A SUMMARY OF THE DEVELOPMENT OF LARGE EXPLOSIVE GUNS FOR REENTRY SIMULATION

PIFR-155

August 1970

Contract No. DA-04-200-AMC-796(X)

by

J. D. Watson

Prepared for

Commanding Officer
Ballistic Research Laboratories
Aberdeen Proving Ground
Maryland 21005

ARPA Order No. 546
Program Code No. 4730

PHYSICS INTERNATIONAL COMPANY
1 MERCED STREET • SAN LEANDRO, CALIFORNIA 94577 • PHONE 357-4610 (415) • TWX 891-9689 (415)

A SUMMARY OF THE DEVELOPMENT OF LARGE EXPLOSIVE GUNS FOR REENTRY SIMULATION

PIFR-155

August 1970

Contract No. DA-04-200-AMC-796(X)

by

J. D. Watson

Prepared for

Commanding Officer
Ballistic Research Laboratories
Aberdeen Proving Ground
Maryland 21005

ARPA Order No. 546
Program Code No. 4730

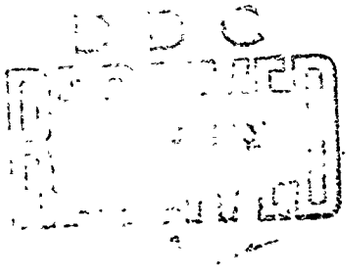

Physics International Company
2700 Merced Street
San Leandro, California 94577

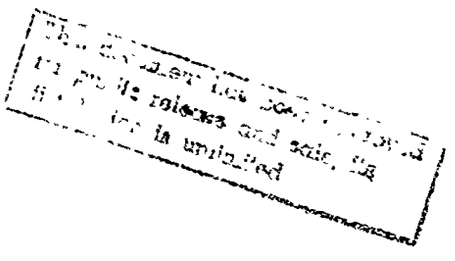

ABSTRACT

This report describes the results of a program to develop an explosive gun capable of launching large saboted models to reentry velocities. A secondary objective was to accelerate small projectiles to the highest possible velocity. Saboted lithium-magnesium models up to 4.5-inch diameter have been launched successfully to 4.8 km/sec. Attempts to accelerate 6-inch-diameter and 7.3-inch-diameter models have not been completely successful. A new velocity-mass record was achieved by accelerating a 2-gram cylindrical projectile to 12.2 km/sec.

FOREWORD

This report summarizes the development of an explosive gun from September 1964 to November 1969, and traces the evolution of the explosive driver and explosive gun parameters. The program was funded by the Ballistic Research Laboratories, Aberdeen Proving Ground, Maryland, under Contract No. DA-04-200-AMC-796(X).

ACKNOWLEDGEMENTS

Many people contributed to the work covered in this report. The author respectfully acknowledges Dr. C. S. Godfrey, who originated the concept of the explosive driver and recognized its potential use in a high-performance launcher, and Mr. E. T. Moore, Jr., who guided the development of this launcher through his continued participation and supervision. The author also wishes to thank the members of the Shock Dynamics Department for their many contributions, in particular Dr. S. P. Gill for his work on the explosive decomposition; Mr. D. M. Mumma and Dr. R. F. Flagg for managing initial phases of the program; Messrs. D. S. Randall, G. B. Steel, and J. S. Marshall for designing and conducting many of the experiments; and the technicians and test site personnel for their enthusiastic efforts. Special thanks are due to Mr. F. D. Milistefr for his inexhaustible support in conducting the large-scale gun experiments.

CONTENTS

CONTENTS (cont.)

ILLUSTRATIONS

ILLUSTRATIONS (cont.)

ILLUSTRATIONS (cont.)

ILLUSTRATIONS (cont.)

ILLUSTRATIONS (cont.)

SECTION 1

INTRODUCTION

Inexpensive methods of simulating reentry phenomena in ground-based facilities are very desirable alternatives to extensive and costly in-flight testing. In the past, hypervelocity range facilities have provided significant data; however, these facilities are presently limited to launching models with diameters of 2 inches or less. Extrapolation of data (generated in these facilities) to full-size reentry vehicles depends on inadequate scaling laws. The explosive gun concept described in this report can be used to inexpensively launch 6-inch to 8-inch diameter models to reentry velocities. Coupled to a range facility, these guns could be used to generate data for reentry vehicles having dimensions which more nearly approach those of an actual vehicle. The usefulness of this data, which would include close observation of the model for several thousand body diameters of flight, would not be as dependent on scaling laws.

Section 2 describes the early experiments with explosive guns and the attempt to launch a 6-inch-diameter plastic cylinder to 6 km/sec. Section 3 summarizes the investigation and solution of the projectile integrity problem, and the subsequent studies resulting in the successful launch of a 3-inch-diameter sphere to 4.8 km/sec. Section 4 includes a discussion of the problem of explosive decomposition in large drivers and the gun design modifications that were required to launch slender cones to 5.5 km/sec. Section 5 presents

SECTION 2

EARLY DEVELOPMENT OF THE EXPLOSIVELY-DRIVEN GUN AND LAUNCHING OF A 6.25-INCH-DIAMETER CYLINDER TO 6.0 KM/SEC

This section presents the initial development of the gas-dynamic cycle of an explosively-driven gun to launch large models to reentry velocities. These investigations were conducted to establish explosive driver parameters such as initial gas pressure, charge-to-mass ratio, and length-to-diameter ratio, and the basic gun parameters such as chambrage ratios and gas mass-to-projectile mass ratios. Several projectile materials were studied for various launch cycles. The reproducibility and scalability of explosively-driven guns were demonstrated experimentally over a wide range of sizes. The experimental methods and instrumentation techniques developed for large-scale gun tests are described.

2.1 THEORY AND OPERATION OF THE EXPLOSIVELY-DRIVEN GUN

The linear explosive driver represents a technique whereby a substantial portion of the chemical energy of an explosive is converted in a controlled manner to the kinetic and internal energy of a gas. Basically, the energy densities in the gas are produced by a strong shock generated by the progressive collapse of a tube. The collapse of the tube is such that it may be represented as a piston propagating into a gas. The model used to describe the ideal operation of the driver is quite similar to that used to explain the basic discontinuous motion produced by a piston in one-dimensional gasdynamics.

the experiment used to verify the solution to the pre-initiation problem followed by a description of the ALPHA-I experiment to launch a 6-inch-diameter slender cone to reentry velocity. Conclusions and recommendations are made in Section 6. A secondary objective of this program was to further the development of a two-stage explosively-driven gun to accelerate small projectiles to extremely high velocities. The results of this effort are given in Appendix A. A hypervelocity range facility for large explosive guns is described in Appendix B.

The operational characteristics of the linear explosive driver are shown in Figure 2.1. A thin-walled metal tube (the pressure tube) containing the driver gas is surrounded by a chemical explosive. After a detonation is initiated in the explosive, a detonation wave propagates in the explosive along the outside of the metal tube. The pressure behind the detonation wave accelerates the tube wall in toward the axis, sealing the tube and forming a conical-shaped piston (Figure 2.1b). The velocity of the piston, D, is equal to the detonation velocity of the explosive. The motion of this piston generates a strong shock wave in the stationary column of the driver gas. If the gas behaves ideally (i.e., the ratio of the specific heats, γ, of the gas is constant), then the velocity of the shock wave, S, is $(\gamma + 1)\ D/2$. The position-time histories of the piston and shock wave are shown in Figure 2.1c for an ideal driver gas ($\gamma = 5/3$). These trajectories are presented in the dimensionless coordinates

$$\bar{x} = \frac{x}{d} \quad \text{and} \quad \bar{t} = \frac{Dt}{d}$$

Where x and t are the distance and time after the shock wave begins to move ahead of the detonation wave, d is the internal diameter of the pressure tube, and D is the detonation velocity of the explosive. The use of these coordinates facilities the comparison of drivers having pressure tubes of different dimensions or utilizing explosives with different detonation velocities. It should be noted that in this coordinate system all slopes are normalized with respect to the detonation velocity of the explosive. For example, in Figure 2.1c the trajectory of the detonation wave has a slope of unity, while that of the shock wave has a slope of four-thirds

$$\left(\frac{S}{D} = \frac{\gamma + 1}{2}\ ,\ \gamma = \frac{5}{3}\right)$$

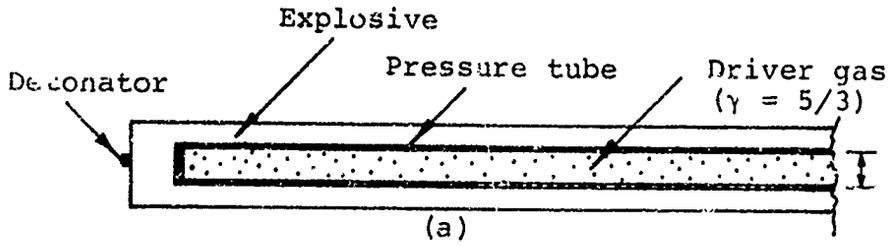

Time $\bar{t}$ = 0, before initiation of the explosive

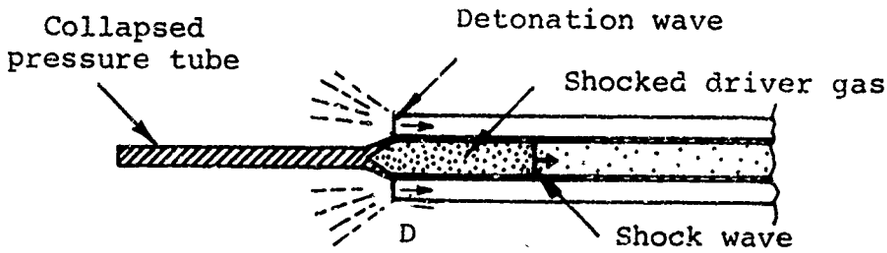

(b)

Time $\bar{t} = \bar{t}_1$, after initiation of the explosive

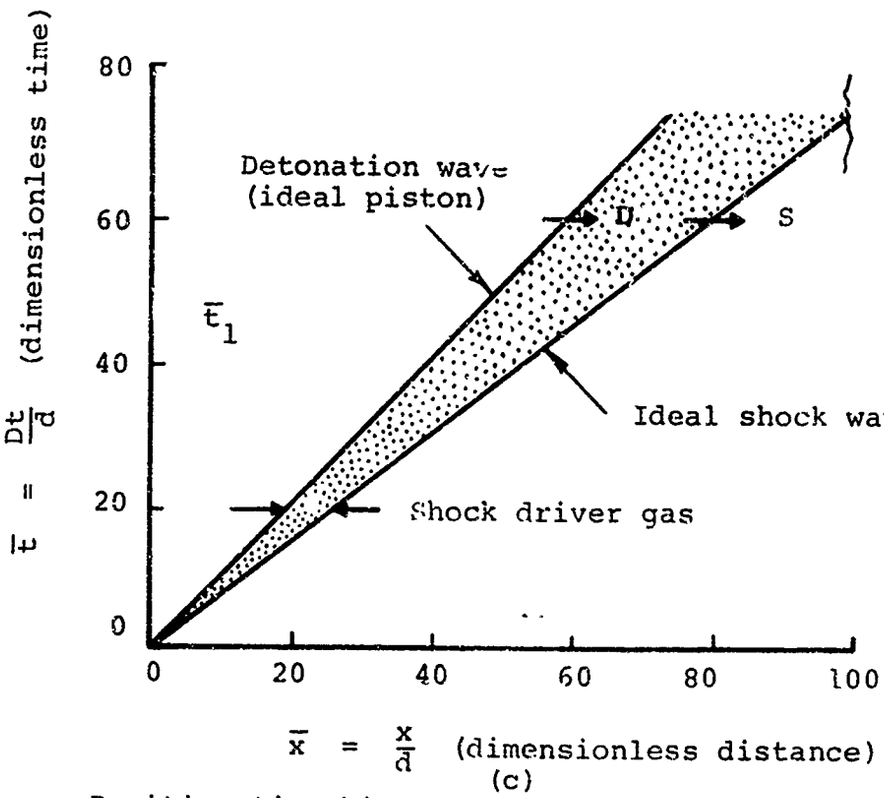

(c)

Position-time history of shock and detonation wave

Figure 2.1 Ideal operation of the linear explosive driver.

The thermodynamic state of the shocked gas (subscripts 1) is described by the following relations:

Pressure: $$P_1 = \rho_o \frac{\gamma + 1}{2} D^2$$

Specific internal energy: $$E_1 = \frac{1}{\gamma + 1} \frac{P_1}{\rho_o} = \frac{D^2}{2}$$

Density: $$\rho_1 = \frac{\gamma + 1}{\gamma - 1} \rho_o$$

Sound speed: $$a_1 = \frac{\gamma (\gamma - 1)}{2} D$$

where ρ_o is the initial density of the unshocked gas. These relations assume that the initial pressure, P_o, and internal energy, E_o, in the unshocked gas are quite small compared to the corresponding quantities in the shocked gas. It is noted that for a given ideal gas the magnitude of each of these properties, except density, is a function only of the piston velocity (detonation velocity).

The performance of linear explosive drivers has been demonstrated over a wide range of experimental parameters. Internal diameters of pressure tubes made of copper, steel, lead, and aluminum have ranged from 1/4-inch to 16-inches; high-explosive weight has ranged from 27 grams to 9200 pounds; the explosive-to-pressure tube mass ratio has been varied from 0.5 to 10; driver gases have included helium, air, argon, and hydrogen; the initial pressure of the driver has been varied from 15 to 2450 psi; and the detonation velocities of the explosives used (liquid and solid) have ranged between 5.5 km/sec and 8.6 km/sec. While some of these tests have been one of a kind, the majority were essential to comprehensive experimental studies of a particular explosive driver design.

Although many of the drivers perform close to the ideal predictions, certain departures may occur. Four phenomena have been incorporated in a model of explosive driver operation to account for observed departures from the ideal driver performance described above. They are: (1) radial expansion of the pressure tube behind the shock wave; (2) decomposition or predetonation of the driver explosive during the period of pressure tube expansion; (3) the effect of boundary-layer growth behind the shock wave; and (4) formation of a metal, gas, or metal-gas jet by the collapsing pressure tube. These phenomena are interrelated through the kinetics produced by the imploding pressure tube. Their interdependence is such that changes in driver behavior resulting from certain experimental parameter changes cannot be attributed solely to a particular phenomenon. However, the ability of the model to explain, predict, and control the behavior of explosive drivers justifies the categorization of these phenomena. A detailed discussion of these four phenomena is presented in References 1 through 5.

The explosive driver is coupled to the barrel of the gun by a massive steel reservoir section. Materials used to form the reservoir section during the course of launcher development included lead, steel, concrete, and explosive . Guns have been operated on both the chambraged or unchambraged mode. When the strong shock generated by the explosive driver reaches the chambrage plane (or projectile location in an unchambraged gun) it reflects and forms a reservoir of very high enthalpy gas. The reservoir of gas is then expanded to accelerate the projectile, as illustrated in the example of a chambraged gun in Figure 2.2.

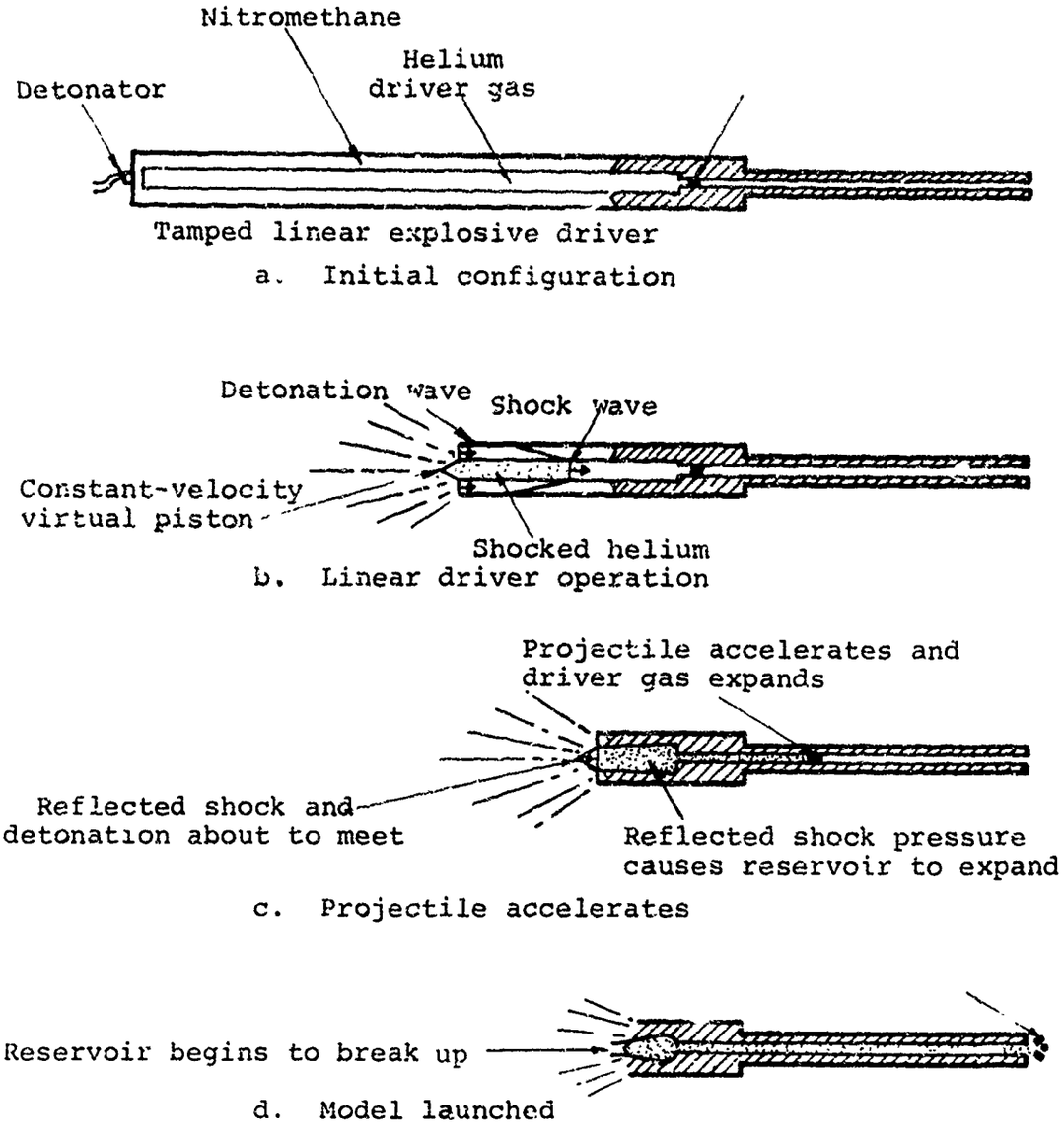

Figure 2.2 Operation of a single-stage explosively-driven launcher.

3479

For launcher applications, the length of shocked gas generated by the explosive driver is usually limited to less than 10 tube diameters to preclude major effects of boundary-layer growth or pressure tube expansion. Jetting of the collapsing pressure tube that forms the piston is usually negligible in launcher applications because of the high gas pressures (2 to 5 kbar).

Using the ideal theory for reflection of a strong shock from a rigid wall, the gasdynamic conditions in the reservoir may be calculated. The pressure and sound speed, for example, are found from the relations

$$P_4 = \frac{\gamma + 1}{\gamma - 1} + 2 \qquad P_2 = \frac{3\gamma - 1}{\gamma - 1} \frac{\gamma - 1}{2} \rho_1 D^2$$

$$a_4 = \frac{(3\gamma - 1)(\gamma - 1)}{2} D$$

Because of the high pressures generated in the reservoir section (guns have been operated with peak reservoir pressures up to 80 kbar), expansion of the reservoir material during the gun cycle has an important limiting effect on the performance of the gun. This effect is covered extensively in subsequent sections of this report.

2.2 CHOICE OF BASIC GUN PARAMETERS

The first series of explosive guns tested under this program were unchambraged designs (pressure tube-to-barrel area ratio of 1:1) with one of two diaphragm methods. In some of the guns a diaphragm was located about halfway down the pressure tube so that the shocked helium driver gas would expand into a void and the pressure history on the rear of the projectile would be accomplished by a steep compression wave and would be relatively gradual. In

other guns, the projectile itself served as the diaphragm and the projectile was loaded abruptly by the direct reflection of a strong shock wave on the base of the projectile.

In the first series of guns the explosive drivers and barrels were relatively short and the initial gas pressures were high (around 2400 psi helium). The gas mass-to-projectile mass ratios ranged from 1 to 2.

When lexan was used as the projectile material, the models were badly fragmented. Nylon projectiles were usually launched intact, but somewhat distorted as a result of peak base pressures ranging as high as 80 kbar. The best combination of performance and projectile integrity was obtained by lowering the initial gas pressure to 1200 psi helium in a gun with a diaphragm located halfway down the pressure tube. A range radiograph from this experiment of the projectile in flight at 4.5 km/sec is shown in Figure 2.3. An intermediate-scale (160-gram nylon projectile)

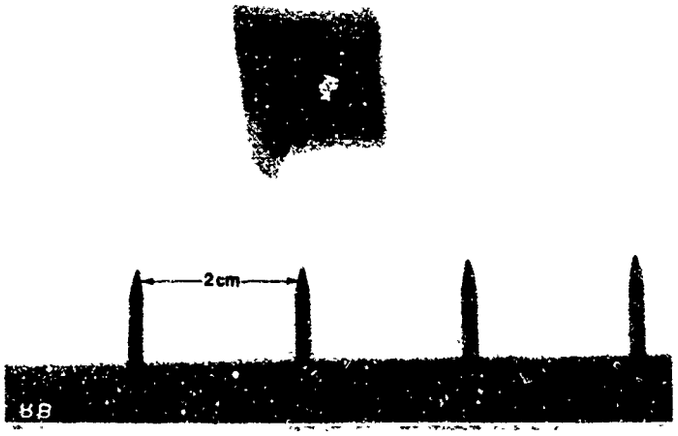

Figure 2.3 Range radiograph of a 4.2-gram projectile launched to 4.6 km/sec (Shot 152-18).

gun was built and fired based on this experiment. However, the barrel of the intermediate-scale gun was formed by a thin steel tube surrounded by a thick layer of concrete. At the time this was not considered a design compromise and, if successful, would have resulted in a substantial cost saving in large-scale guns. However, the experiment was unsuccessful due to severe projectile damage. The final velocity was only 2 km/sec. Subsequent small-scale tests (Reference 6) demonstrated that the concrete/steel barrel construction was responsible for the failure.

On the basis of successes obtained in another explosive gun program (NASA Contract No. NAS W-978), the design of the gun was modified to include a 4:1 area reduction between the pressure tube and barrel (chambraged gun). In this design the explosive driver and barrel lengths were increased and the initial gas pressures were further lowered to 645 psi. The gas mass-to-projectile mass ratio for this design increased to 2 as a result of these changes. Polyethylene was substituted for nylon as the projectile material because of its lower density, and the technique of gradually loading the projectile by a compression wave was abandoned in favor of the more reliable direct shock loading method. Polyethylene projectiles were now launched consistently to 6 km/sec with minimal distortion.

Another intermediate scale (101-gram polyetheylene projectile) gun was tested based on the success of the small-scale chambraged gun design. The projectile was accelerated intact to 5.65 km/sec, and recorded by the range radiograph and high-speed framing camera (Figure 2.4). The small decrease in velocity compared to the small-scale experiment is probably a result of not scaling exactly the pressure tube-to-barrel area ratio. The ratio was about 10 percent in the intermediate-scale experiment.

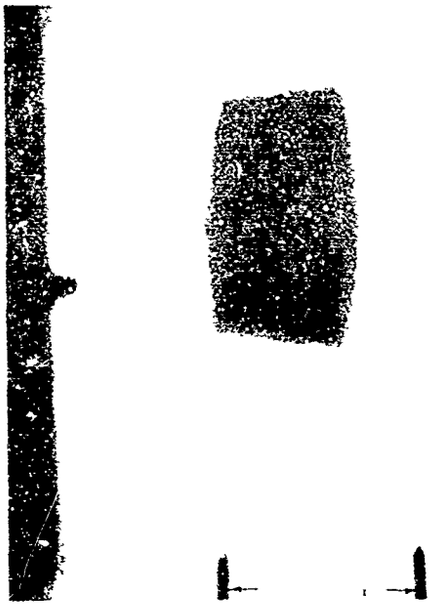

Figure 2.4 Range radiograph of a 102-gram projectile launched to 5.75 km/sec (Shot 152-101).

After the intermediate-scale gun experiment, an attempt was made to further optimize the performance of this design before scaling the gun to launch a 6-inch diameter projectile. The results of this investigation revealed that slightly higher performance was possible with a longer barrel, and that the existence of scratches and pits on the internal surface of the barrel would not adversely affect projectile integrity or the performance of the gun (Reference 4).

2.3 LARGE GUN EXPERIMENT (SHOT 1000)

The design of the large-scale gun was based on the results of the successful intermediate-scale experiment (Shot 101) and subsequent small-scale optimization tests. The large-scale gun was a chambraged gun with a pressure tube-to-barrel area ratio of

4:1 and a driver gas mass-to-projectile mass ratio of 2:1. The 6.25-inch-diameter, high-density polyethelene projectile weighed 2.36 kg and the barrel was 13.5 feet long. Because of availability and scheduling considerations, the barrel was fabricated from a salvaged propeller shaft section and was only three-quarters of the desired length. The gun contained 3200 pounds of nitromethane high explosive.

In all of the small- and intermediate-scale guns leading up to this test, the projectiles were seated in the breech by tapering the projectile and forcing it into the barrel. With this method, the projectile would not move under the initial gas loading pressures of 645 psi, but would accelerate properly under the pressures of many kilobars developed during the operation of the gun. In most of these shots 3- or 4-degree tapers were sufficient to seat the projectile; tapers up to 5-degrees had been tried successfully. Since the viscous properties of the projectile do not scale, the large-scale projectile required a 7-degree taper to prevent premature extrusion out of the barrel.

The assembled gun (Figure 2.5) was brought to the Physics International Tracy Test Site, and placed concentrically inside an 8-foot culvert pipe, 8 feet below the surface of the ground. The entire shot was covered with sand to a minimum depth of 4 feet to attenuate the coupling of the explosive blast into the air and to reduce the shrapnel hazard. The "cover factor," or apparent reduction in explosive weight (calculated from the work of B. Perkins, Jr. at the Ballistic Research Laboratory, Reference 7), was 3-1/2 and was seen 4-1/2 miles from the explosion. That is, the 3200 pounds of nitromethane buried to a depth of 4 feet would appear as a 530-pound surface explosion. This calculation is valid for a spherical charge and overestimates the effect of a long cylindrical charge such as the explosive gun.

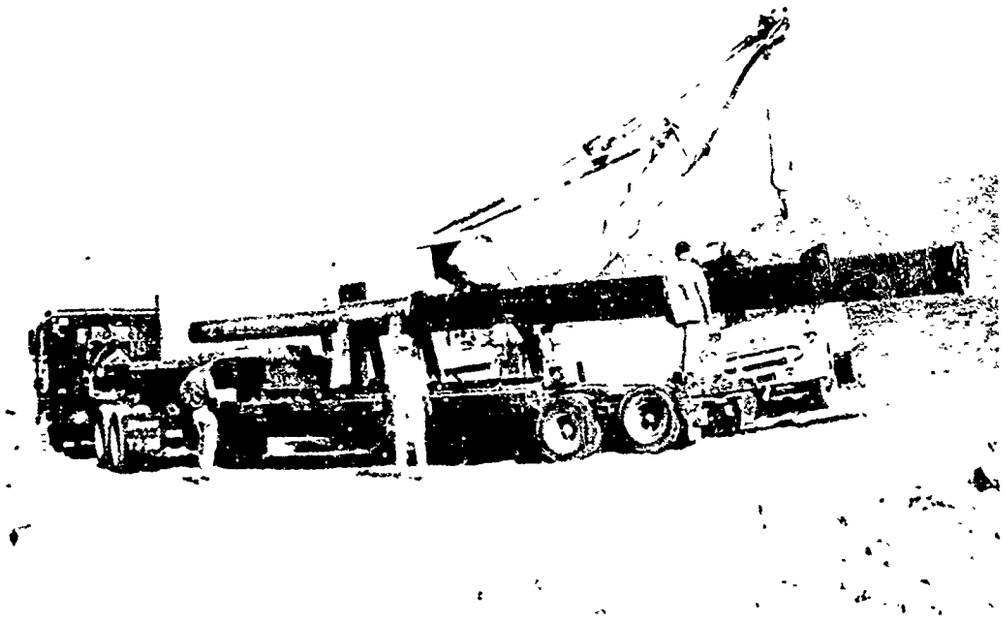

Figure 2.5 Six-inch bore explosive gun arriving at the Tracy Test Site (Shot 1000).

The explosive driver was instrumented with pin switches to measure the shock and detonation wave trajectories. High-speed framing cameras and a 600-kV Marx X-ray unit were used to record the projectile velocity and condition. A 400 frame/sec Milliken camera was placed on a nearby hill to obtain an overview of the test.

The Seismographic Department of the University of California, Berkeley, was given a zero-time pulse to monitor ground shock transit times from the explosion. The Meteorological Department of the Lawrence Radiation Laboratories monitored overpressures with microbarographs located 4-1/2 and 6 miles from the explosion, directly in line and at 90 degrees from the muzzle of the gun.

The projectile was launched to a velocity in excess of 6 km/sec; however, it was badly damaged. It was felt that the large projectile taper required to seat the projectile was responsible for the breakup, probably because of the radially convergent stress pulse sent into the polyethylene as the projectile was extruded into the gun barrel. Pin switch data on the driver indicated that the trajectory of the driver shock was normal. No data was recorded on the detonation wave trajectory. With the available data and inspection of the recovered portion of the driver, it was concluded that driver operation was normal. The observed performance of the gun is shown in the x-t plane (Figure 2.6).

Both microbarograph stations located 4-1/2 miles from the shot recorded 75 microbars; no overpressure was observed in the town of Tracy, six miles away. The normal expected overpressure at the 4-1/2 mile stations, if located at the point of pressure focusing, would be around 800 microbars for a 500-pound spherical charge detonated on the surface. From this it was concluded that the calculated cover factor could possibly be increased from 6 to 80 without causing overpressure disturbances to surrounding communities. That is, a 3200-pound explosive charge such as that used in the large gun experiment would be equivalent to a 40-pound sphere detonated on the surface. The post-shot condition of the firing area is shown in Figure 2.7.

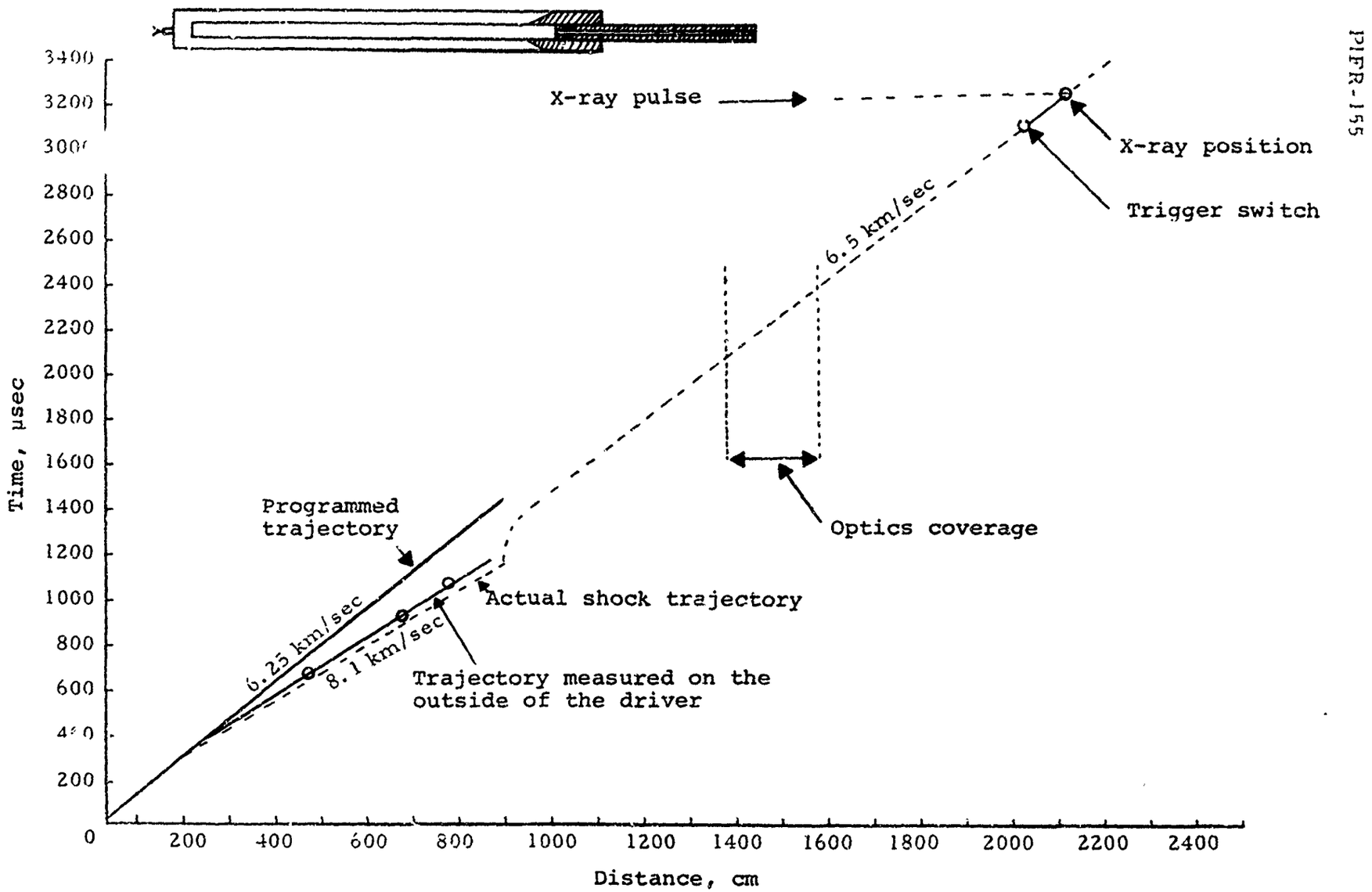

Figure 2.6 Observed performance of Shot 1000.

Figure 2.7 Crater formed by Shot 1000 (target stand is in the foreground).

2.4 SUMMARY

The results of the first large-scale gun experiment demonstrated the basic feasibility of using large-scale explosively-driven guns to accelerate models to reentry velocities. A 2.36-kg, 6.25-inch-diameter polyetheylene cylinder was accelerated to 6 km/sec. Fragmentation of the model was probably not caused by the basic operation of the gun, but by the particular method used to seat the projectile in the barrel prior to launch. The operation of the explosive driver appeared to scale over a considerable range (1.5-inch-diameter to 12-inch-diameter), although the data recorded on the 12-inch-diameter driver was limited to shock trajectory measurements. Gun performance also scaled reasonably well over this range of size, and the performance of the given

gun design was shown to be quite reproducible. A chambraqed gun geometry with direct shock loading of a polyetheylene or nylon projectile appeared to be the best configuration for optimizing projectile velocity and integrity. The problem of the airblast and shrapnel hazards in large-scale guns appeared to be solved by using a culvert for decoupling and a reasonable amount of sand covering.

Areas remaining to be investigated were the projectile integrity problem and the task of upgrading the performance of the gun to launch more complex and massive projectiles for a given barrel bore size. In order for the gun to be useful in reentry research, the 2/3-caliber-long cylindrical models would have to be replaced by up to 1-1/2- to 2-caliber-long saboted sphere and cone configurations with no loss in final projectile velocity. The solutions to these problems are discussed in subsequent sections.

SECTION 3
LAUNCHING OF A 3-INCH-DIAMETER SPHERE TO 4.8 KM/SEC

This section describes the analytical and experimental efforts leading to the design of an explosively-driven gun capable of launching saboted models. In particular, projectile integrity was significantly improved by using advanced time-dependent computer programs and a new aerospace metal alloy. Reproducibility, range accuracy and scalability of the gun design were confirmed. Continued experiments and analysis revealed several nonideal phenomena affecting the operation of explosive drivers. Small-scale spheres and cones were launched to 5.0 km/sec. The gun was then scaled-up and used to successfully launch a 3-inch-diameter sphere to 4.8 km/sec from a 4.5-inch sabot.

3.1 PROJECTILE INTEGRITY

The previous section demonstrated the basic feasibility of using an explosive driver to launch large cylindrical models to 6 km/sec. It was recognized, however, that as the models became more complex, the performance of the launchers would be largely limited by the ability of keeping the model intact during its acceleration. Although the importance of the gasdynamic cycle of a launcher has been widely acknowledged, the correlation of this cycle with projectile integrity had never been treated in a comprehensive manner. Since one of the distinctive advantages of explosively-driven launchers is the precise and reproducible control that can be exercised over the gasdynamic cycle, an extensive analytical program was conducted in conjunction with the

experimental efforts to correlate the gasdynamic cycle with the detailed response of specific model configurations (References 1 and 8). Using advanced computer techniques, this analytical study resulted in considerable progress in this much neglected area of gun design. For instance, it was shown that the peak pressures (or accelerations) that a given model can withstand are strongly dependent on the nature of the wave interactions occurring within the projectile. It was also shown that very high pressures are permissible if the gasdynamic cycle and the dynamic response of the barrel material are properly integrated with the projectile design. Indeed, a study of the detailed wave systems generated in the projectile during launch resulted in the establishment of guidelines which led directly to improvement in the condition of the models launched by explosively-driven guns.

This approach to projectile design was based on simulating the interaction of the driver gas, projectile, and walls of the gun on one- and two-dimensional computer programs.* It then became possible to observe the wave systems that were generated in the driver gas as they interacted at the projectile and barrel interfaces and propagated into the projectile and barrel materials. By examining on the computer the results of typical launcher problems, any destructive wave systems generated in the projectile could be traced back to their origin in the gasdynamic cycle or the specific geometry of the gun. The destructive wave system could then be altered or eliminated by design changes in the

*The programs used are one- and two-dimensional, time-dependent Lagrangian and coupled Eulerian-Lagrangian codes. These codes solve the conservation and constitutive relations in hydrodynamic and elastic-plastic media, employing the Von Neumann-Richtmeyer artificial viscosity method to handle shock discontinuities. These codes describe the dynamic and thermodynamic properties of material as a function of position and time. In addition, they allow the localized stress, strain, and distortional energy to be evaluated.

geometry and/or gasdynamic cycle of the gun. The impracticality of a given launcher design, or at least potential problem areas for model integrity and deformation, could be ascertained. This approach, while pertinent to any light-gas-gun cycle, has given valuable insights into the more frequnt causes of model breakup which occur in explosively-driven gas guns.

The projectile in an explosively-driven gun is usually set in motion by reflecting a strong shock from the base of the projectile. The projectile is then accelerated by a repetitive internal wave system of strong downstream-running shock waves and upstream-running rarefaction waves. For the simplest case of a one-dimensional gun, this accelerating wave system is shown in Figure 3.1a.

When a material is put into severe net tension in a time comparable to that required for a sound wave to traverse the specimen, a fracture process known as spalling will arise. Spalling may occur in a projectile if a strong rarefaction wave produced in the driver gas (e.g., by stopping the piston driving the reservoir gas) propagates downstream, overtakes the accelerating projectile and interacts with an upstream-running rarefaction within the projectile (Figure 3.1b). Spall fracture can also be caused by the presence of pressure spikes* in the driver gas. Large pressure spikes can cause the projectile to spall even after the acceleration is essentially complete; thus projectile failure can be caused at any point in the barrel.

A two-dimensional calculation of the shock acceleration of a nylon projectile in an unchambered gun (Figure 3.1c) revealed that

---

* A pressure profile in which a strong shock is immediately followed by a strong rarefaction.

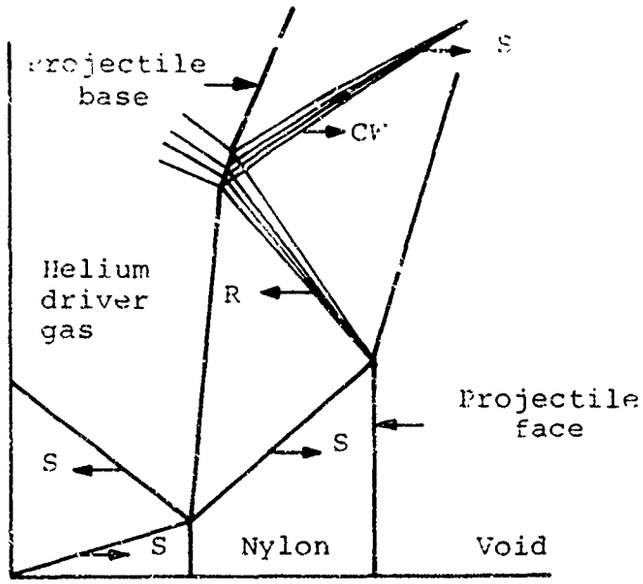

a. Axial wave system in a shock-accelerated projectile (unchambered gun)

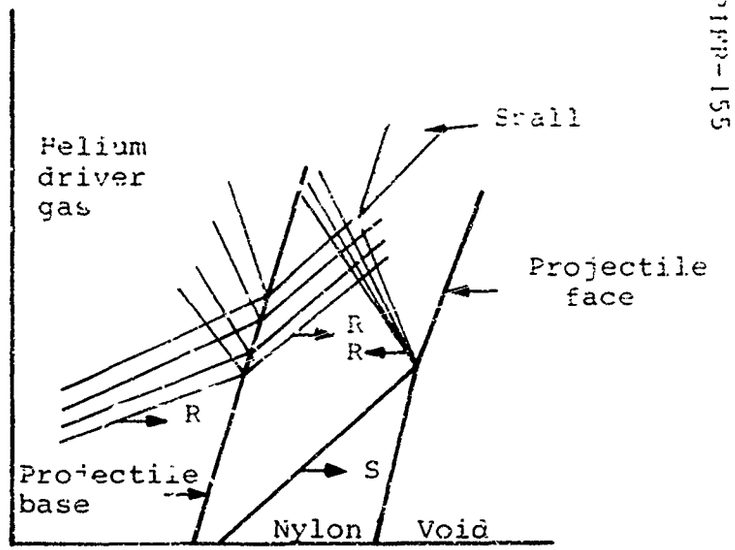

b. Spall fracture of projectile resulting from downstream-running rarefaction in the driver gas

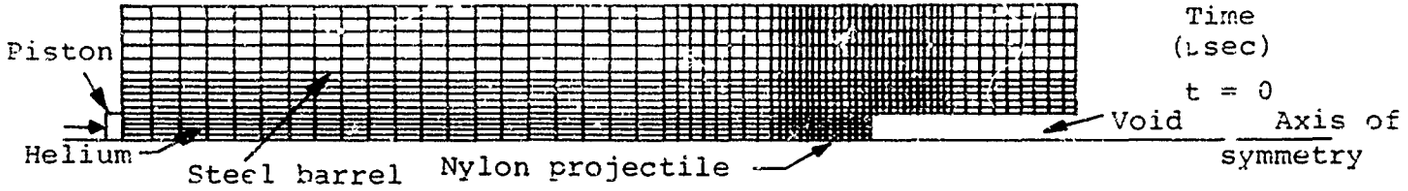

c. Initial configuration of two-dimensional calculation of an unchambered gun.

Note: Gas initially at 6.4 km/sec and 2 kb

Figure 3.1 Projectile acceleration in an unchambered gun.

the wave systems generated in the driver gas and in the projectile are essentially one-dimensional. There is a small amount of energy transfer between the projectile and the barrel during each wave transit in the projectile, but this has an insignificant effect on the condition of the projectile.

In a chambered gun (Figure 3.2) large radial stress waves will develop if the shock velocity in the barrel material is higher than that in the projectile material. If, in addition, the yield strength of the barrel is much higher than the yield strength of the projectile, the radially converging shock will be followed by a radially converging rarefaction. The formation of large radial shocks or pressure pulses can lead to fracture in the projectile and ultimately result in breakup of the projectile. For large area ratios at the chambrage plane, the axial plastic wave in the barrel can propagate ahead of the projectile and cause significant distortion of the barrel ahead of the accelerating projectile. For rapidly accelerating projectiles, the complex flow through the area discontinuity can result in an unequal distribution of pressure on the base of the projectile. Large radial variations in pressure across its base can cause destructive shear waves to propagate through the projectile. The strong two-dimensional nature of the gas flow through an area change is illustrated in Figure 3.3 for the limiting case when the projectile mass approaches zero.

Several examples of distorted and fragmented projectiles launched by explosively-driven guns are shown in Figure 3.4. Most of the failures can be attributed to improper integration of the gasdynamic cycle with the projectile configuration; only small design changes are usually required to eliminate these. As projectile configurations become more complex, this computer technique becomes a powerful research tool. A detailed discussion of this technique applied to the projectile integrity problem is given in Reference 8.

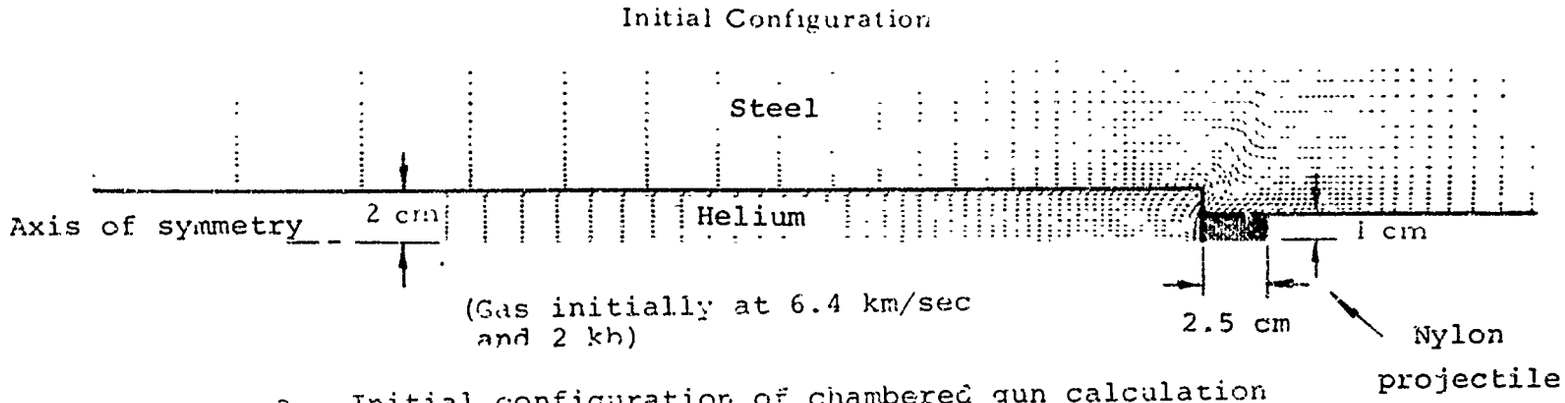

a. Initial configuration of chambered gun calculation

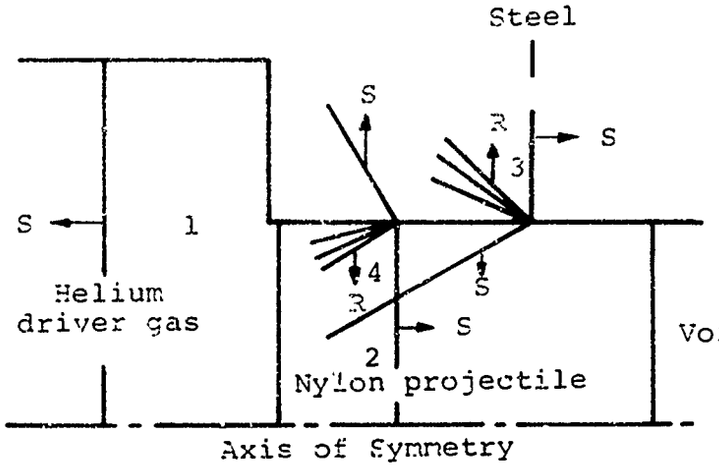

Material Properties

Helium: Ideal gas

Nylon: Initial density = 1.14 gm/cm^3
Initial sound speed = 3 km/sec
Yield strength = 0.7 kb

Steel: Initial density = 7.84 cm/gm^3
Initial Sound speed = 5.86 km/sec
Yield strength = 6.0 kb

Region	Axial Stress (kb)	Radial stress (kb)
1	12	12
2	12	11.3
3	12	6
4	16.8	16.5

b. Formation of radially converging stress pulse after reflection of gasdynamic shock

Figure 3.2 Two-dimensional effects associated with a chambered gun.

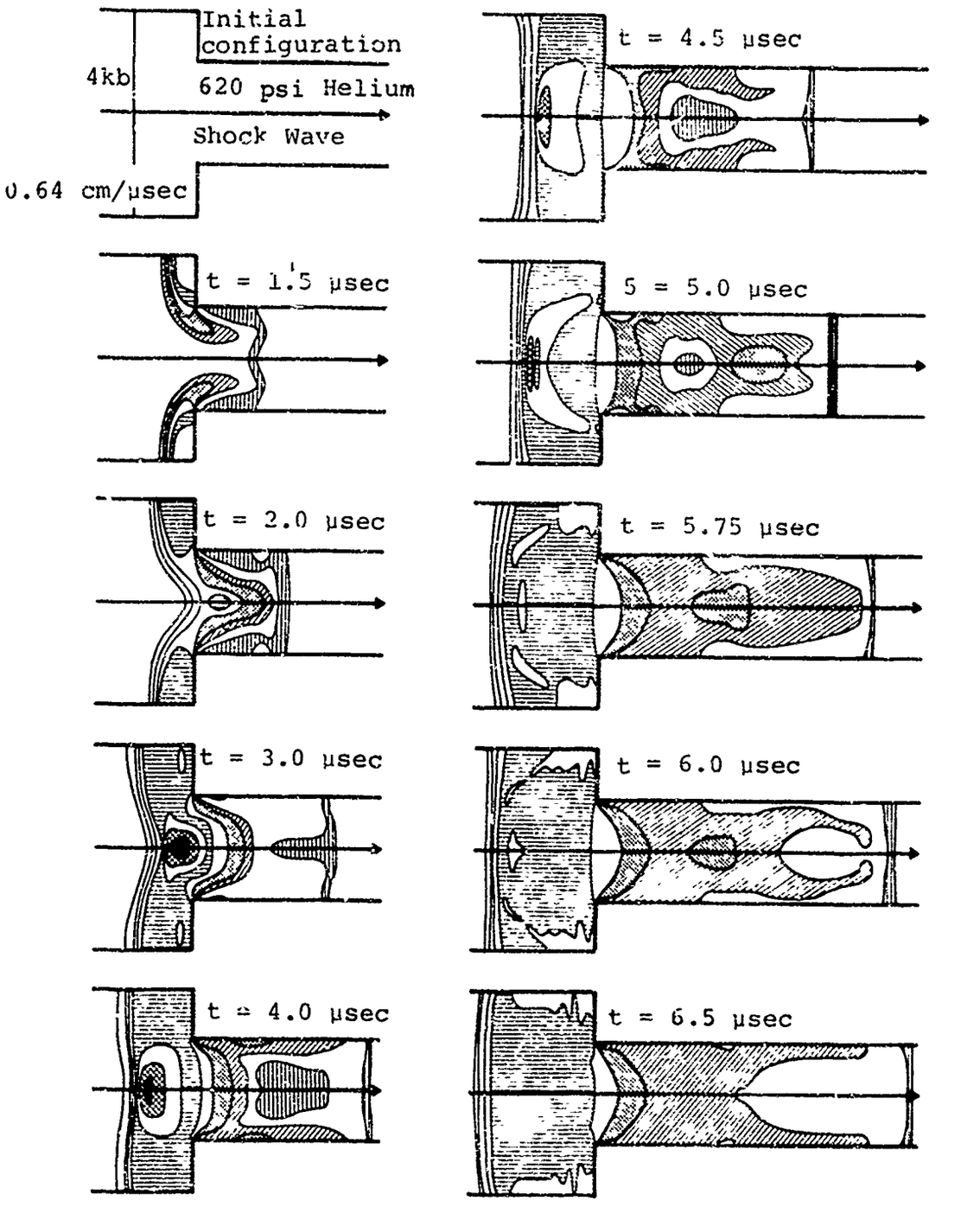

Figure 3.3 Interaction of a shock wave with an area discontinuity showing isobaric regions at various times.

Direction of flight ——————→

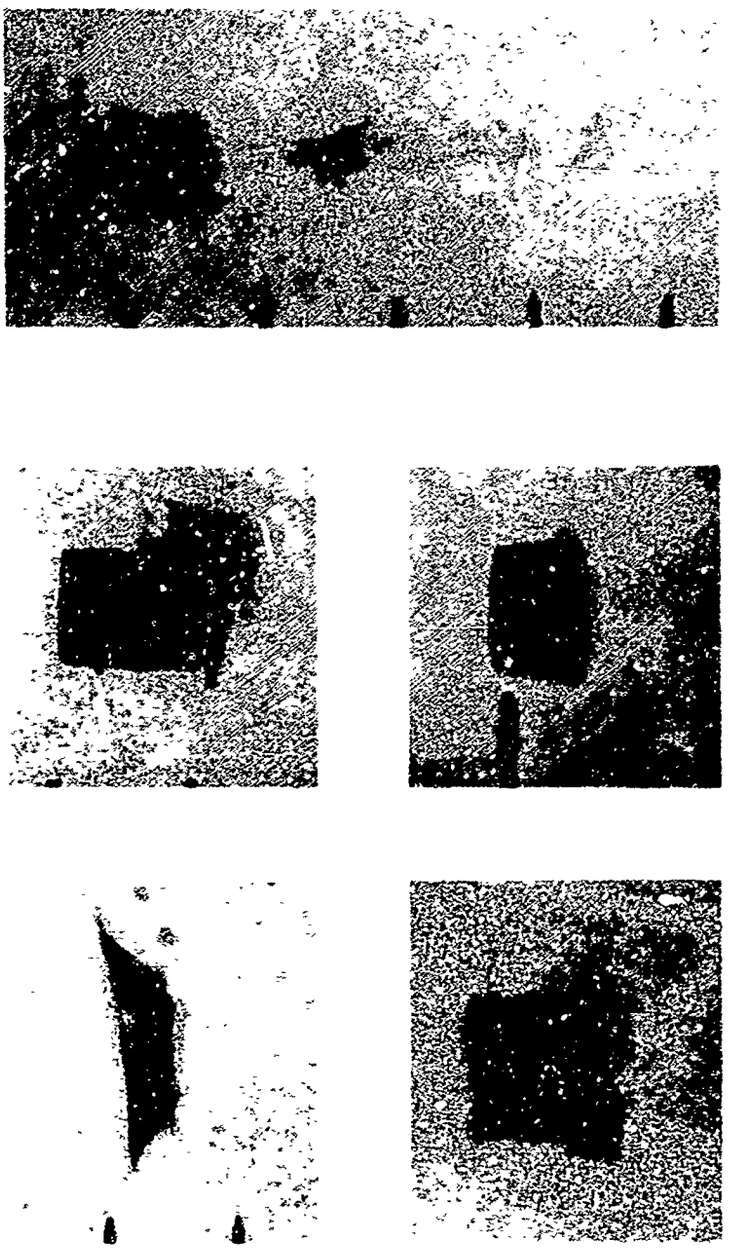

Figure 3.4 Typical modes of projectile failure in erly explosively-driven guns.

3.2 SMALL-SCALE DRIVER AND GUN DEVELOPMENT TESTS

Experiments were conducted that demonstrated four observed departures from ideal explosive driver operation. These phenomena are (1) formation of a metal, gas, or metal-gas jet by the collapsing pressure tube; (2) radial expansion of the pressure tube behind the shock wave prior to the arrival of the detonation wave (piston); (3) decomposition or pre-detonation of the driver explosive during the period of pressure tube expansion; and (4) the growth of a boundary layer behind the shock wave and its interaction with the piston formation or collapse process.

Jetting phenomena, while nearly always present, are generally not a major problem except in low-pressure drivers (initial gas pressures of a few atmospheres). Radial expansion is always a factor in the high-pressure drivers used in launcher work; however, it can be controlled by surrounding the explosive with a thick-walled steel tube (often referred to as a tamper) which is used to elastically or inertially restrict radial expansion of the pressure tube within acceptable levels. This, of course, will enhance compression of the driver explosive prior to the arrival of the detonation wave. In large-scale drivers or drivers with sensitized explosive this can result in decomposition or pre-detonation of the explosive. Also, in long drivers (length-to-diameter ratio of over 50), the flux of boundary-layer gases built up behind the shock impinges on the explosively formed piston, alters the momentum balance of the collapse process, and eventually results in a leakage of boundary-layer gases through the collapse region. This phenomena ultimately limits the length of shocked gas that can be generated by an explosive driver, in practice, to about 20 tube diameters of shocked gas.

The detailed observed performance of an early driver design demonstrates these phenomena. The driver was made very long in an attempt to generate a long column of shocked gas. The explosive was surrounded by a thick-walled steel tube to control radial expansion. The observed performance shown in the x-t plane (Figure 3.5) reveals both a shock and detonation wave speedup. This was subsequently attributed to predetonation of the sensitized driver explosive. When the same driver was operated with unsensitized explosive, the detonation trajectory was normal and the shock velocity, although starting out normally, eventually decayed to a velocity equal to the detonation velocity (Figure 3.6). This was caused by a combination of radial expansion and boundary-layer gas leakage. In both driver experiments the initial shock trajectory is overdriven, due in part to the formation of a metal and gas jet generated during the start-up process. A comprehensive analytical and experimental discussion of observed driver performance can be found in References 2, 3, and 5.

During this period, the attention of small-scale gun experiments was focused almost exclusively on the breech area of the gun and the projectile itself. In two experiments a nylon cylinder and saboted sphere were launched to 5.0 km/sec, but were fragmented. Both models were located at the area change of a chambered gun and both were exposed to peak base pressures of nearly 40 kbar. The mechanism of failure was attributed to the impedance and strength mismatch of the projectile and barrel materials, as discussed in the section on projectile integrity. A new projectile material, lithium-magnesium LA141A, was then substituted because of its higher strength and shock impedance. This new aerospace metal has a density of 1.38 g/c^3 and mechanical properties approaching those of aluminum. Because of the high longitudinal sound velocity of LA141A (~ 6 km/sec, or about that of steel),

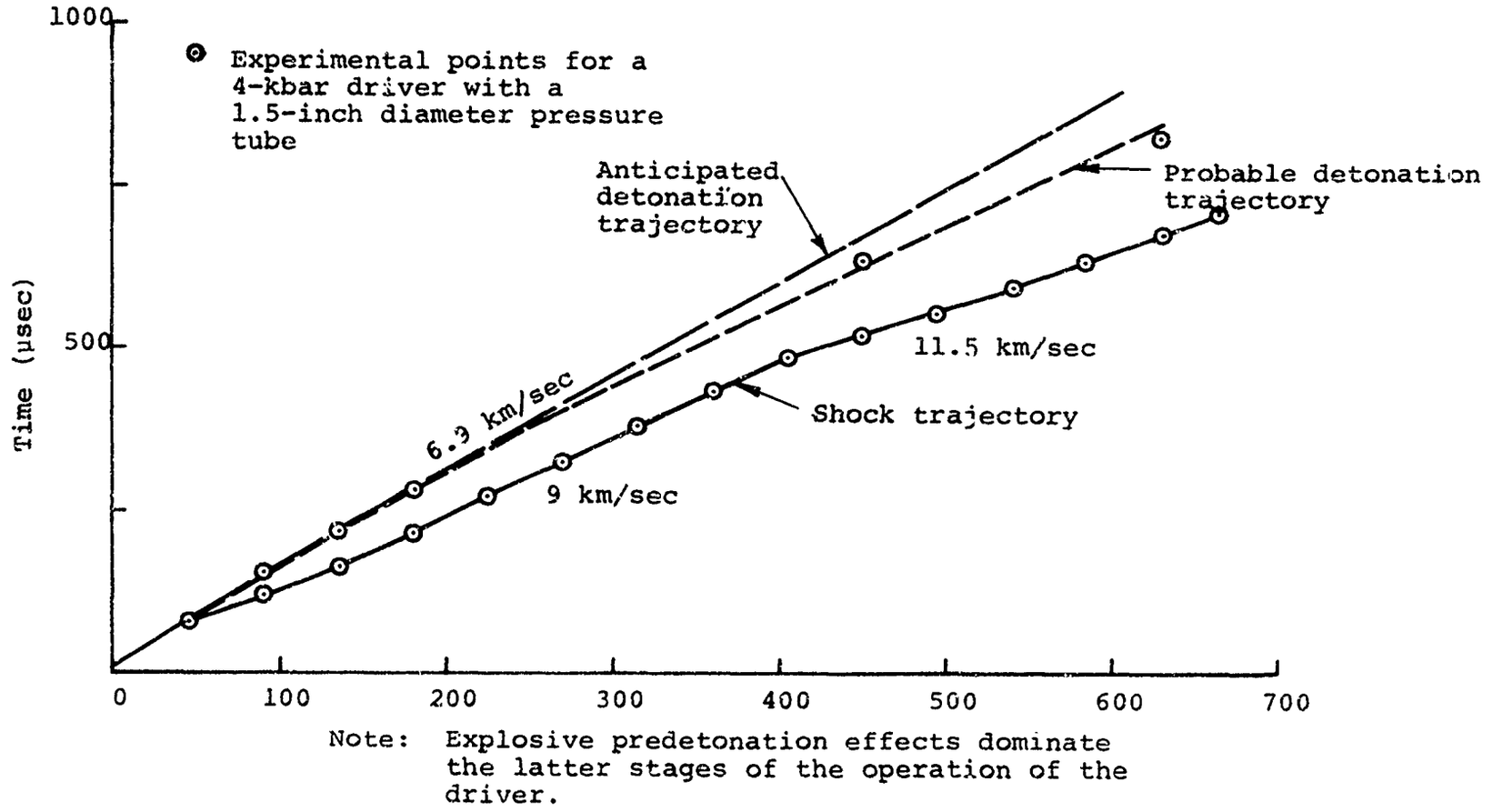

Figure 3.5 Performance of a long-tamped-driver with sensitized nitromethane (Shot 152-60).

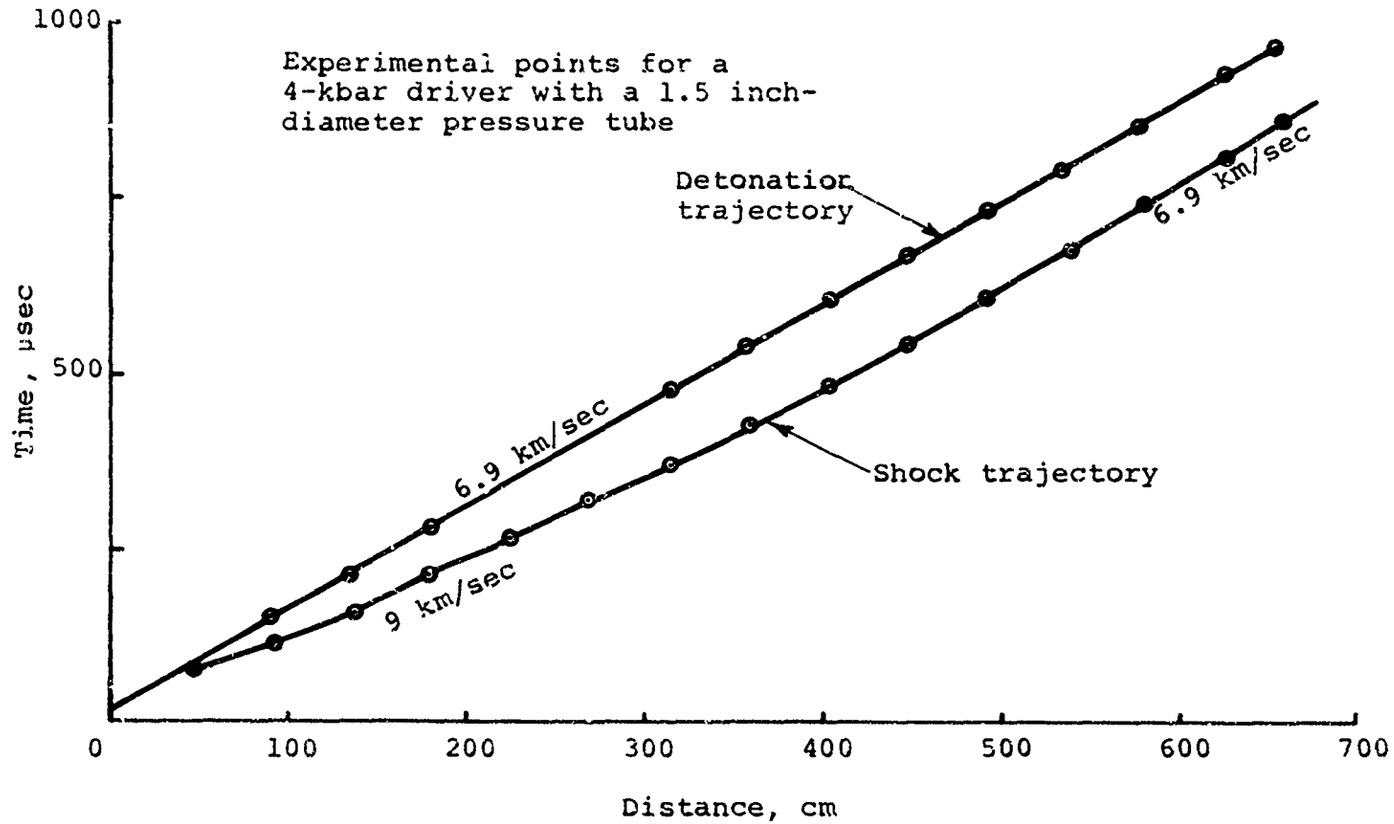

Note: Boundary layer effects dominate the latter stages of operation of the driver.

Figure 3.6 Performance of a long-tamped driver with unsensitized nitromethane (shot 152-61).

the failure mechanism present in the case of nylon projectiles was ineffective. The superiority of LA141A as a projectile material is demonstrated in the range radiographs of a nylon and LA141A projectile launched by the same gun designs and exposed to the same peak base pressures (Figure 3.7).

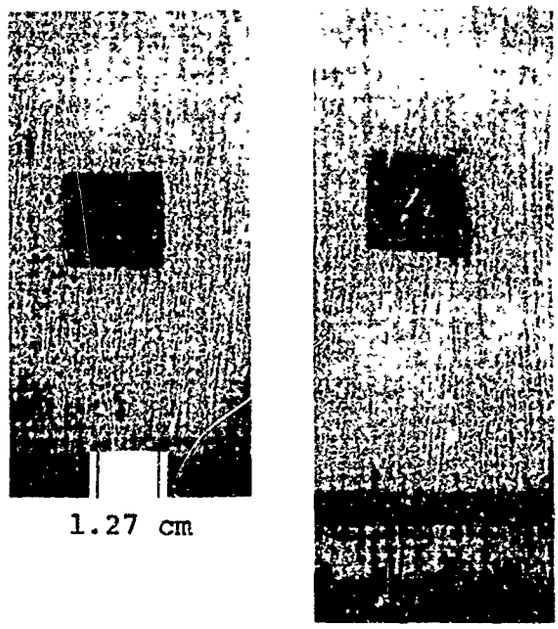

a. Lithium-magnesium (829) Velocity = 4.36 km/sec

b. Nylon (6.99) Velocity = 5.05 km/sec

Figure 3.7 Range radiographs of lithium-magnesium and nylon projectiles launched from the same explosively-driven gun design.

Several saboted sphere models made from LA141A were then launched in an attempt to increase the projectile velocity and reduce model distortion. It was found that model distortion could be reduced by initially placing the projectile two body-diameters downstream of the area change. The flow of gas through the area change and subsequent non-uniform radial distribution of the pressure loading on the base of the model was found to be quite important in reducing model distortion and was studied extensively

(see Figure 3.3). In order to optimize performance, the length of the projectiles was shortened somewhat so that the length-to-diameter ratio of the model was 0.8. Examples of saboted spheres and cones launched to 5.0 km/sec during this phase of the program are shown in the range radiograph of Figure 3.8.

The reproducibility and range accuracy of the explosive gun was demonstrated in a trilogy experiment (Figure 3.9). Three identical guns were fired simultaneously, and the results indicated that the performance of all three drivers was nearly identical. The spheres were all launched in good condition (Figure 3.10) to 5.07 ± 0.06 km/sec and the off-axis trajectory dispersion upon impact at the target was within $0^{o}\ 8^{1}$.

Other experiments were carried out to optimize barrel length and reservoir length in preparation for a large-scale gun experiment. These tests are reported in more detail in Reference 1. Attempts were made to accurately calculate the gasdynamic cycle of this gun design. These calculations were carried out using a one-dimensional Lagrangian code which could simulate area changes using the one-dimensional stream tube approximation. This code was later modified to include radial motion of the inner walls of the gun. These calculations were accurate to the degree that they could simulate the manner in which the reservoir walls yielded and expanded during the launch cycle and to the degree they could simulate the stopping process of the explosively-formed piston.

3.3 LAUNCHING OF A 3-INCH-DIAMETER SPHERE (SHOT 450)

A large explosive gun experiment was planned based on the design of the gun used in the trilogy experiment. The dimensions of the large gun were six times larger than the small-scale design.

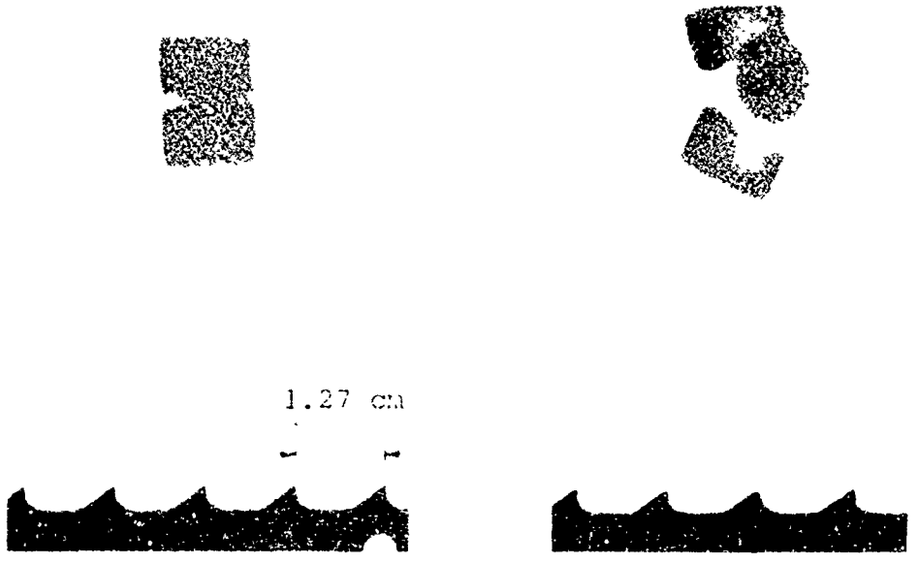

87 cm from muzzle 28 cm from muzzle

a. Sphere 5.03 km/sec

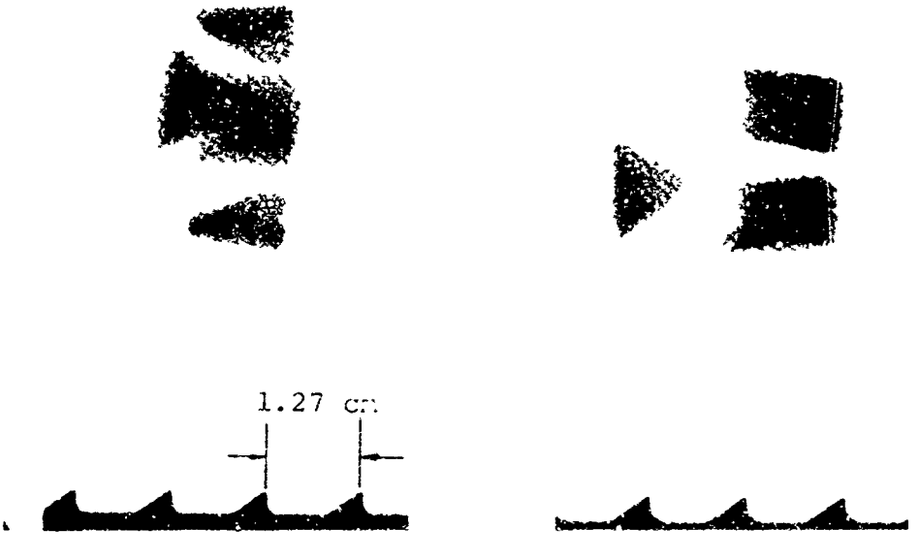

45 cm from muzzle 90 cm from muzzle

b. Cone at 5.18 km/sec

Figure 3.8 Radiographs of lithium-magnesium sphere and cone launched by explosively-driven gun.

3498

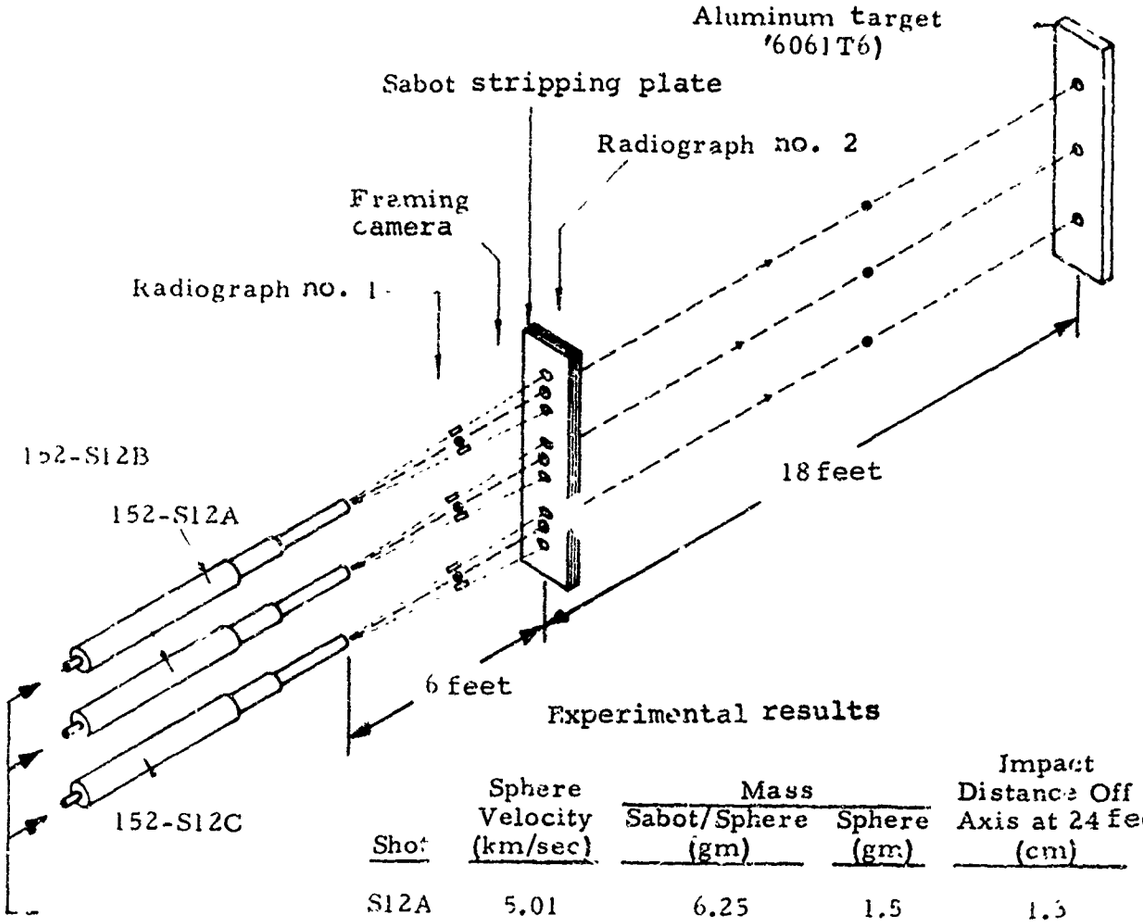

Experimental results

Shot	Sphere Velocity (km/sec)	Mass Sabot/Sphere (gm)	Mass Sphere (gm)	Impact Distance Off Axis at 24 feet (cm)
S12A	5.01	6.25	1.5	1.3
S12B	5.07	6.25	1.5	1.7
S12C	5.13	6.25	1.5	0.4

Figure 3.9 Experimental configuration used in the trilogy reproducibility and range accuracy experiment.

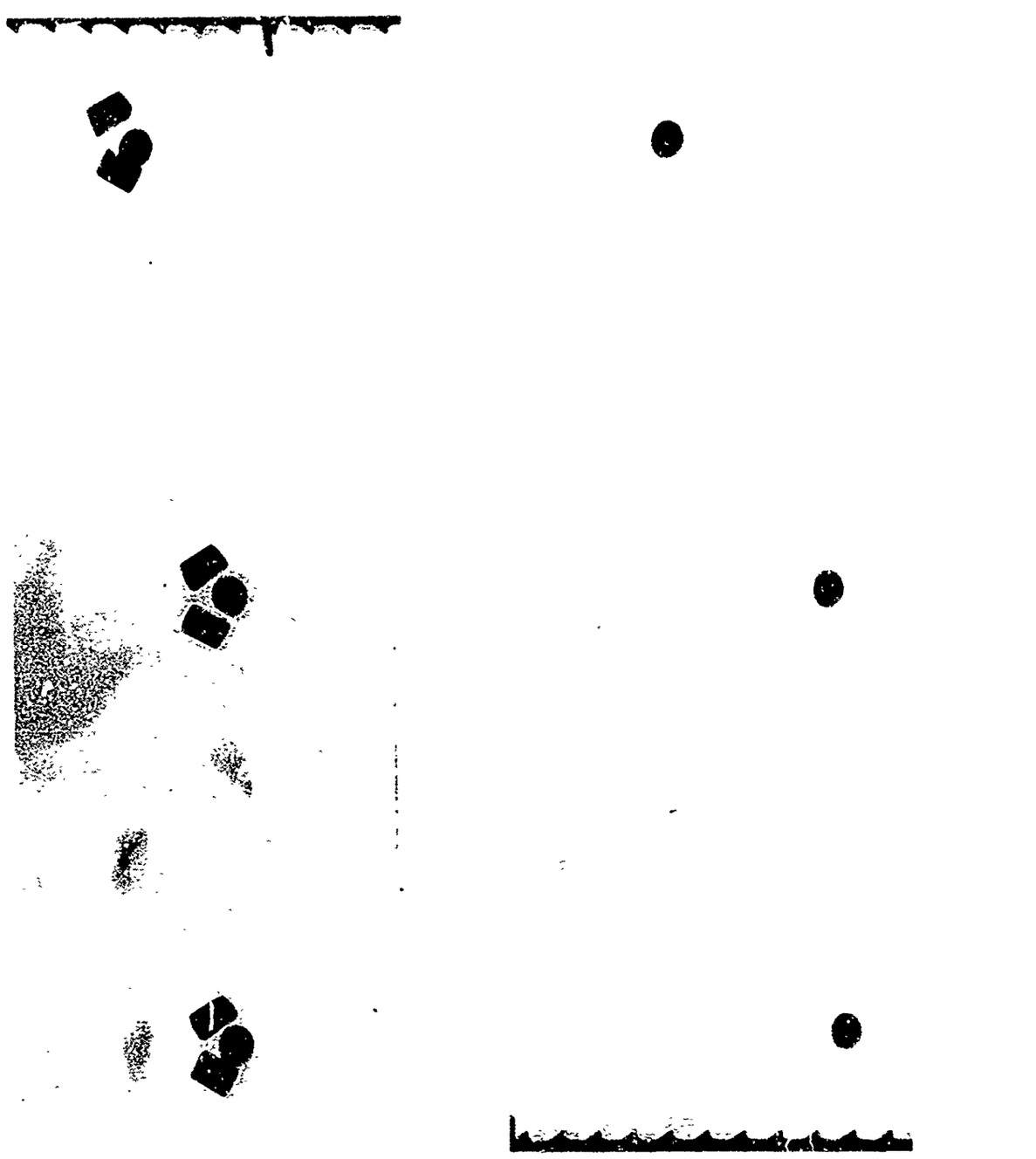

Note: Range atmosphere is air at 1 atmosphere.

Figure 3.10 Radiographs of sabots and spheres launched from identical guns in the trilogy experiment.

The gun was chambraged with a pressure tube-to-barrel area ratio of 3.17. This is only 85 percent of the corresponding ratio used in the small-scale experiments and was dictated by the limited choice of large commercial tubing. The driver gas-to-projectile mass ratio of the large gun was approximately 1.2; the 4.5-inch-diameter LA141A sabot and sphere weighed 1346 grams. The 3-inch-diameter sphere contained in the sabot weighed 346-grams. The barrel of the launcher was 15 feet long and the 18.5-foot-long driver contained 1200 pounds of nitromethane. The schematic layout of the experiment is illustrated in Figure 3.11.

The explosive driver was instrumented with piezoelectric and contact pins to monitor the shock wave trajectory and ionization pins to monitor the detonation wave (piston) trajectory. The condition and velocity of the sphere in free-flight were determined by two high-intensity, 600-kV Marx X-ray units. High-speed framing and streaking cameras were used to measure projectile velocity.

As shown in the range radiograph (Figure 3.12), the model was accelerated to 4.8 km/sec in excellent condition. The velocity was slightly lower than the anticipated 5.0 km/sec, probably because the pressure tube-to-barrel area ratio and reservoir thickness were not precisely scaled due to the limited selection of available large commercial tubing. The sphere was in excellent condition and only slightly elliptical (major to minor diameter ratio of 1.08) after launch. Part of this eccentricity can be attributed to ablation during flight down the range of atmospheric air. The sabot pieces separated properly in less than 16 feet, and the sphere impacted less than 6 inches from the center of the target, 232 feet downstream of the muzzle.

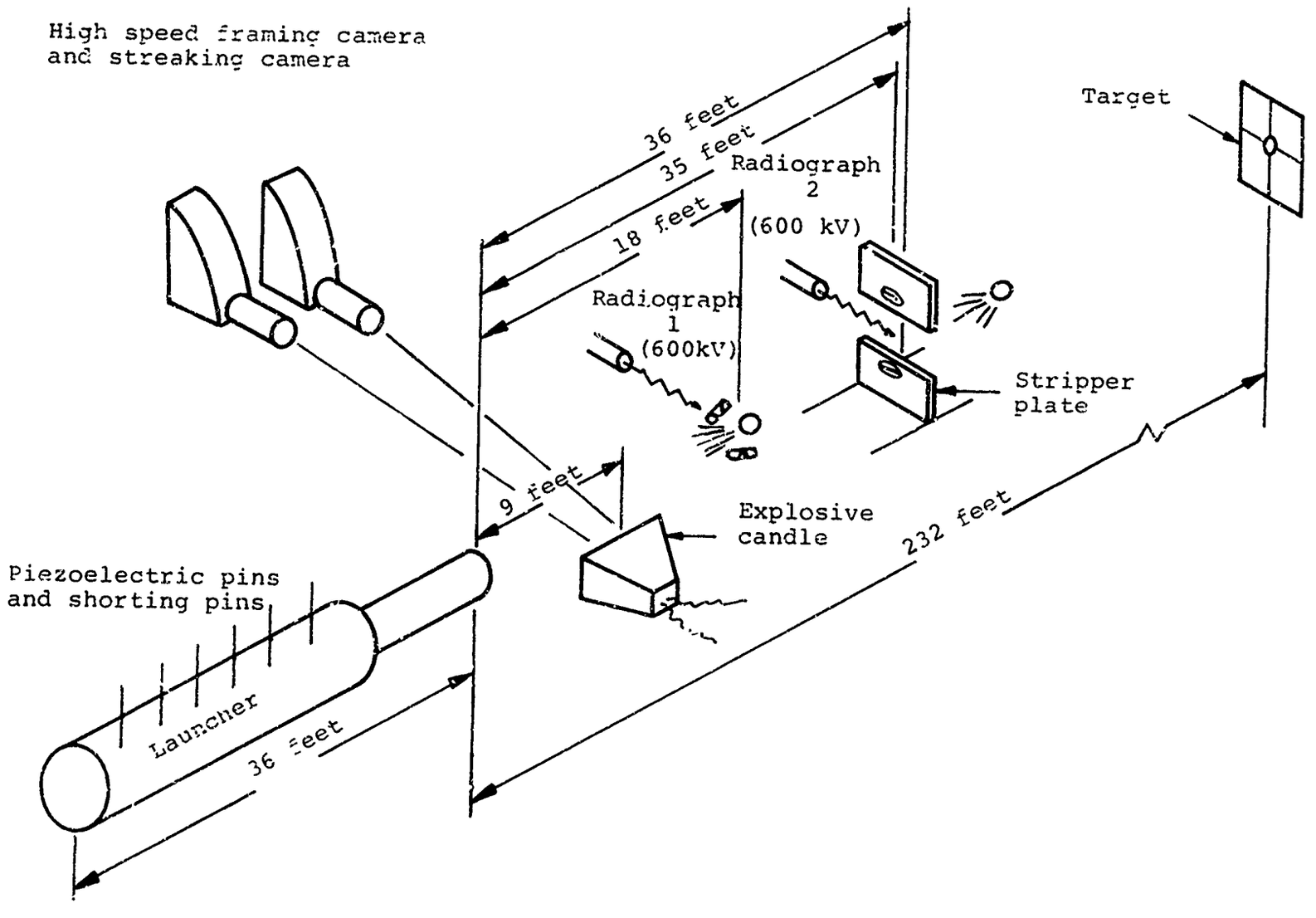

Figure 3.11 Range instrumentation layout in the experiment to launch a 3-inch-diameter sphere to 4.8 km/sec (Sabot 450).

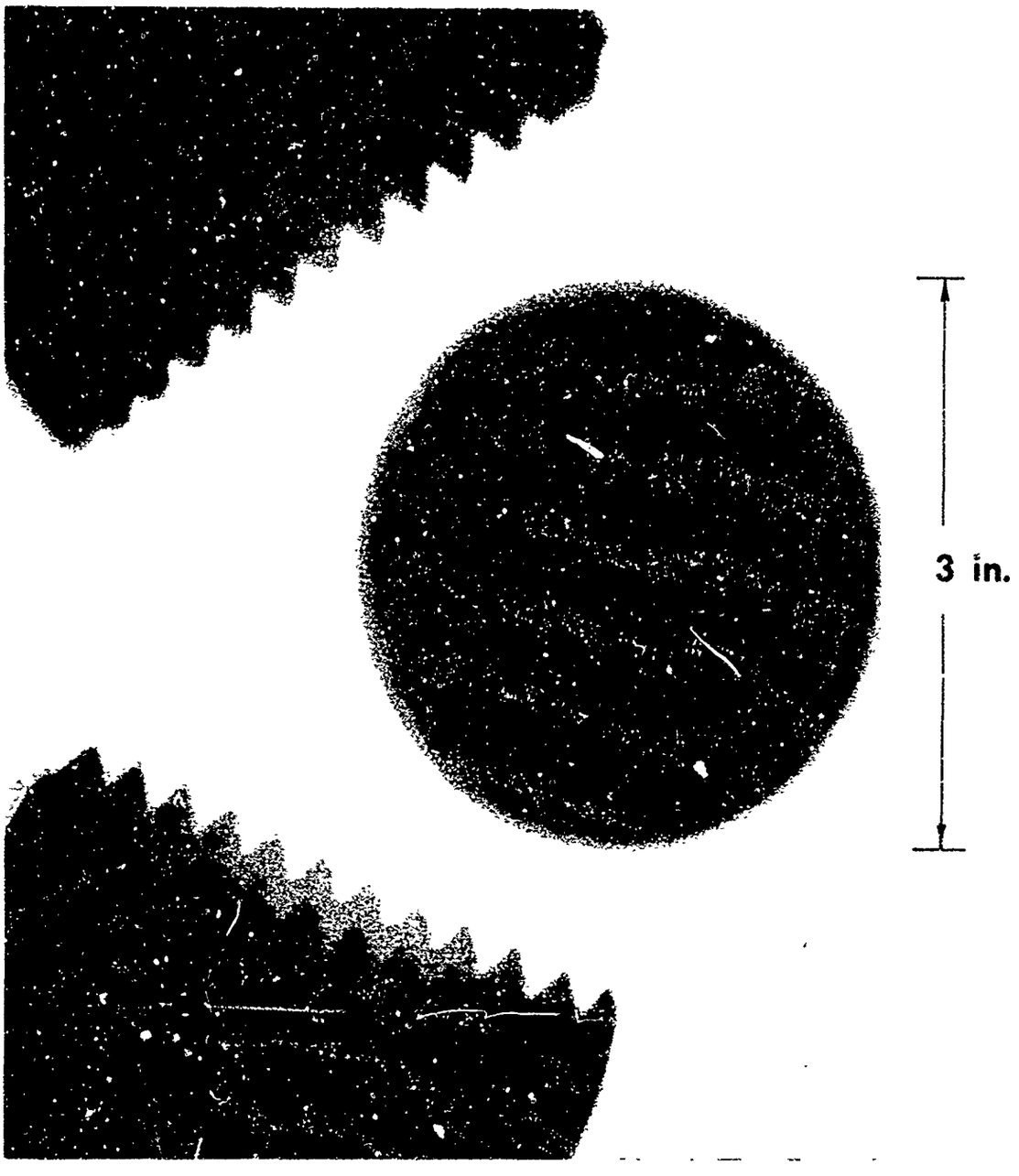

Figure 3.12 Range radiograph of sabot and 3-inch-diameter magnesium-lithium sphere launched to 4.8 km/sec (Shot 450).

The trajectories of the shock and detonation waves of the small- and large-scale experiments are shown in Figure 3.13a and b, respectively. The pressure tube diameter of the small driver was 1.37 inches, that of the large driver was 8 inches. The scalability of this driver design is evident in Figure 3.13c. This shows that in dimensionless coordinates the shock trajectories of the drivers are nearly identical. The start-up or piston formation, expressed as the time and distance required for the shock wave to appear ahead of the detonation wave, also scales.

In terms of explosive weight, this experiment was only one-third that of the first large-scale gun experiment (Shot 1000); the logistics of this experiment were correspondingly less complex than those of the first experiment.

3.4 SUMMARY

The successful firing of the second large-scale launcher demonstrated that explosively-driven guns could be used to launch complex saboted models to velocities in the vicinity of 5 km/sec. It also provided further evidence that the guns were scalable over a wide range of projectile masses with little variation in performance. The performance of this gun design was also shown to be reproducible and the range accuracy of explosive guns was established. During this phase of the program, insights were gained into the problem of projectile integrity by making use of advanced computer techniques. Understanding of the detailed operation of the explosive driver was increased substantially through various experimental and analytical programs. The ability to calculate and predict the performance of explosively-driven guns was demonstrated during this phase of the development. The choice of a chambraged gun geometry was reaffirmed, especially with the

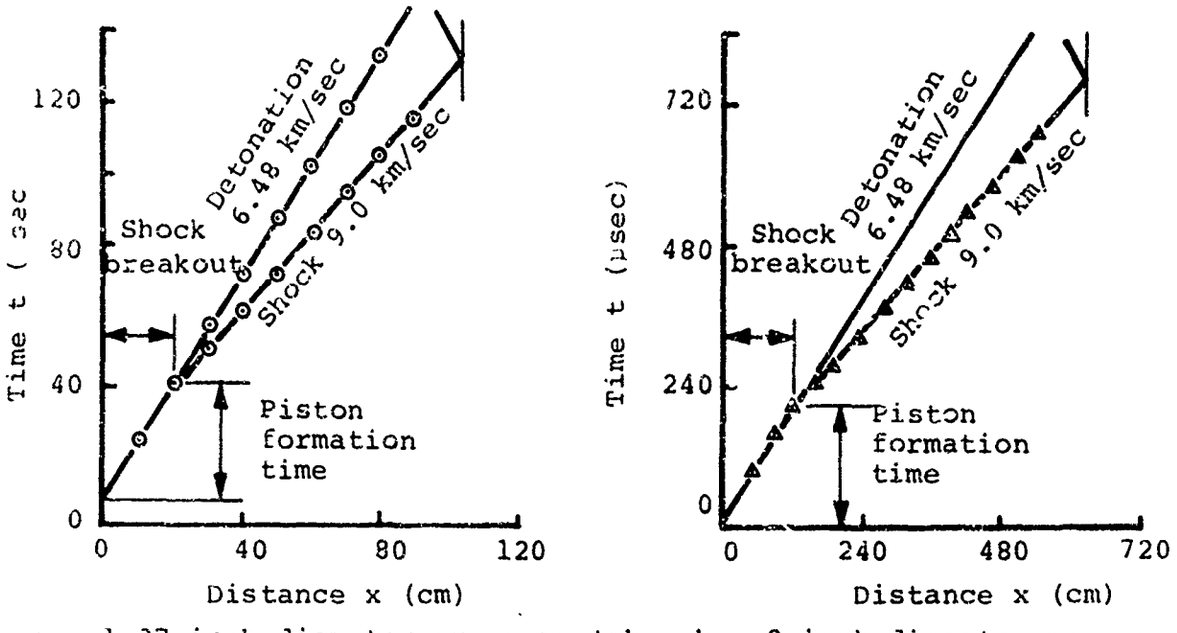

a. 1.37-inch-diameter pressure tube b. 8-inch-diameter pressure tube

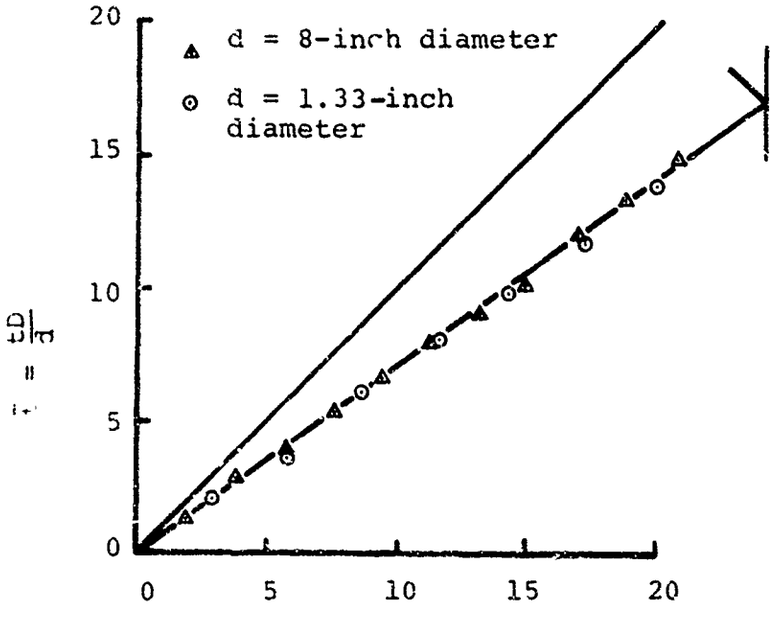

c. Dimensionless distance-time comparison

Figure 3.13 Scalability of explosive driver performance for 8-inch-diameter and 1.33-inch-diameter pressure tubes.

3472

emergence of the boundary-layer problem as a limit on the length of shocked gas generated by the explosive driver.

The principal area remaining to be investigated determines the gas-dynamic cycle required to launch slender cones since the length-to-diameter ratio of the projectile would have to be increased from 0.8 to about 1.66. The problem of decomposition of the driver explosive in large-scale drivers had been uncovered, but the full implications of this phenomenon were not yet realized.

During this period there was related progress made in another area. A two-stage explosive gun had proved successful in launching small projectiles to velocities that were considerably higher than reentry velocities. The two-stage gun design is basically a single-stage gun modified by surrounding the gun barrel with an explosive lens to form a second-stage piston. With the development of the explosive lens a wide range of second-stage piston trajectories, including a constant base pressure trajectory, became possible. An outline of this is presented in Appendix A.

SECTION 4

DETERMINATION OF THE GASDYNAMIC CYCLE TO LAUNCH A 6-INCH-BASE-DIAMETER SLENDER CONE TO 5.5 KM/SEC

This section describes the analytical and experimental investigations of the driver start-up process, the pressure tube expansion and the reservoir expansion. The purpose of these studies was to determine the gasdynamic cycle of a gun to launch slender cones to 5.5 km/sec. The problem of premature driver explosive decomposition is addressed and the method of overcoming this problem in large-scale explosive drivers is outlined.

4.1 INVESTIGATION OF DRIVER START-UP PROCESSES, PRESSURE TUBE EXPANSION AND RESERVOIR EXPANSION

In an explosive driver the start-up process is defined as the initial formation of the conical piston and the gasdynamics leading to the emergence of the driver shock. The time and distance in an x-t diagram at which the shock wave overtakes and passes the detonation wave are called the "breakout" coordinates. The start-up process has a direct effect on driver design since the driver must be lengthened by the "breakout" distance. Also, the emerging shock may be overdriven if the start-up gasdynamics are sufficiently violent and the shock may require substantial distance to recover its steady-state velocity.

To investigate start-up, several one-dimensional analytical models of the start-up process were proposed and the resulting start-up dynamics were calculated. Three start-up experiments were then carried out to test the accuracy of the analytical models. The simplest analytical model assumed the shock wave originated at the instant the conical piston was first formed and that it then moved at the ideal shock velocity. This model is discussed fully in Reference 3; it predicts a breakout distance of eight pressure tube diameters for a typical explosive driver design. However, this model does not conserve mass and therefore implies that (1) two-thirds of the gas mass is lost, (2) the density ratio behind the shock is three times the compression of a simple strong shock, or (3) that the density is not uniform everywhere. Another analytical model that does conserve mass was used to predict a breakout distance of 2.7 pressure tube diameters, or one-third of that predicted by the first analytical model.

The start-up experiments that are described in References 3 and 9 revealed the highly two-dimensional nature of the start-up process, which is further complicated by the formation of a small, transient metallic jet. The breakout distance observed in these experiments was about 4.3 pressure tube diameters, a value intermediate to those predicted by the one-dimensional analytical models.

Expansion of the pressure tube has been observed both directly by means of high-intensity flash radiography (Figure 4.1) and indirectly by its observed effect on the trajectory of the driver shock wave. In the design of drivers, especially high-pressure drivers, it is important to prevent excessive pressure tube expansion that could result in rupture of the pressure tube

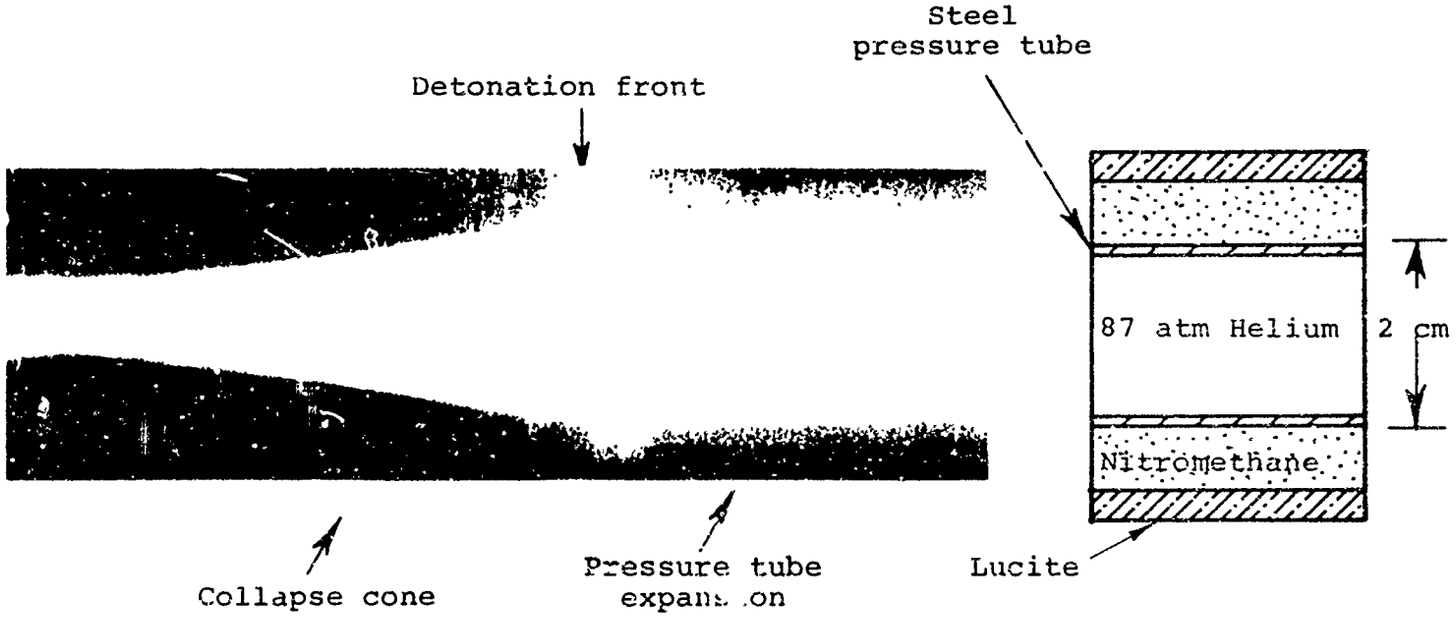

Figure 4.1 Flash radiograph of explosive driver operation showing expansion and collapse of the pressure tube (Shot 152-19).

and disruption of the operation of the driver. Also, in large-scale drivers the pressure tube may be fabricated in welded sections, and the design and placement of these welds require an understanding of the expansion process and a quanitative measure of expansion rates. An analytical and experimental investigation of this phenomenon is described in Reference 3. It was found that pressure tube expansion could be best calculated by employing the Physics International one-dimensional Lagrangian code, POD, in cylindrical geometry, assuming that the driver gas pressure remains constant (Figure 4.2). This method accounts for the wave nature of the expansion process (the expansion rates are comparable to the material sound velocities) and can quantitatively evaluate the effect of thick-walled, explosive-containing tubes to elastically or inertially control the rate of expansion. For design purposes, the driver parameters are chosen to keep pressure tube expansion below 30 percent. Experiments have shown that no rupture occurs below these expansions for the driver designs used in most launchers.

The reservoir section of an explosively-driven gun is usually made from a thick-walled steel or lead cylinder. Since the moving column of gas generated by the driver is brought to rest in the reservoir by the reflection of a strong shock, the reservoir must contain the full stagnation pressure of the gas. These pressures are typically an order of magnitude greater than the strength of the reservoir material. Therefore, it is inevitable that the inner reservoir walls expand and the rate of expansion has a major limiting effect on the performance of the gun. High-speed framing and streaking cameras have been used to measure outer reservoir wall expansion during the critical phases of the launch cycle (Figure 4.3) and these observations

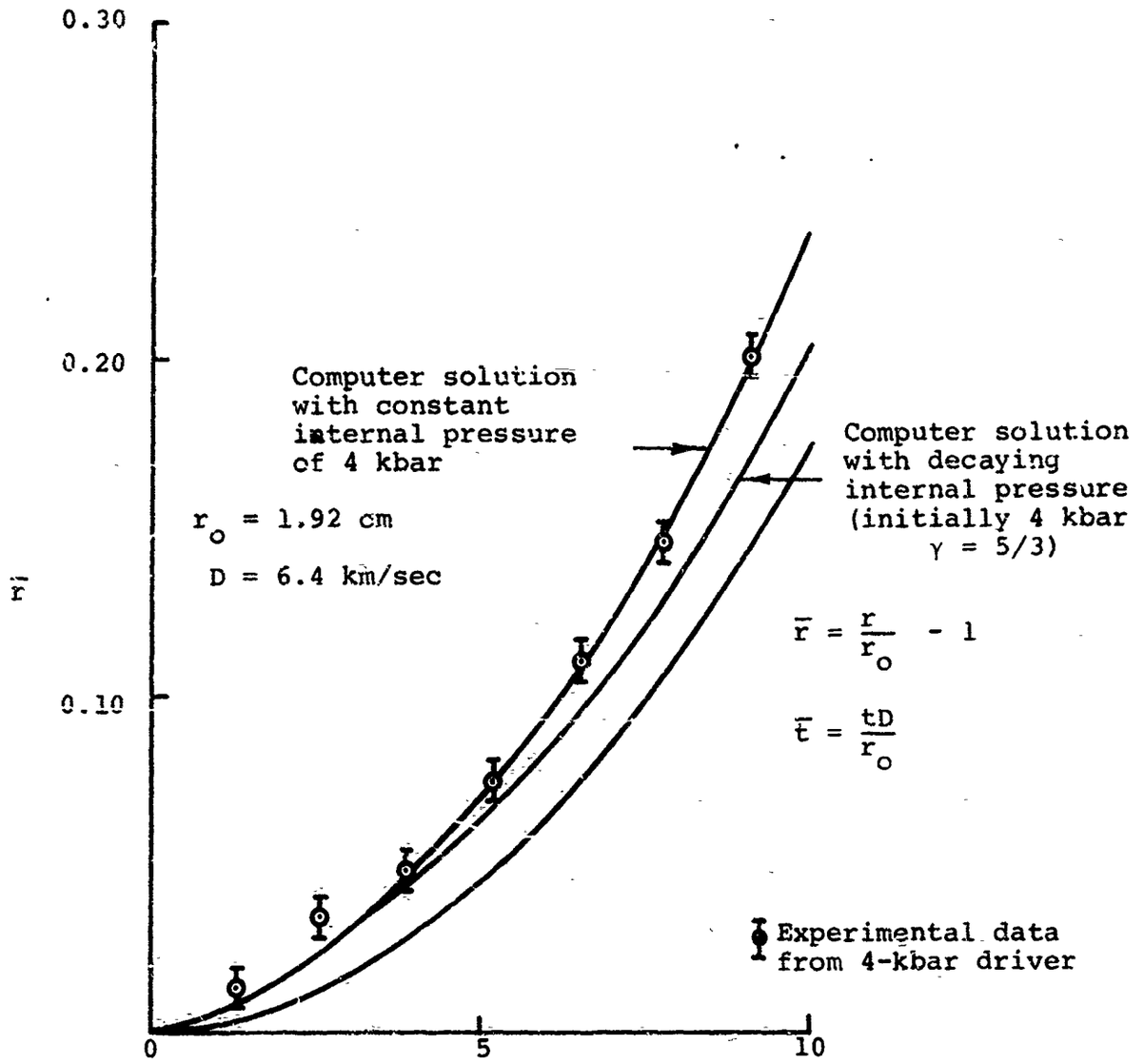

Figure 4.2 Radial expansion histories for an explosive driver (observed and calculated solutions for a 4-kbar untamped driver).

5806

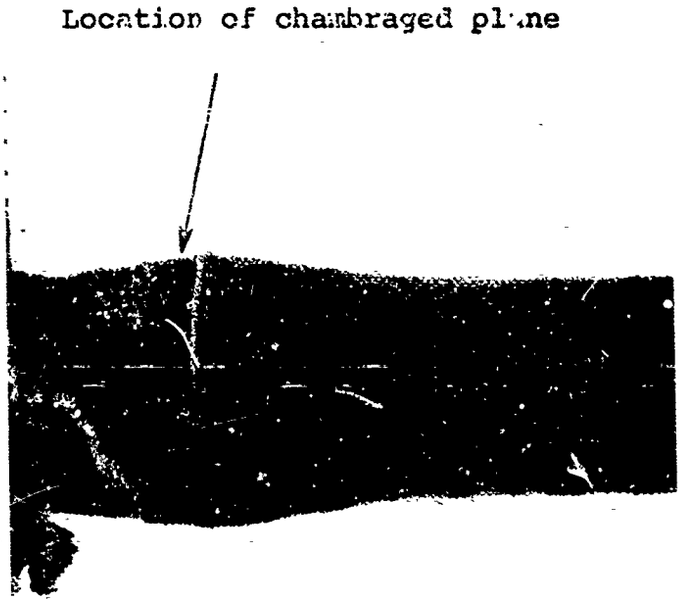

Note: The 0.750-inch-diameter, 0.600-inch-long projectile had accelerated for 59 μsec when this picture was taken. The projectile is in the barrel for a total of 177 μsec.

Figure 4.3 High-speed framing camera record of reservoir expansion (Shot 351-2).

have been correlated to inner wall expansion using the Physics International one-dimensional Lagrangian code in cylindrical geometry (Figure 4.4). These experiments and calculations are especially important in the design of large-scale guns where it is necessary to know how much reservoir material is really effective in controlling expansion and whether other materials such as lead or concrete would be suitable alternatives. For instance, these studies have shown that for the high reservoir pressures (20 to 40 kbar) used in most gun programs, lead or

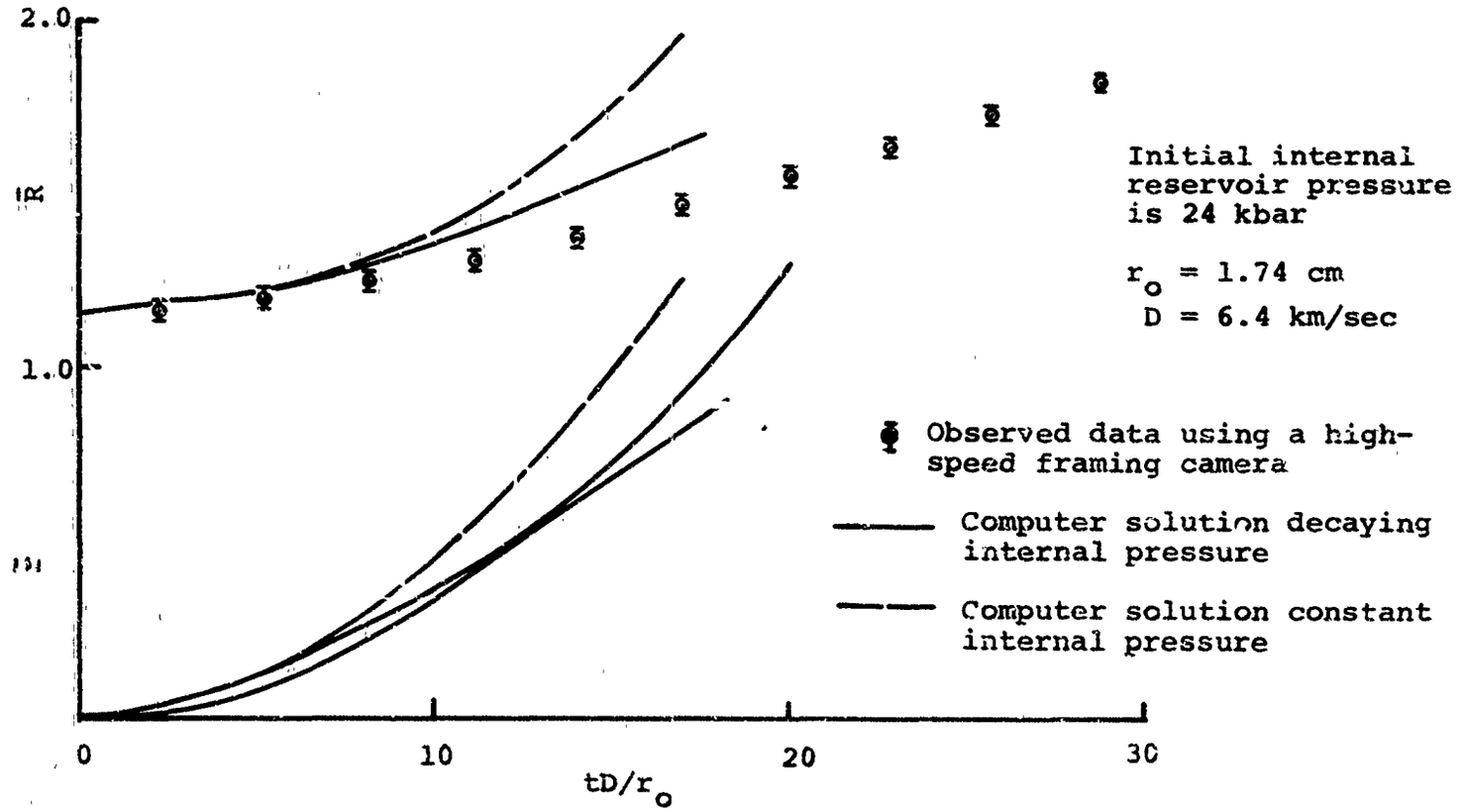

Figure 4.4 Dimensionless radius-time plot of reservoir expansion

steel are equally suitable and concrete is unacceptable. They have also shown that inner wall expansions of up to 50 percent can have an important effect on the final velocity of the projectile and imply that any major rupture of the inner walls during this period could seriously affect gun performance.

Calculations and experiments were also made to investigate the use of explosives in controlling reservoir expansion. This technique, referred to as dynamic confinement, is illustrated in Figure 4.5 and discussed fully in Reference 3. It was found that while the technique worked for guns in which the projectile accelerated rapidly to velocities greater than the sound velocity of the reservoir material, the concept was not workable in the reentry gun, whose projectile velocity never exceeded the reservoir material sound velocity. In this case, the transient stress wave generated by the reservoir explosive could overtake and damage the projectile. This was confirmed experimentally (Reference 3).

4.2 SMALL-SCALE GUN EXPERIMENTS TO LAUNCH SLENDER CONES TO 5.5 KM/SEC

Several experiments were carried out to improve the performance of the gun to launch slender cones to higher velocities. The explosive driver was redesigned with the new design data on start-up processes and pressure tube expansion to generate a 6.5 kbar driver shock by increasing the initial gas pressure to 920 psi. Nitromethane continued to be used as the driver explosive because of its low cost and ease of handling.

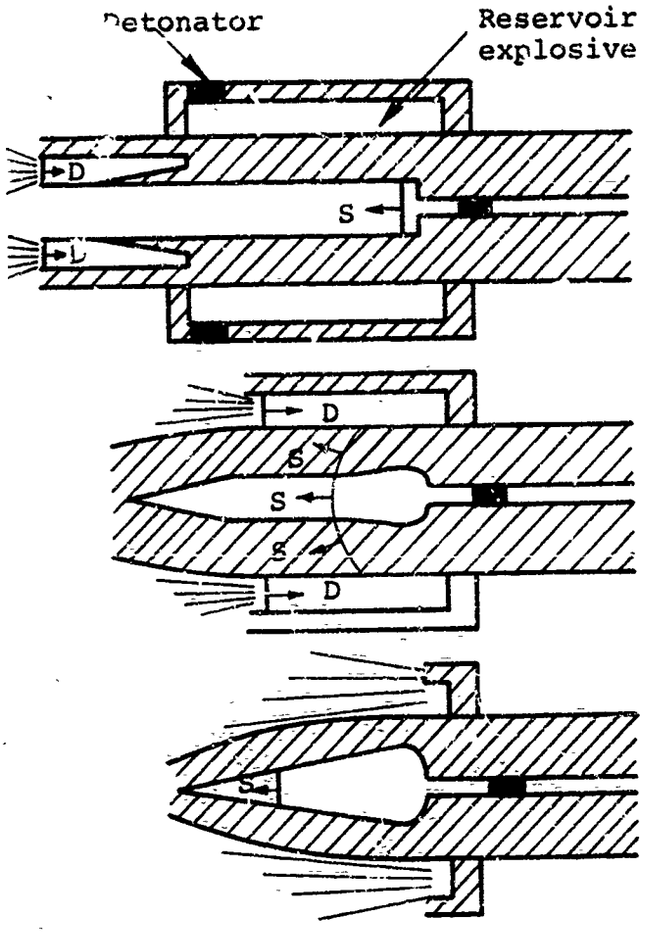

Shock reflects from area change generating pressures well above the yield strength of the steel.

Reservoir explosive is initiated as the reservoir walls begin to expand.

Reservoir explosive has forced the reservoir walls inward.

Figure 4.5 Schematic operation of a dynamic confinement technique to contain a high-pressure reservoir.

In preliminary small-scale experiments lithium-magnesium projectiles with a length-to-diameter ratio of 1 were accelerated to 6.3 km/sec, and the saboted cones were launched in good condition. Lead and steel reservoir designs were tested with little variation in overall gun performance. An intermediate-scale gun (145-gram projectile) was successfully fired (Figure 4.6). However, the velocity of 5.7 km/sec was slightly lower than anticipated. The loss of performance was attributed to imprecise scaling of the reservoir thickness and pressure tube-to-barrel area ratio.

In subsequent small-scale experiments the length-to-diameter ratio of the projectile was increased to 1.66; the launch velocity observed in these tests was 5.5 km/sec. Several experiments were carried out to evaluate the use of explosives to control reservoir expansion, but this technique could not be made workable (Reference 3). The design of the cone and its sabot was optimized during these experiments. Based on the guidelines set forth in the projectile integrity studies, the saboted model was constrained to be a right-circular cylinder of constant density. Therefore, optimizing the design of the cone and sabot consisted of trying to maximize the cone base diameter-to-sabot diameter ratio while minimizing distortion of the cone. It was found that cones with base diameters up to 0.85 of the sabot or barrel bore diameter could be launched successfully (Figure 4.7).

In some of these experiments, the design of the nozzle coupling the reservoir to the barrel was investigated. Normally, the base of the projectile was initially located two barrel diameters downstream of the nozzle inlet. Calculations of the initial two-dimensional gas flow into the nozzle and supporting experiments suggested that the projectile could be

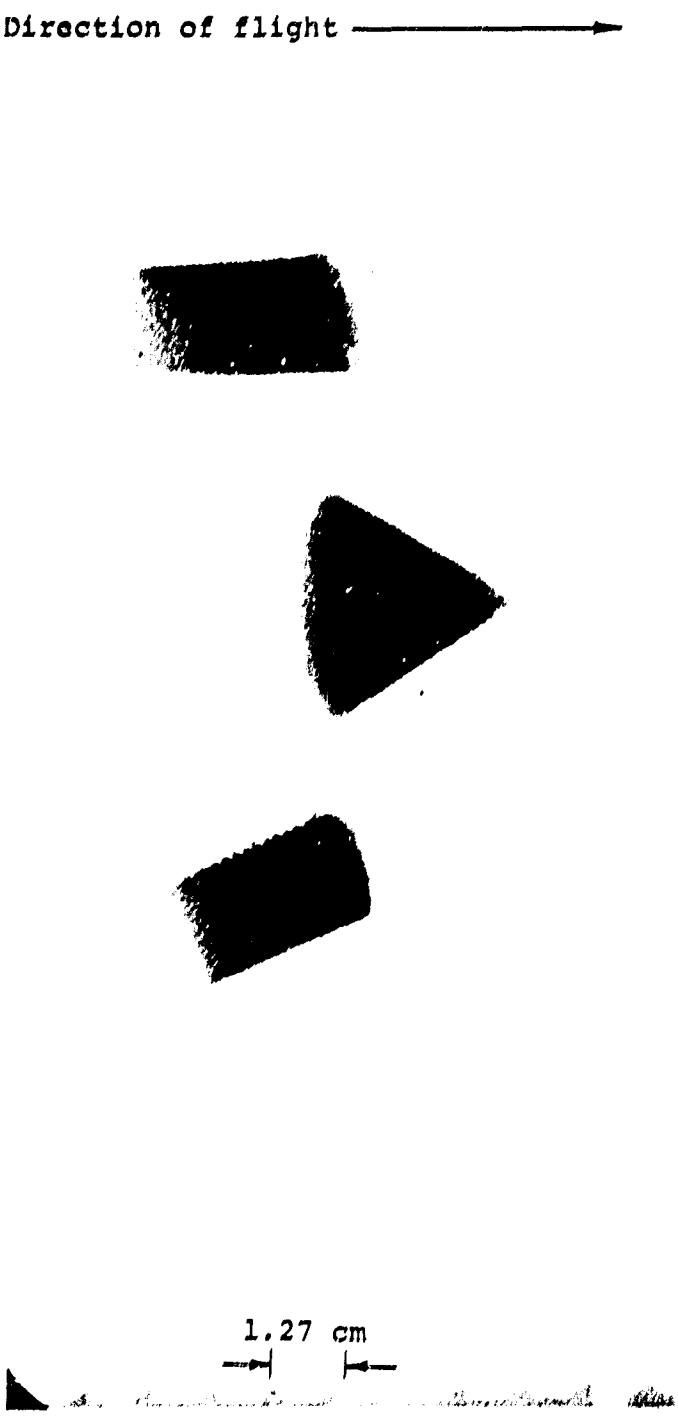

Figure 4.6 Radiographs of a 2-inch-diameter cone launched to 5.65 km/sec by an explosively-driven gun (Shot 351-9).

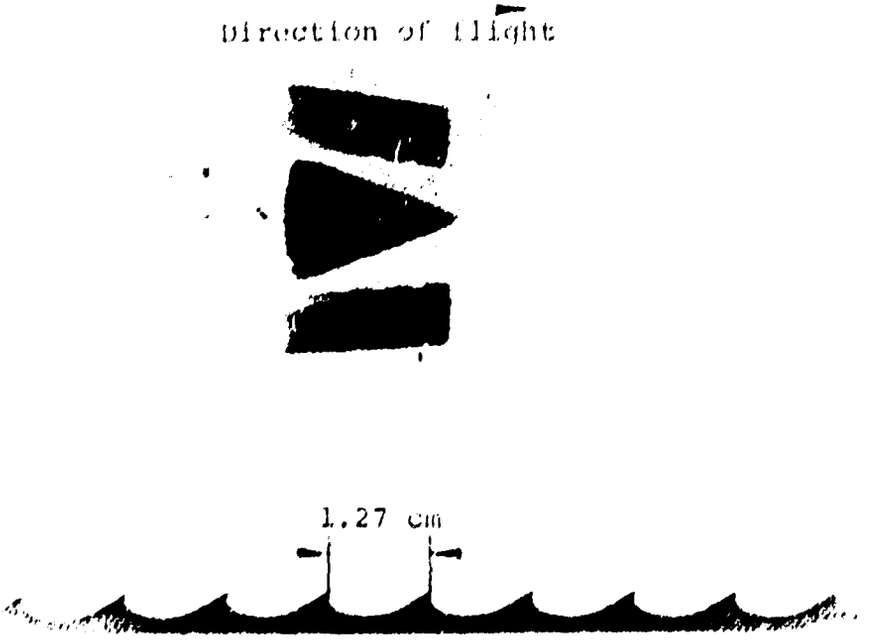

Note: The pusher plate has not been separated from the cone.

Figure 4.7 Range radiograph of a scale model of the cone to be launched by the ALPHA-I gun (Shot 351-19).

launched with less overall deformation by placing the base of the model three diameters downstream of the nozzle inlet. This apparently small change in initial projectile location would result in a more uniform radial distribution of pressure during the initial projectile acceleration when pressures were highest. The resultant shear stresses in the projectile would be less and the deformation of the projectile would be reduced. This was confirmed experimentally (Figure 4.8). There was, however, an

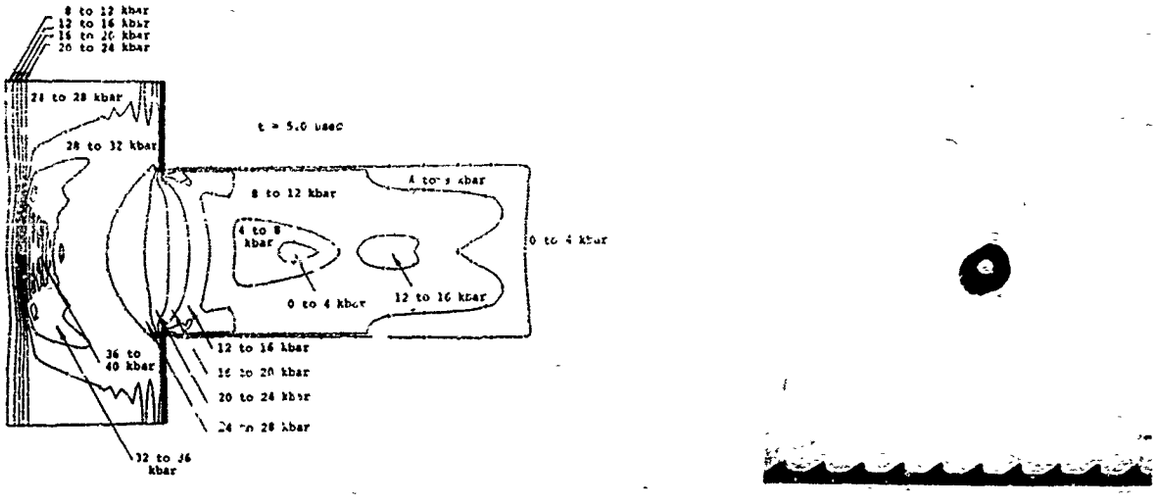

a. Projectile in flight that was initially located two diameters downstream of the area change. The calculated pressure distribution at the beginning of acceleration is shown.

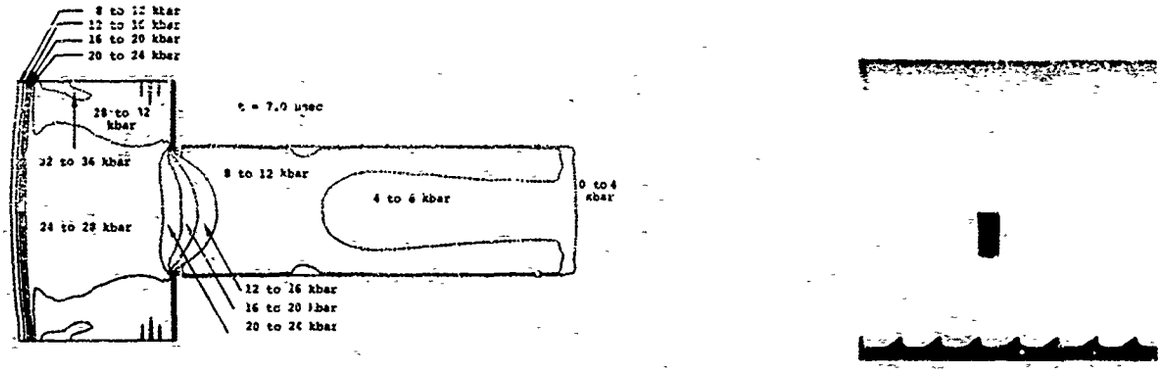

b. Projectile in flight that was initially located three body diameters downstream of the area change. The calculated pressure distribution at the beginning of the acceleration is shown.

Figure 4.8 Two-dimensional gasdynamics at an area change in the breech section of a gun with a 6-kbar driver.

unexpected decrease in launch velocity which has never been fully explained. Since the loss of performance (up to 25 percent) more than cancelled the improvement in projectile condition, this change was never incorporated and the initial position of the base of the projectile remained at two barrel diameters downstream of the nozzle inlet. Since most of the deformation of the projectile was confined to the base plate of the sabot, this was considered acceptable.

4.3 THE PROBLEM OF PREMATURE DECOMPOSITION OF THE DRIVER EXPLOSIVE

During the period of pressure tube expansion in an explosive driver the explosive is put through a rapid compression cycle. If a thick-walled steel tube surrounding the explosive is used to control expansion, then the pressures developed in the explosive may exceed the driver gas pressure by nearly a factor of two because of wave reflections from the surface of the outer tube (Figure 4.9). For a 6-kbar driver, then, the explosive is compressed to nearly 12-kbar prior to arrival of the programmed detonation wave. In this environment the explosive may begin to decompose or in some cases even pre-detonate. Because this is a nonscalable chemical process, the operation of large-scale drivers could be seriously affected. Other investigations (Reference 10) have reported this phenomenon in nitromethane exposed to pressures of 10 kbar for hundreds of μsec. Our own experience with large drivers (Reference 3) has suggested the possibility of premature explosive decomposition; well-documented, small-scale drivers using sensitized nitromethane have actively exhibited pre-detonation (Figure 3.5).

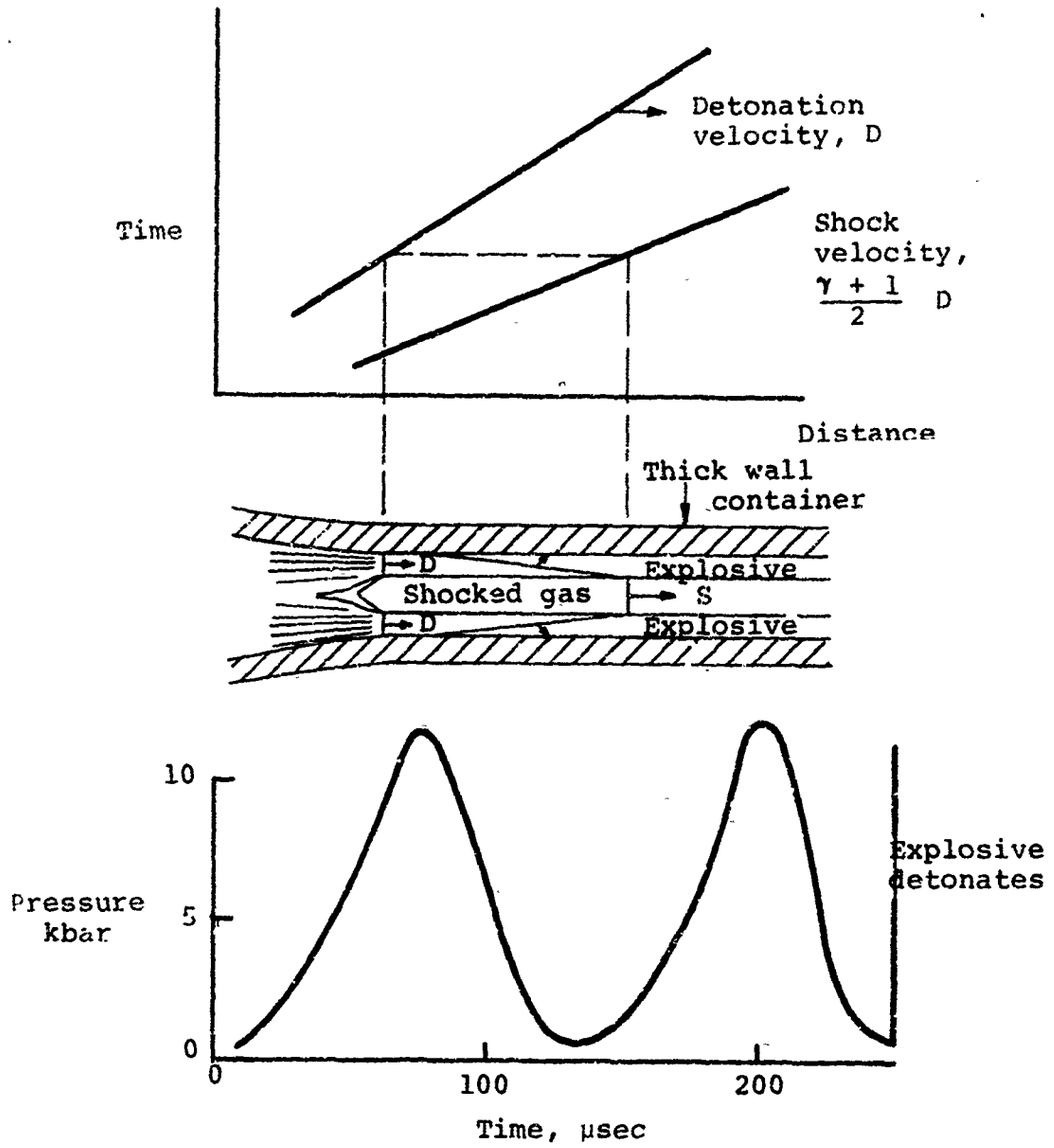

Figure 4.9 Calculated pressure environment in an 8-inch explosive driver (similar to the ALPHA-1/2 driver).

Before designing, building and testing a large-scale gun to launch a slender cone to reentry velocity, an analytical and experimental program was undertaken to determine whether the problem of explosive decomposition would affect the performance of a 16-inch-diameter, 6-kbar driver and, if so, how this premature decomposition could be suppressed. A redesign of the driver and gasdynamic cycle of the gun to circumvent the decomposition problem was considered, but this approach was rejected because of the cost, schedule, and technology limitations (Reference 3).

Early analytical investigations found that, based on an Arrhenius reaction-rate theory and extrapolated data at 80 kbar, nitromethane below 20 kbar should not react significantly for several hundred seconds. From out experiments and the limited work of others to the contrary, it was therefore concluded that a new mechanism of initiation described in terms other than an Arrhenius reaction theory was dominating the behavior of the nitromethane. A number of possible alternative physical mechanisms were proposed and all but one of these mechanisms were rejected on the basis of analysis or experiments (Reference 3 and 4).

The one proposed mechanism that appeared to satisfy the limited data was the adiabatic compression of minute gas-filled bubbles to high temperatures and the subsequent initiation of a reaction at the bubble surface. Isentropic compression of a real air (Reference 11) results in a temperature of approximately 2700 K, well above the temperature necessary to ignite nitromethane in a few microseconds. Further analysis (Reference 4)

of the thermochemical behavior of the nitromethane gas bubble system lead to the conclusion that bubbles as small as 10^{-4} cm could give rise to significant chemical reaction in a few microseconds in the 10-kbar environment.

Bubbles of this size would be extremely difficult to remove in a large-scale driver in the field, therefore a simple method of overcoming the problem was sought. Since the decomposition of nitromethane is still ultimately governed by the exponential Arrhenius reaction rate, relatively small changes in the compression ratio of the bubbles would result in an increase in chemical induction times of several orders of magnitude. Therefore, the simplest solution seemed to be pre-pressurization of the explosive to reduce the bubble compression ratio. The effect of this on chemical induction time of the nitromethane is shown in Figure 4.10 for a pre-pressurization of 40 atmospheres or a reduction of the bubble compression ratio by a factor of 40.

Experimentally, it would have been desirable to investigate the problem in the environment generated by a large-scale explosive driver. However, this approach was rejected because of the excessive cost per experiment and the unknown number of experiments that might be necessary to resolve the problem. An inexpensive test chamber that would simulate the driver explosive environment was then conceived and developed as an alternate method of studying the pre-initiation problem. The design and performance of this chamber are described in detail in Reference 3.

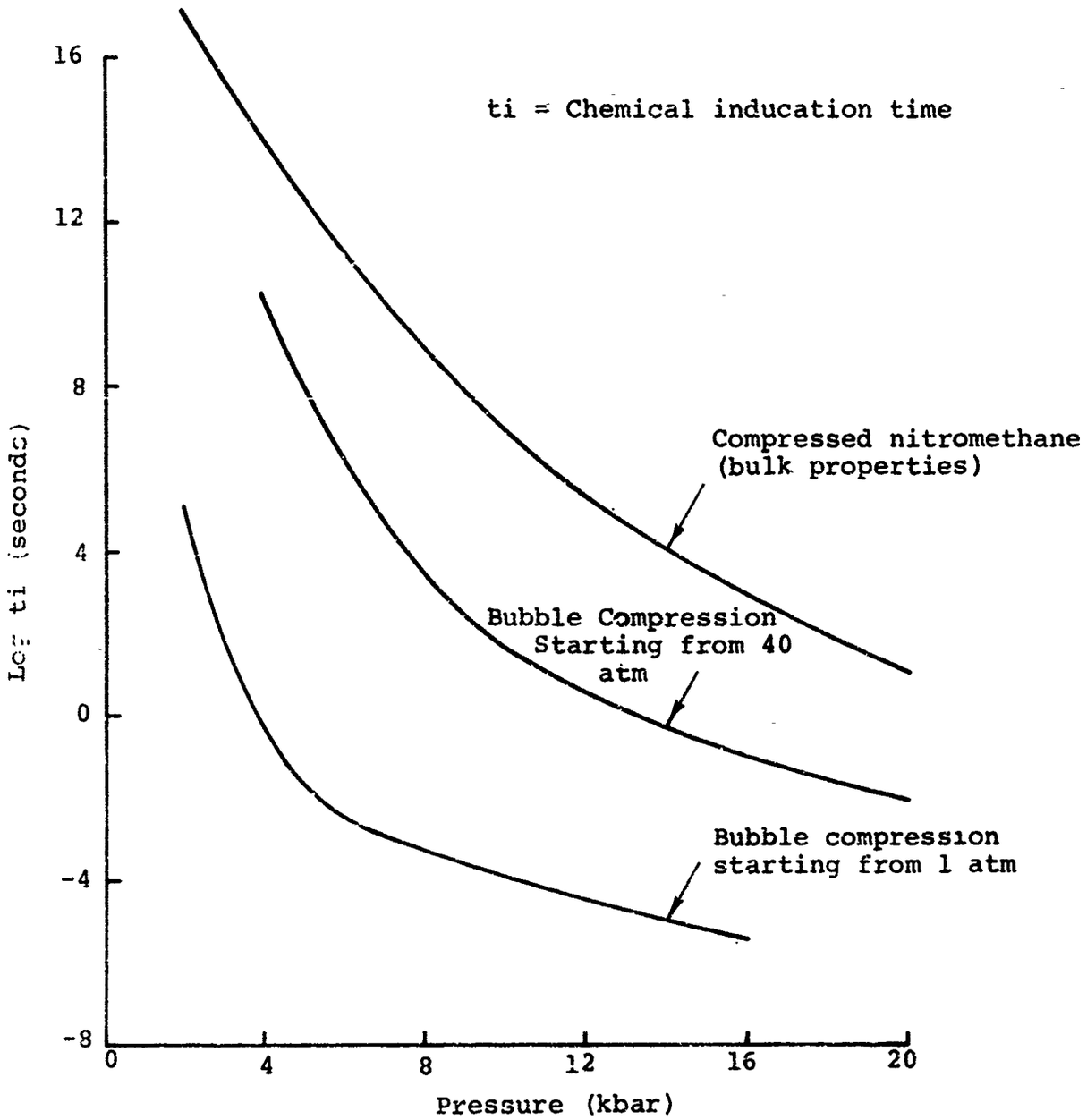

Figure 4.10 Chemical induction time as a function of pressure for real air bubbles greater than 10^{-4}-cm diameter.

5019

Several attempts were made to measure long-term pressure histories (10-20 kbar for hundreds of μsec), but these attempts met with limited success because of the difficulty in keeping the diagnostics intact for long periods of time in such a hostile environment. However, strain gages mounted on the outside of the chamber did indicate that both sensitized and unsensitized nitromethane began to decompose over a period of several hundred microseconds (Figure 4.11) and that the decomposition could be suppressed by pre-pressurizing the explosive.

4.4 SUMMARY

The investigations into driver start-up pressure tube expansion, and reservoir expansion led to a better understanding of driver and gun performance. By eliminating many of the unknowns in driver and reservoir operation, considerable savings in the material costs of large-scale guns were made possible. The basic gasdynamic cycle for launching slender cones to 5.5 km/sec was developed during this period and improved techniques for saboting the cones were successfully tested.

Much of the effort during this period was diverted to investigating the premature decomposition of nitromethane in an explosive driver environment. This problem was unanticipated and ultimately required a large effort to overcome. Adiabatic compression of trapped bubbles in the nitromethane was found to be the mechanism of premature decomposition; pre-pressurization of the driver explosive was proposed as a means of overcoming the problem.

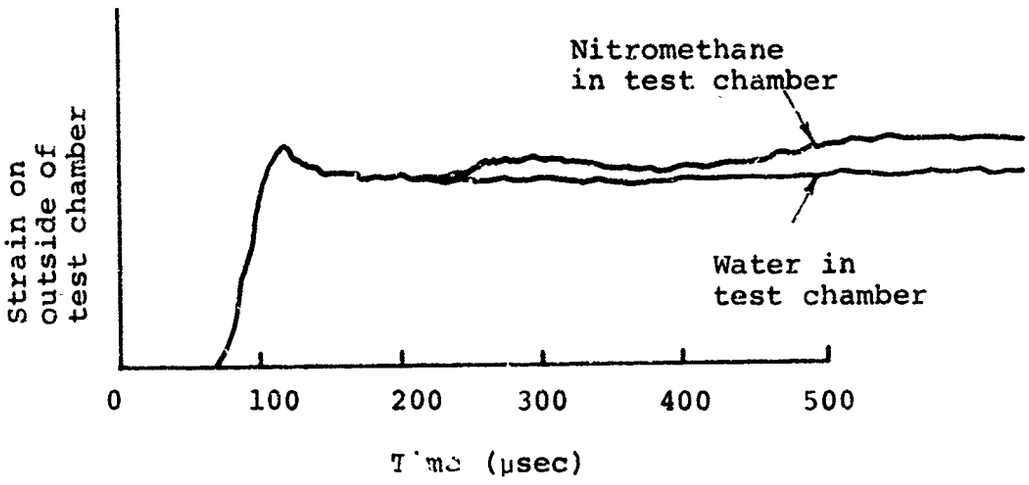

a) Apparent slow decomposition

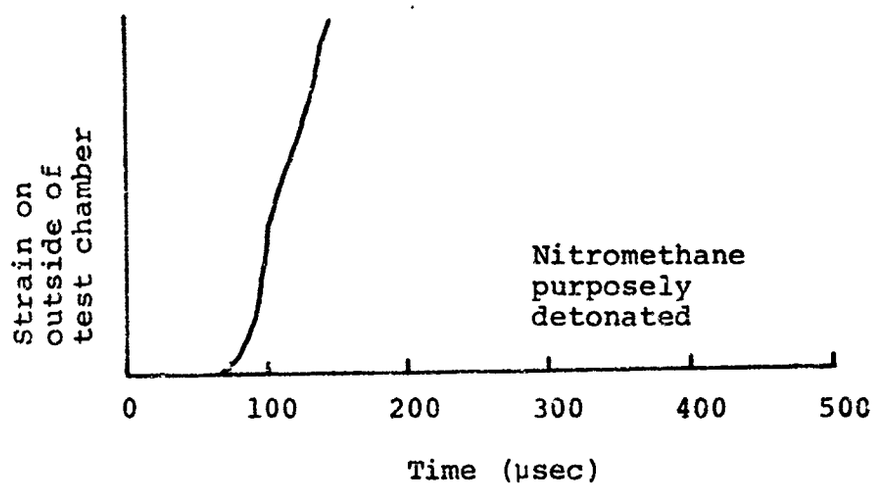

b) Detonation

5020 Figure 4.11 Strain gauge response for a slow decomposition and for a detonation in the test chamber.

Planning for a large gun to launch a 6-inch-base-diameter cone experiment, ALPHA-I, was initiated during this period. Based on the small-scale experiments, preliminary designs of the driver, reservoir, projectile, and barrel were put forth and suppliers of large-diameter tubing were sought.

A pre-proposal brief outlining the preliminary design and costing of a large ballistic range facility was submitted during the period. The range itself was to be 1500 feet long and was to allow testing and diagnosing of 6-inch-base-diameter cones in various atmospheres including simulated dust and rain environments. A unique feature of this facility is a large protective berm to isolate the gun and explosive from the instrumented range. A brief discussion of this facility is presented in Appendix B.

Before testing a large-scale gun to launch a 6-inch-base-diameter slender cone to reentry velocities, it remained to test the solution of the explosive decomposition problem in a large driver experiment. The detailed design of the ALPHA-I gun, the logistics of the experiment, and final small-scale testing of the gun design were the principal tasks remaining.

SECTION 5

DESIGN AND TESTING OF THE ALPHA-1 GUN TO LAUNCH A 6-INCH-BASE-DIAMETER SLENDER CONE

This section describes (1) the large driver experiment to verify that pre-pressurization of the driver explosive is a solution to the problem of premature explosive decomposition; (2) small-scale gun experiments which establish the final configuration and method of construction of the ALPHA-I gun; and (3) the design, construction, experimental logistics, and firing of the ALPHA-I gun.

5.1 LARGE EXPLOSIVE DRIVER EXPERIMENT WITH PRE-PRESSURIZED EXPLOSIVE

A large driver experiment was designed to test the effect of pre-pressurizing the driver explosive to 640 psi (43.5 atmospheres) for suppressing premature decomposition of the nitromethane. The driver design used in this experiment was based on the results of an analytical driver optimization study to minimize the weight of explosive while maintaining pressure tube expansion within the acceptable limits (less than 30 percent) and ensuring proper collapse characteristics. In the analytical study, the Physics International one-dimensional POD code was used to calculate in cylindrical geometry the expansion and collapse of the pressure tube (Figure 5.1). A constant pressure corresponding to the driver pressure is applied to the inner surface of the pressure tube. The explosive, described by its unreacted liquid equation-of-state, is compressed by the expanding pressure tube until the appropriate

Initial inside diameter of the pressure tube is 8-inches. Internal pressure is 6 kbar.

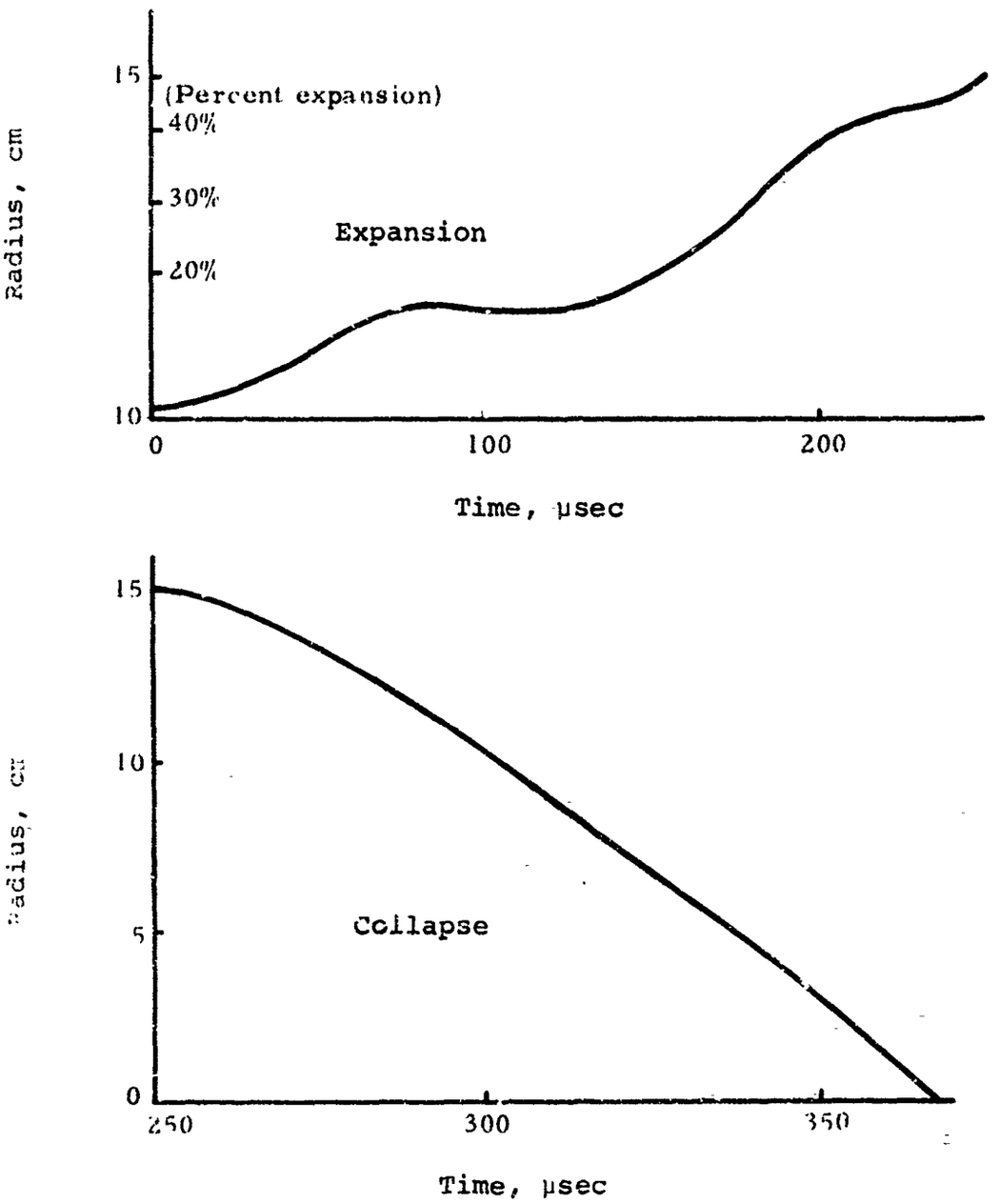

Figure 5.1 Calculated expansion and collapse histories for the inside of the pressure tube for the ALPHA-1/2 driver.

time, when it is "detonated" by changing its equation-of-state to a reacted explosive products description. The pressure tube is now forced to collapse by the high-pressure explosive products. The expansion phase of the calculation is quite accurate (Reference 3). The collapse phase of the calculation is not quantitatively valid; however, the qualitative effect of varying the parameters is valid with this technique.

Using this method the pressure tube dimensions of the optimized driver used to test the pre-pressurized explosive were an 8.50-inch OD and 8.00-inch ID. The overall length of the driver was 33 feet, the initial helium gas pressure was 920 psi, and the driver contained 1275 pounds of nitromethane.

Before implementing the large driver experiment, a one-quarter scale (2-inch-ID pressure tube) driver was tested to determine the wave dynamics and behavior of the optimized driver design. The results of this test are shown in the x-t plane (Figure 5.2) and indicate near-ideal driver operation. The shock trajectory was determined by piezoelectric pins, barium titanate crystals, and capped shorting pins. The detonation wave trajectory was determined by strain gauges, barium titanate crystals, ionization pins, and a high-speed framing camera. As seen in Figure 5.2, the strain gages, barium titanate crystals, and ionization pins sometimes report the arrival of the detonation wave earlier than expected. However, the unambiguous optical records demonstrated that the behavior of the other diagnostics that were exposed to the high-pressure environment could be erroneous.

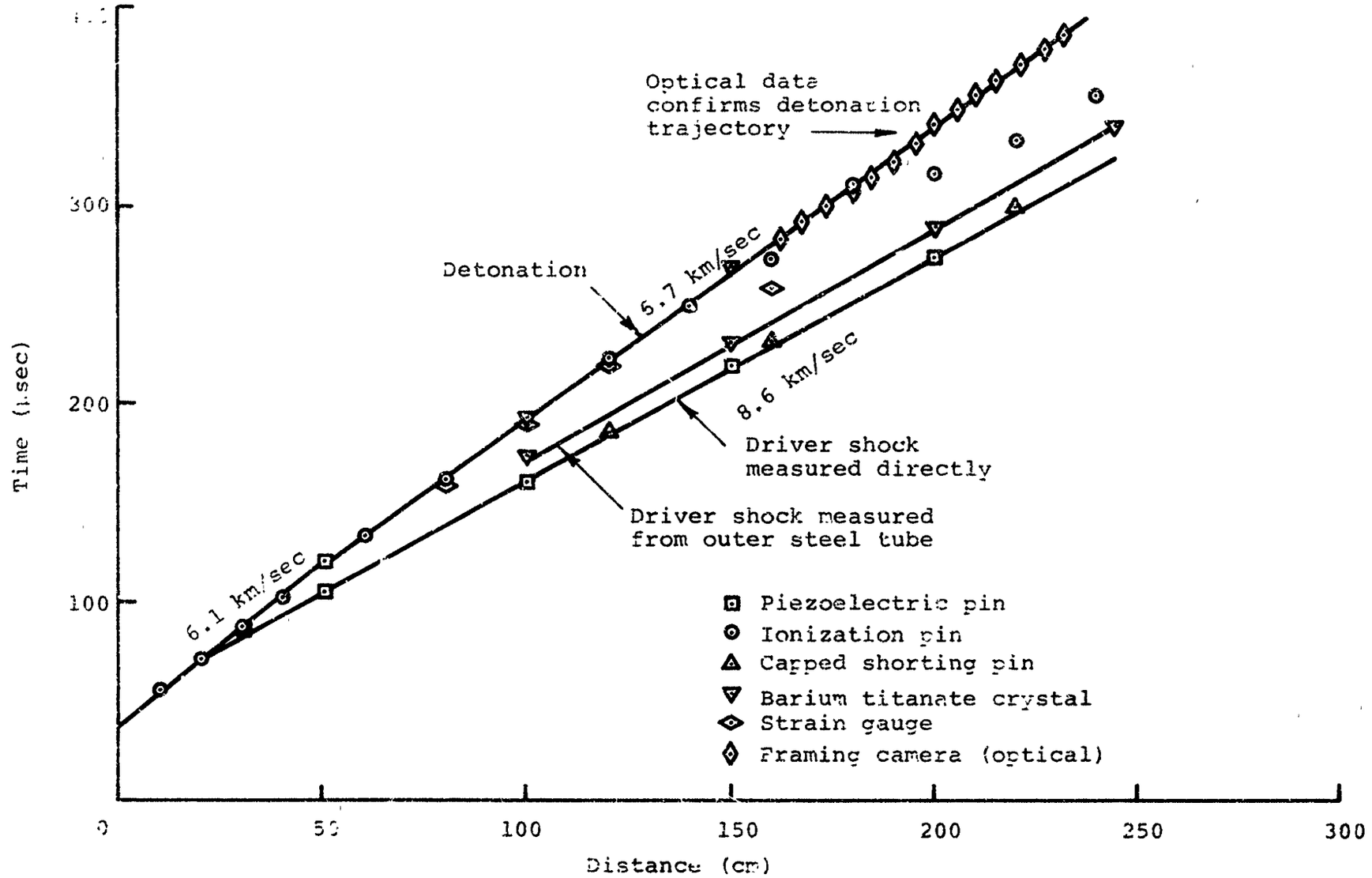

Figure 5.2 Performance of the 2-inch, 6-kbar driver in the x-t plane (Shot 538-2).

Experiments on initiating pressurized nitromethane had shown that the standard method of initiation would not work. The pre-pressurized explosive was very insensitive and the standard detonator and booster pellet arrangement had to be replaced by a more effective method, shown schematically in Figure 5.3. A solid bar is wrapped with a plastic explosive (EL 506-C6) and the explosive, when detonated, drives a convergent stress wave into the bar and forms a Mach disc. This Mach disc is driven into the explosive and generates pressures of hundreds of kilobars, sufficient to initiate the pre-pressurized explosive. This technique* was used in a series of preliminary initiation experiments. It was also used to initiate the explosive in the 2-inch-diameter driver described above.

The 8-inch-diameter driver was one-half the diameter but approximately the same length as the driver anticipated for the large-gun ALPHA-I experiment. The instrumentation used in this experiment was not allowed to penetrate the outer steel tube in order to avoid any interaction between the instrumentation and the explosive. The inner surface of the explosive-containing tube was sandblasted and the final surface finish was approximately a 750 finish. Other than being cleaned, the outer surface of the pressure tube was as delivered. During assembly at the test site, a small layer of dust accumulated on the surfaces of the explosive chamber. The roughness of the surfaces and the accumulated dust in the explosive chamber could only contribute to the problem of explosive decomposition by acting as locations to which for small bubbles would adhere. However, pre-pressurization of the explosive as a solution to the decomposition problem is, within limits,

*First employed by Lou Zernow of Shock Hydrodynamics Company, Sherman Oaks, California.

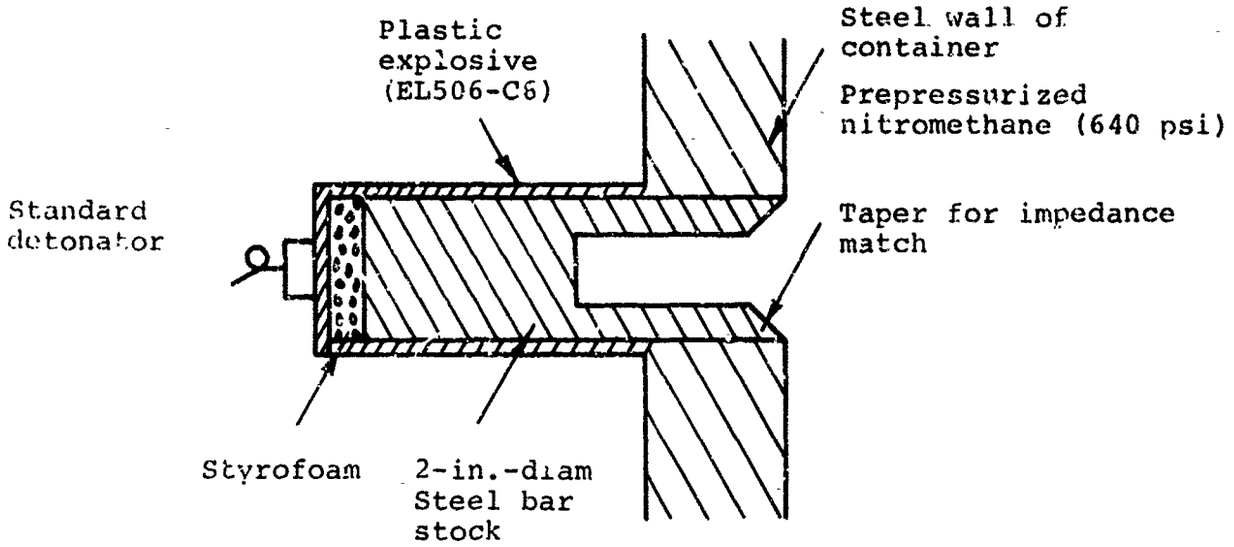

a. Initial configuration

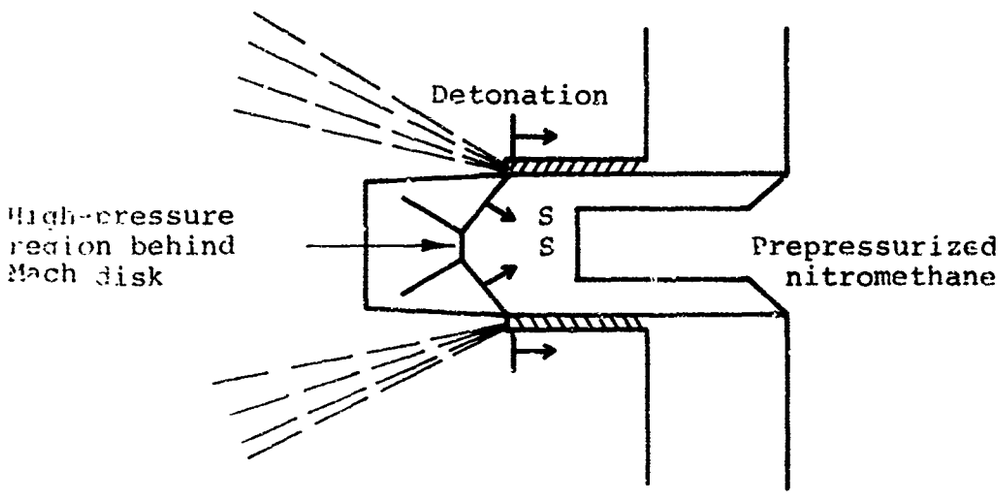

b. Formation of Mach disk on axis of steel bar

Figure 5.3 Operation of a Mach disk generator to initiate pre-pressurized nitromethane.

7235

independent of the number and size of bubbles* and these surface irregularities and contaminants were not considered harmful.

The shock trajectory was monitored by contact pins, strain gauges, and barium titanate crystals mounted on the outside of the driver. Since these diagnostics record the arrival of the driver shock on the outside of the driver, they must be adjusted by the communication time to give the position of the shock inside the tube. Kistler pressure transducers and several other pressure-sensing pins were used to sense the driver shock inside the outer tube at the extended downstream end of the pressure tube, and thus determined the actual communication (or transit) time.

The primary objective of this experiment was to determine detonation trajectory, as any irregularity could indicate decomposition of the explosive. Barium titanate crystals and strain gauges were used for this purpose; however, three high-speed framing cameras were employed as the principal method to detect the detonation.

The nitromethane in the 6-kbar driver was pre-pressurized to 43.5 atmospheres and initiated by five Mach disc generators of the type shown in Figure 5.3. The driver appeared to operate normally, as shown in Figure 5.4. Determination of the detonation trajectory using the optical records was more difficult than in the case of the 2-inch-diameter driver, although no irregularities are apparent within the accuracy of the measurements. When the results of the 2-inch- and 8-inch-diameter driver

*As long as the bubbles are small enough that the heat flow across the bubble-nitromethane boundary is laminar.

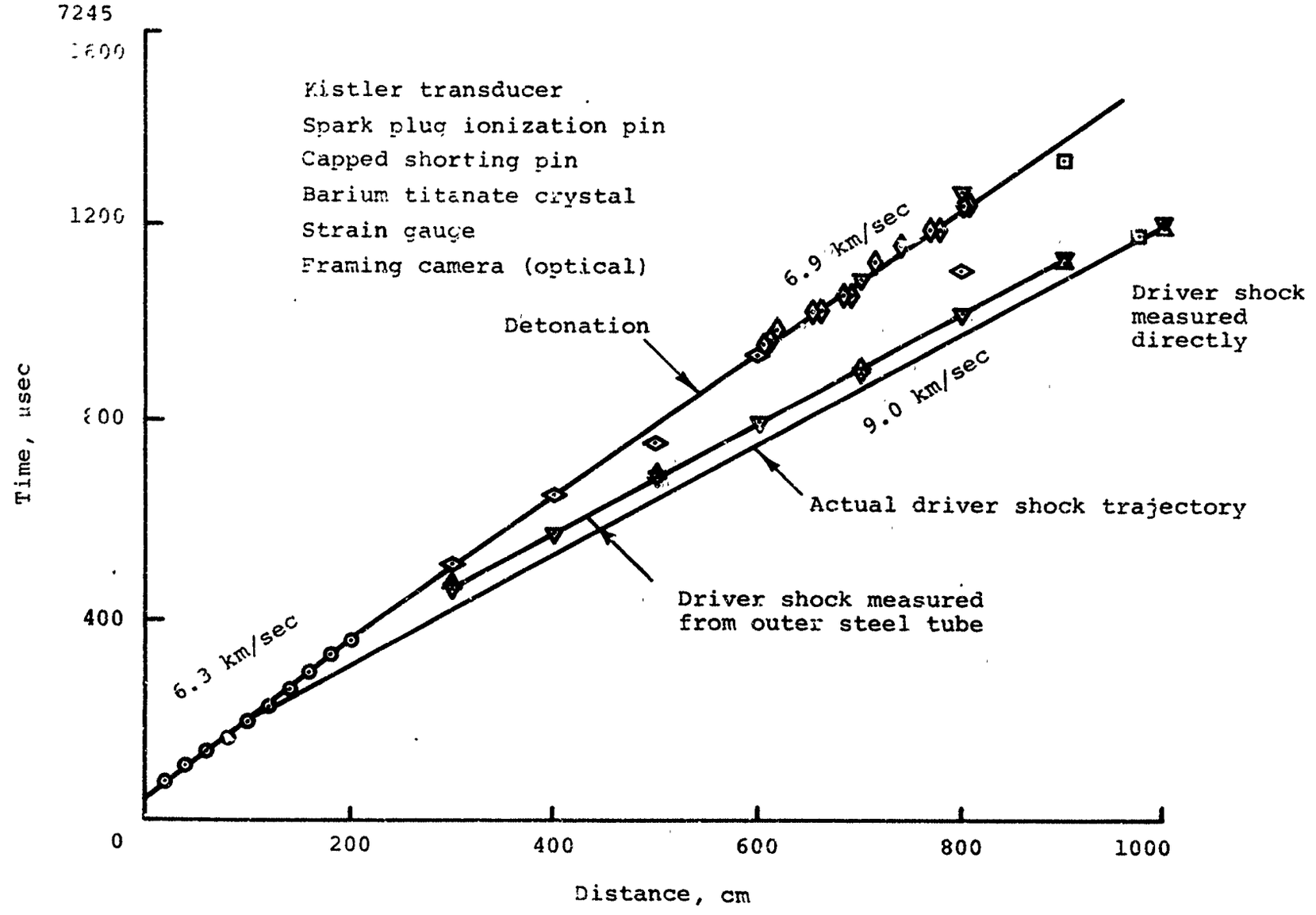

Figure 5.4 Performance of the 8-inch, 6-kbar driver in the x-t plane (Shot ALPHA-½).

experiments were non-dimensionalized with respect to tube diameter and detonation velocity, the shock trajectories collapsed into a single curve (Figure 5.5), demonstrating the simularity of operation as well as the scalability of the design.

The rates of expansion of the outer surface of the tubes containing the explosive were determined from the high-speed framing camera record and compared with the values calculated for this driver design ing the one-dimensional Lagrangian code (POD) in cylindrical geometry. A comparison of the observed and calculated expansion histories for two locations along the driver are shown in Figure 5.6. The observed data, though scattered because of the resolution of the optical records, did not exhibit any abnormal deviation from the calculated curve, as might be expected if significant explosive decomposition (energy release) were occurring.

Since the pre-pressurized driver explosive in the 8-inch-diameter driver experiment was subjected to pressures of over 10 kbar for nearly 300 μsec with no discernable decomposition, it was concluded that the 16-inch-diameter ALPHA-I driver would not preinitiate if the explosive were pre-pressurized.

5.2 SMALL-SCALE GUN EXPERIMENTS OF ALPHA-I DESIGN

Physics International has previously acquired a 8.25-inch-diameter surplus Naval gun barrel from Watervliet Arsenal in Watervliet, New York. This barrel and the 10,000-pound-maximum explosive weight limit at our Tracy Test Site limited the size of the explosive driver to a 16-inch-diameter pressure tube. Therefore, in order to use the Watervliet barrel in the ALPHA-I gun,

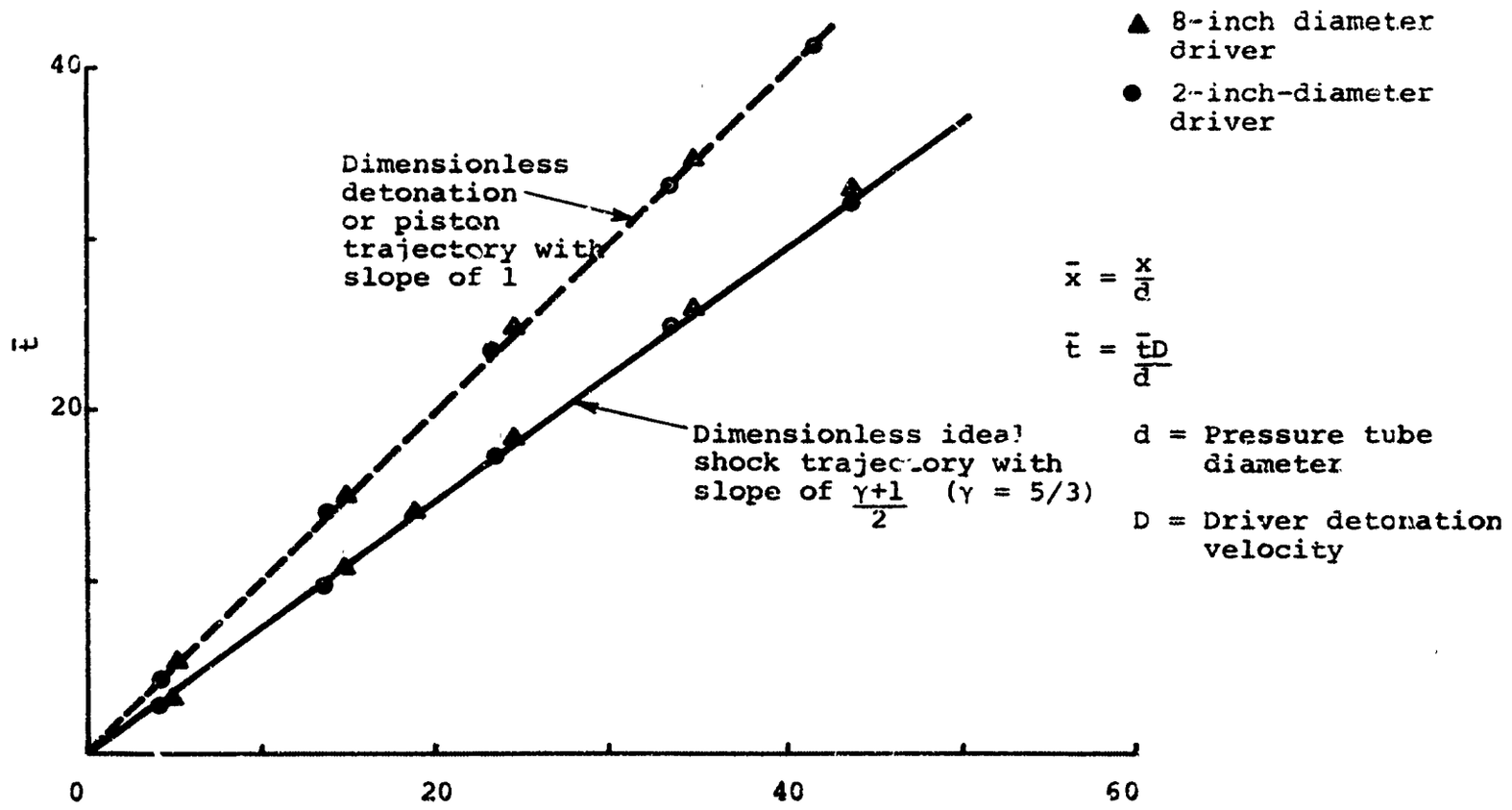

Figure 5.5 Performance of the 2-inch-diameter and 6-inch-diameter drivers in the dimensionless $\bar{x}$ - $\bar{t}$ plane demonstrating scalability of the driver.

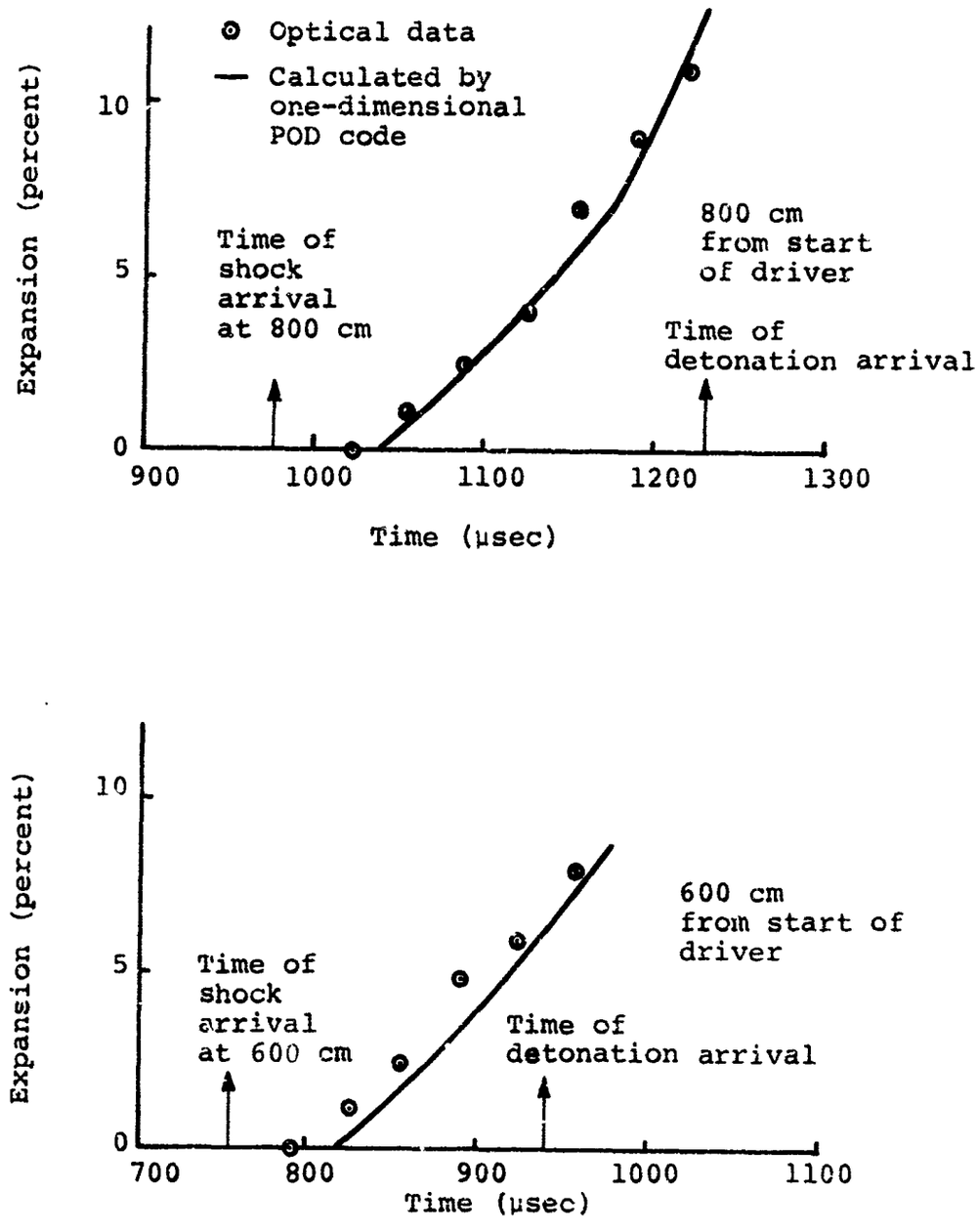

Figure 5.6 Calculated and observed expansion of the outside of the explosive-containing tube (ALPHA-1/2).

the pressure tube-to-barrel area ratio was fixed at 3.75. Several small-scale guns were tested with this pressure tube-to-barrel area ratio and in all cases the observed projectile velocities were low, ranging from 4.3 to a high of 5.0 km/sec. The decision to incorporate this barrel into the final ALPHA-I gun design was delayed pending further investigation.

The pressure tube-to-barrel area ratio was isolated as the cause of low performance in a comparison test in which all parameters were held constant except this critical ratio. The standard gun had a pressure tube-to-barrel area ratio of 4.8 and the projectile was launched to 5.5 km/sec. The gun with the 3.75 pressure tube-to-barrel area ratio was used to accelerate the projectile to 5.0 km/sec. Both guns utilized the same driver design and breech design, and both guns had a driver gas mass-to-projectile mass ratio of 1.5.

The standard one-dimensional ballistic analysis of Seigel (Reference 12) does not predict such a large velocity change (5.5 to 5.0 km/sec) for the relatively small change (4.8 to 3.75) in the pressure tube-to-barrel area ratio. The observed effect in the case of this explosively-driven gun is probably due to enhancement of the effect of reservoir expansion as the pressure tube-to-barrel ratio is decreased.

It was also established during these experiments that use of the optimized driver design tested in the 2-inch- and 8-inch-diameter experiments on explosive decomposition resulted in lower projectile velocities. It was speculated that the decrease in performance was not due to the operation of the driver itself, but rather to the termination process of the explosively formed piston. The reduced thickness of explosive in the optimized

driver design was not enough to collapse the taper section (Figure 5.7) and properly close off the end of the reservoir. The proper closing off of the reservoir is vital to the successful operation of the gun as shown in References 3 and 13. Because of scheduling considerations, further experimentation with this driver design was discontinued and the standard driver design using a larger quantity of explosive was accepted as the design used for the ALPHA-I experiment. As a result, the gun modifications that would be required to incorporate the government-furnished barrel into the final design were judged to be excessive. A cost study showed that it was less expensive to fabricate a new barrel.

a. Taper from the 8-inch-diameter driver showing incomplete closure.

b. Taper from the 2-inch-diameter driver showing incomplete closure.

Figure 5.7 Recovered taper sections from the 8-inch-diameter ALPHA-I driver and the 2-inch-diameter driver (Shot 538-2).

At this point a small-scale gun experiment which incorporated all the parameters of the proposed ALPHA-I gun, including the saboted cone design and proposed method of assembly of the ALPHA-I gun, was conducted. The main features of this gun design are illustrated in Figure 5.8. The operation of the driver was normal; however, the model that was launched badly fragmented. The experiment was repeated with the same results.

A detailed examination of both experiments revealed the probable cause of projectile failure. Prior to testing, the barrel ahead of the projectile was evacuated and filled with helium at 1 atmosphere in order to reduce the counter-pressure during acceleration, thus increasing muzzle velocity by a few percent. During evacuation of the barrel, it was possible that the pieces of the sabot were drawn slightly apart under the action of trapped gases. Thus, the projectile assembly contained small gaps which, when shocked loaded, resulted in model breakup as these gaps were abruptly closed.

The gun experiment was repeated without evacuating the barrel and flushing it with helium. This time the performance of the gun was excellent, as shown in the x-t plane (Figure 5.9) and the projectile was launched in good condition to 5.7 km/sec, as shown in the range radiograph (Figure 5.10). This gun design was accepted as the final design for the ALPHA-I experiment and the practice of evacuating the barrel and flushing with helium was discontinued because of the possibility of opening gaps in the projectile prior to launch.

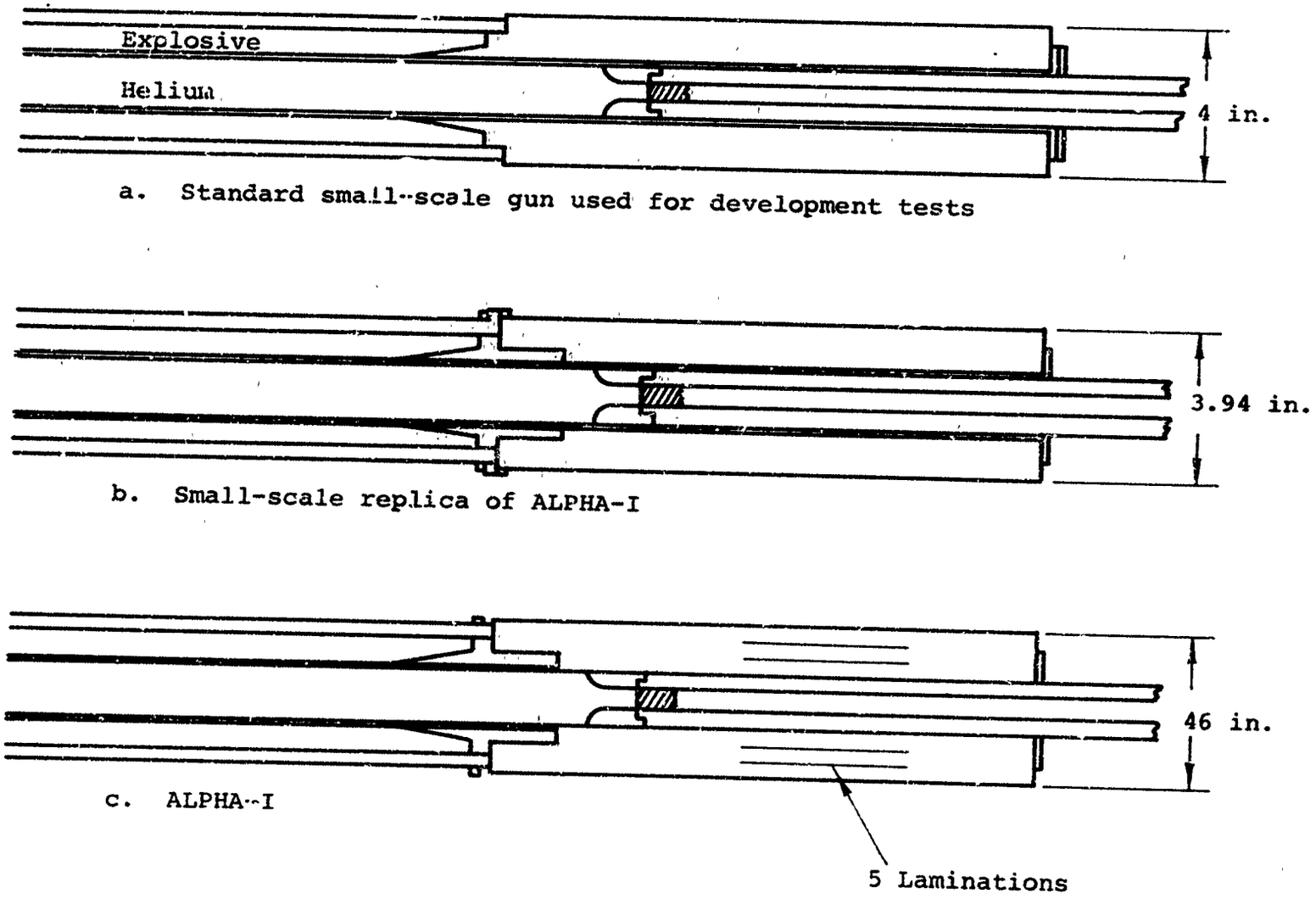

Figure 5.8 Method of construction of ALPHA-I and small-scale guns.

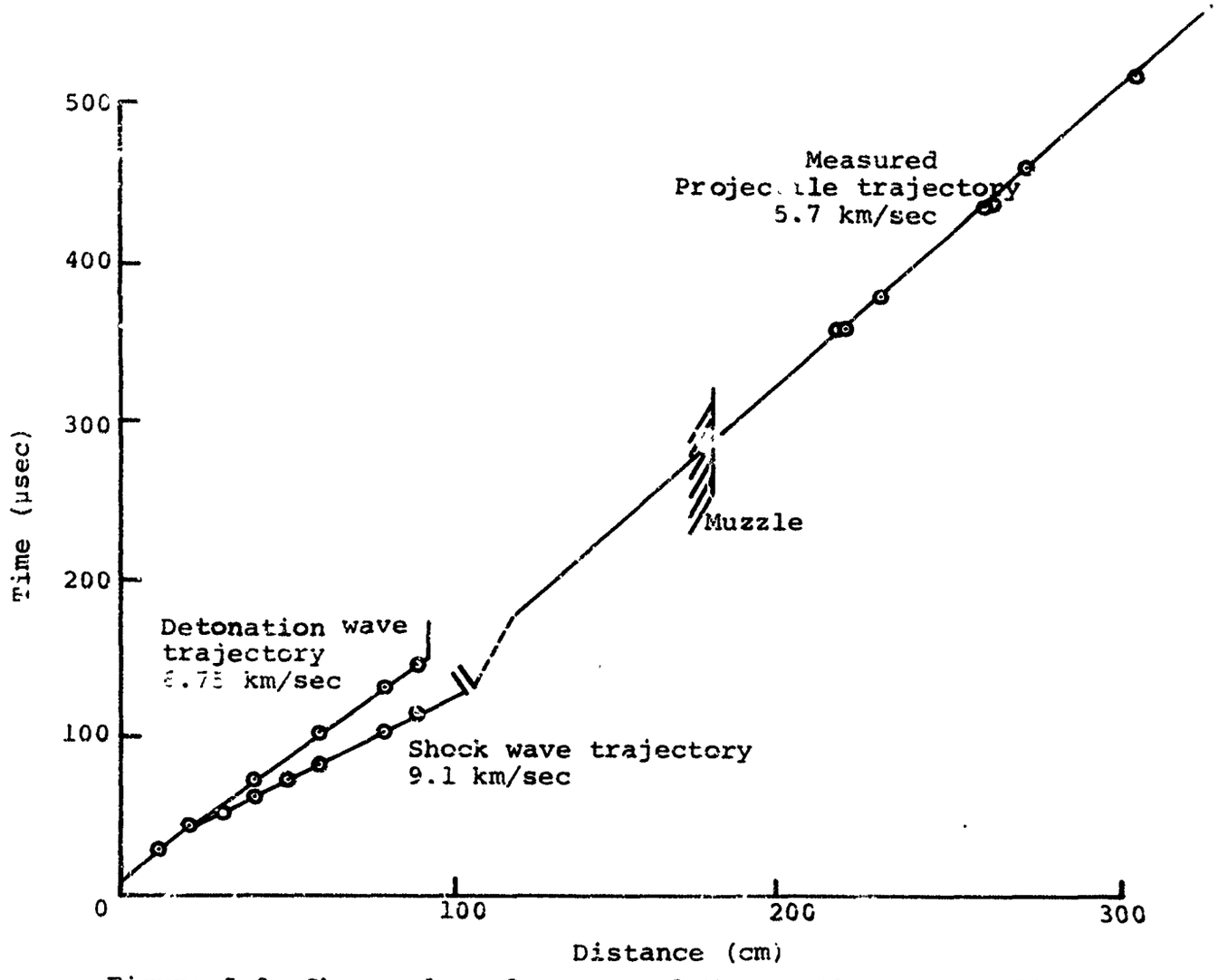

Figure 5.9 Observed performance of the small-scale replica of the ALPHA-I gun (Shot 538-11).

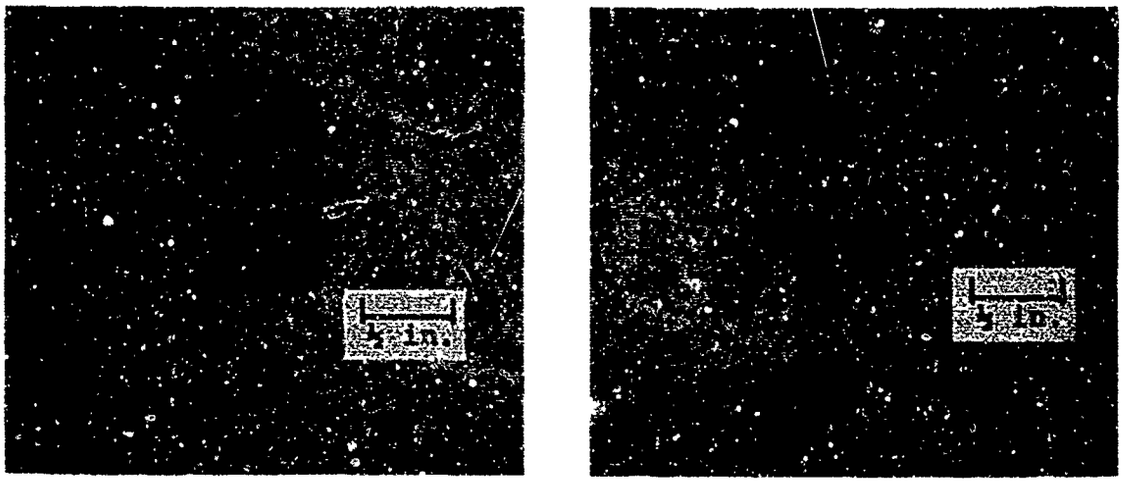

a. Cone is 29 barrel diameters downstream of the muzzle.

b. Cone is 58 barrel diameters downstream of the muzzle.

Note: The cone is flying at 5.7 km/sec into air at 1 atmosphere.

Figure 5.10 Range radiograph of a 0.514-inch-base diameter, small-scale replica of the ALPHA-I cone.

5.3 DESIGN OF THE ALPHA-I GUN

The final design of the ALPHA-I gun was based on the small-scale gun experiment described above. The methods of construction of the ALPHA-I gun, the gun used in the final small-scale experiment, and the guns used in most of the previous small-scale development tests were slightly different, these differences are shown schematically in Figure 5.8. Apart from these constructional differences, the important physical parameters controlling gun performance were the same. Table 5.1 summarizes the dimensions of the principal ALPHA-I components. The dimensions of the ALPHA-I gun were 11.68 times larger than the corresponding dimentions of the small-scale guns.

The following is a summary discussion of the ALPHA-I gun design. The driver parameters such as charge-to-mass ratio, initial gas pressure, and outer tube thickness were chosen from a driver design that had been employed in a large number of small-scale tests. The length of the shocked gas column (6.5 pressure tube diameters) and the pressure developed (6.5 kbar) by this driver design were sufficient to accelerate slender cones to the required velocity of 5.5 km/sec. The design of the taper section, which gradually terminates the explosive to prevent shearing of the pressure tube, was satisfactory for closing off the end of the reservoir. This is a vital characteristic in the successful operation of the gun. The explosive weight used in the 16-inch-diameter driver was 9200 pounds; this is within the maximum weight limit of 10,000 pounds imposed on the Physics International Tracy Test Site. The explosive-containing tube was a massive thick walled tube (40-inch OD x 30.65-inch ID) designed to limit the expansion of the pressure tube to less than 30 percent (Figure 5.11) to make efficient use of the explosive, and to hold the pre-pressurized nitromethane at 640 psi. The pressure tube (17.5-inch OD x 16-inch ID) was pressurized to 935 psi with helium and the total mass of gas was approximately 18,000 grams. When detonated, the nitromethane collapses the pressure tube at approximately 6.7 km/sec and generates approximately a 6.5-kbar shock in a 260-cm-long column of helium.

The reservoir section of the ALPHA-I gun was made from a surplus Naval gun breech section with a 46-inch OD by 16-inch ID. The thickness of the steel reservoir walls was sufficient to contain the high reservoir pressures (up to 40 kbar) generated when the 6.5-kbar driver shock reflects at the entrance to the nozzle section and the base of the projectile. Upon shock reflec-

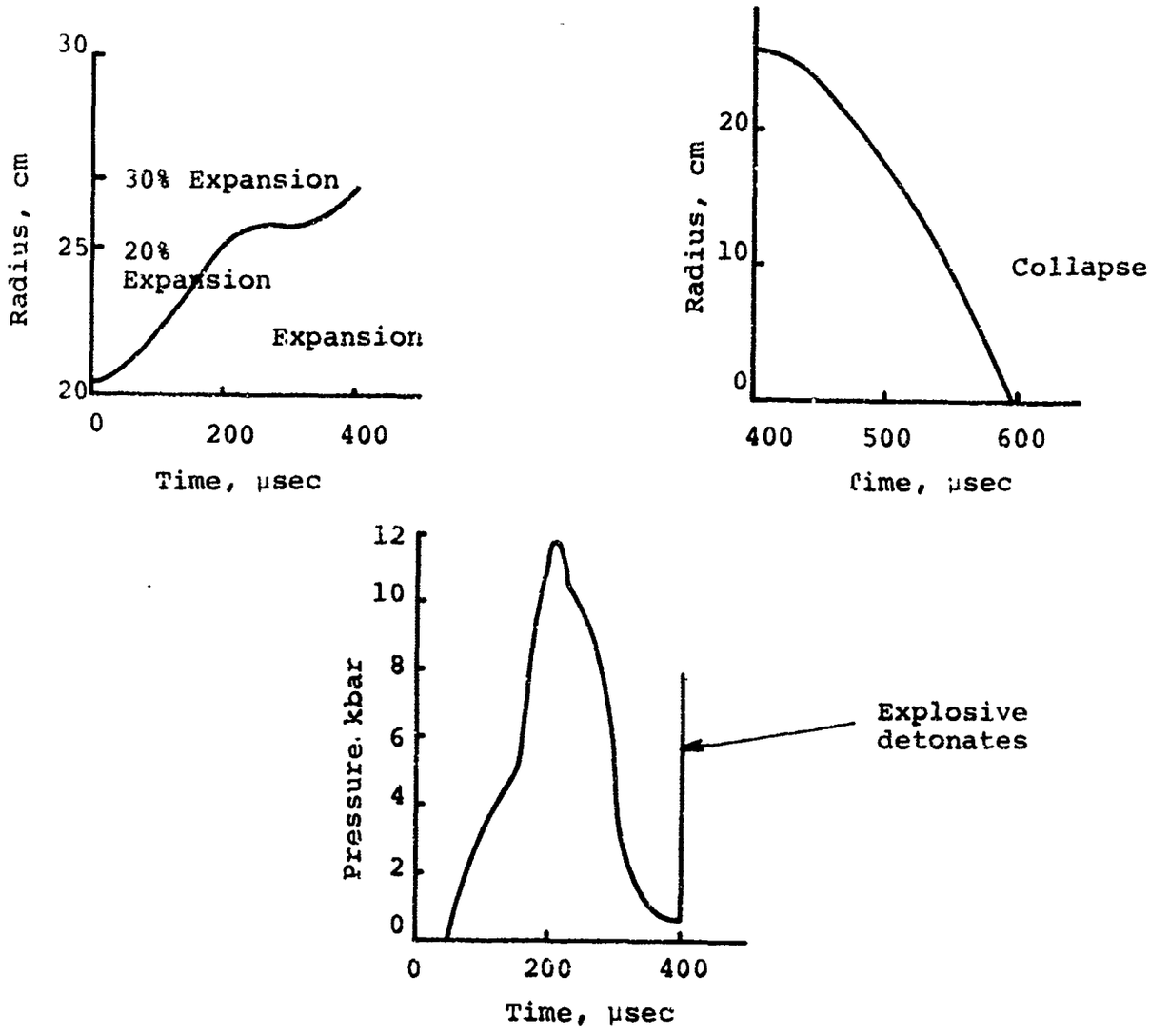

Figure 5.11 Calculated expansion and collapse histories of the pressure tube and presusre history in the center of the explosive for the ALPHA-1 driver.

tion the reservoir walls begin to expand; however, the inertia of the walls keeps the reservoir pressure from decaying too quickly during the acceleration of the projectile.

The final nozzle section design allows the projectile to be located two body diameters downstream of the nozzle inlet or chambrage plane. The nozzle entrance is radiused to improve the flow characteristics. This design was evolved from a series of small-scale experiments and results in the best combination of projectile integrity and velocity.

The new barrel had a bore diameter of 7.3 inches and the pressure tube-to-barrel area ratio, which was found to be a sensitive parameter, was kept at 4.8, as in all the successful small-scale experiments. If the large government-furnished barrel (C.25-inch bore) were used and the pressure tube-to-barrel area ratio of 4.8 maintained, the explosive driver would require 11,800 pounds of explosive; this would have been an unacceptable weight for the Tracy Test Site. In addition, the cost of the gun would have been increased considerably as a new and larger reservoir section would have been required. The barrel used in the ALPHA-I gun was 28 feet long; this length was chosen to allow the projectile to exit from the muzzle with essentially zero base pressure.

The projectile itself (Figure 5.12) was 12-inches long and weighed 11,400 grams. Thus, the driver gas-to-projectile mass ratio was 1.58. The cone and three sabot pieces were all made of a lithium-magnesium alloy, LA141A, with a density of 1.38 g/cm^3. The cone itself was 10.73 inches long with a base diameter of 6-inches and an included angle of 31 degrees. As shown in Figure 5.12, the cone was hollowed to improve its stability in free flight.

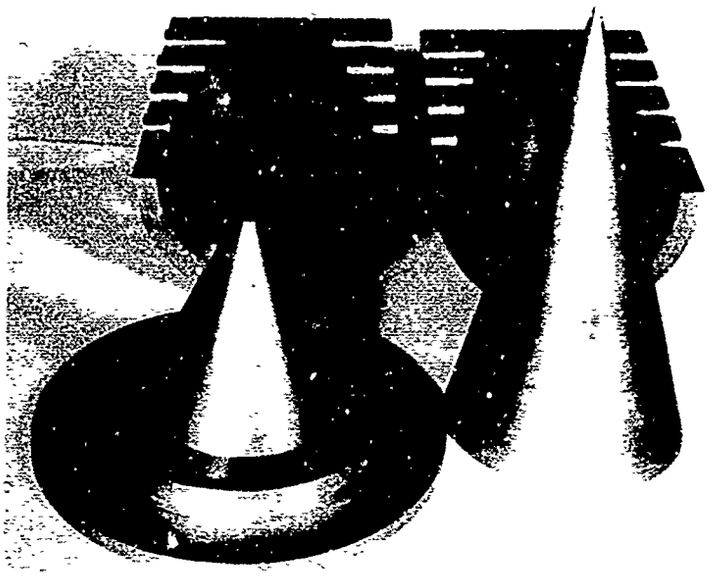

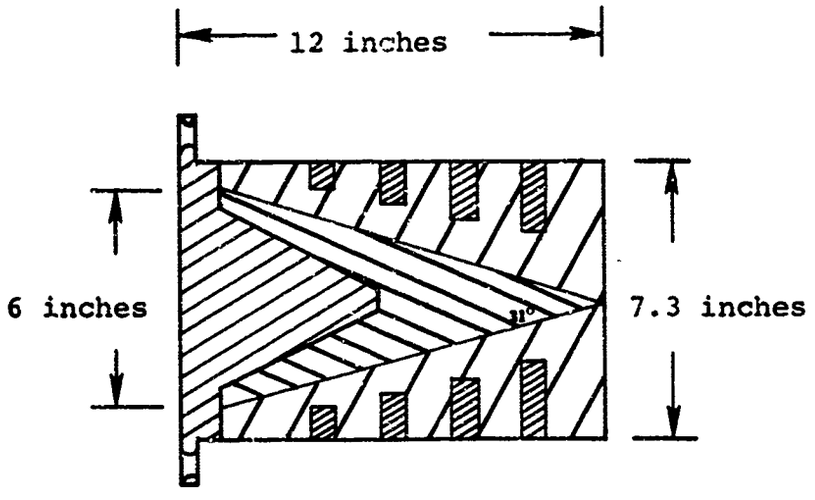

Figure 5.12 The ALPHA-I projectile.

5.4 CONSTRUCTION AND ASSEMBLY OF THE ALPHA-I GUN

In scaling the design of the successful small-scale gun, considerable care was excerised in maintaining all important dimensions and methods of assembly. The process of procuring very large tubing for the barrel, reservoir, and driver components presented many problems.

An engineering study of the ALPHA-I design showed that the most cost-effective method of fielding this experiment without significant delays was to fabricate the reservoir section from a 14-foot-long section of a readily available surplus 16-inch Naval gun. The 46-inch OD by 16-inch ID laminated (five laminations) section met the scaling requirements exactly.

The pressure tube, explosive-containing tube, and barrel were all specially made from certrifugally cast low-strength alloy (ASTM-A27) steel by ACIPCO Steel Products of Birmingham, Alabama. Because of the limitations of their equipment, the barrel was constructed in a laminated fashion (Figure 5.13) with one full-penetration circumferential weld. The pressure tube and explosive-containing tube were not laminated, but also required several full-penetration circumferential welds. The design and location of these welds are illustrated in Figure 5.13. The weld material used was chosen to duplicate the strength and ductility of the parent material within 10 percent and was the same type of low-strength alloy steel. One of the welds in the pressure tube was located at a critical position where the pressure tube would expand 14 percent before the arrival of the detonation wave. The positioning of this weld was inevitable and required a small-scale experiment to determine if it affected

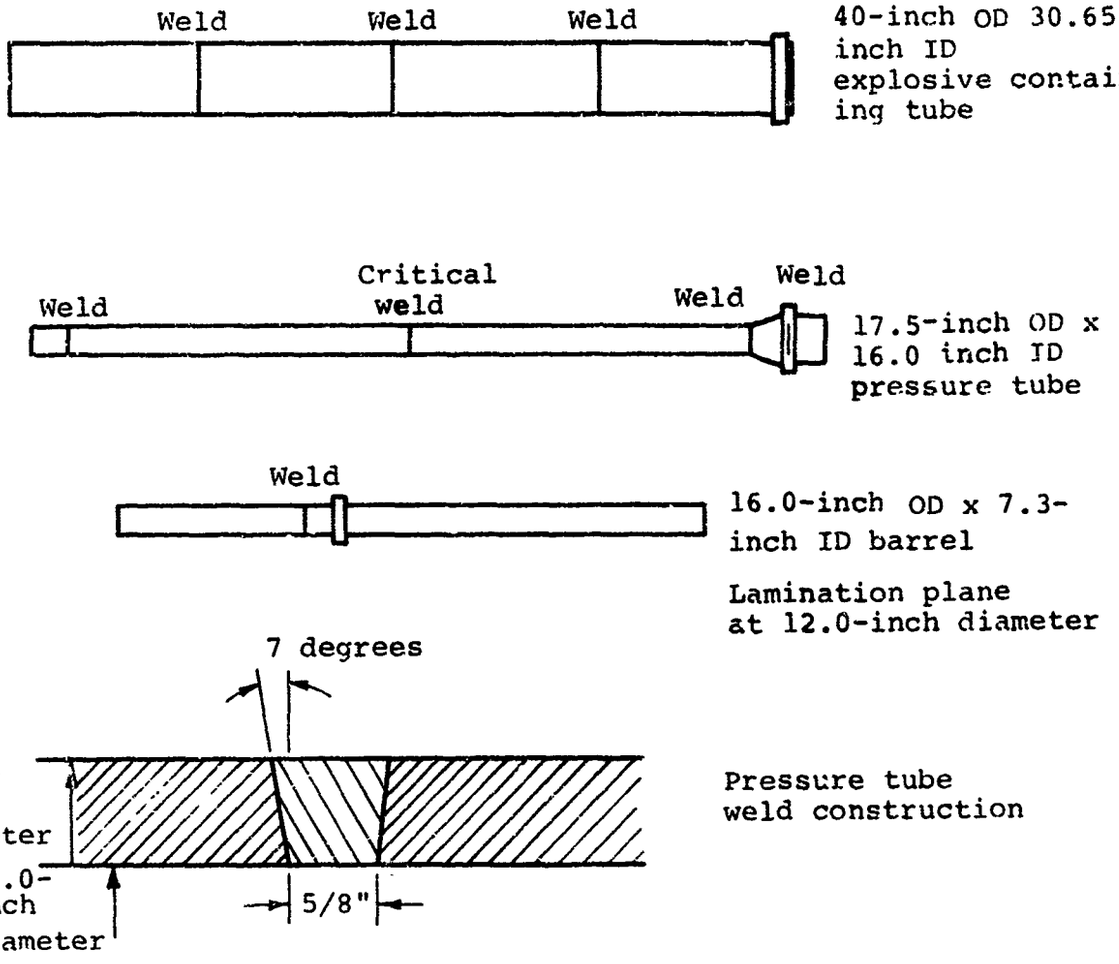

Figure 5.13 Full penetration circumferential grove welds used in the construction of the ALPHA-I gun.

performance. A small-scale driver was constructed and full-penetration circumferential welds were located at positions where 7-, 14-, and 19-percent expansion were anticipated. The explosive-containing tube was made from clear plastic, thus enabling the pressure tube to be viewed by a high-speed framing camera which would detect any tube rupture. In addition, the driver was made very long so that any perturbations caused by rupturing could be observed as a variation in the shock or detonation trajectories near the end of the driver.

This experiment was successful and demonstrated that the welds did not rupture even at pressure tube expansions of nearly 20 percent. The observed performance of this driver is shown in the x-t plane (Figure 5.14). Because the quality of welds used in this experiment was inferior to the quality of welds used in the ALPHA-I gun, it was concluded that successful operation of the large gun would not be jeopardized by the use of welds in the pressure tube. After manufacture the welds in the pressure tube were radiographed and found to be void free and virtually indistinguishable from the parent material.

The choice of tolerances specified for all manufactured parts was dictated by assembly requirements; all tolerances were well within those established in the small-scale experiments for successful operation of the gun. The surface finishes specified for the manufactured parts varied from a rough machined surface for all outside parts to a 125 finish for the barrel bore explosive-containing tube ID, and pressure tube OD and ID. These finishes were more than adequate, surpassing the number specified (see Table 5.1).

TABLE 5.1

DIMENSIONS OF THE ALPHA-I GUN COMPONENTS

Component	Outer Diameter (inches)	Inner Diameter (inches)	Length (inches)	O.D. Finish Design/ Actual	I.D. Finish Design/ Actual	Weight (pounds)	Material	Yield Strength (psi)	Comment
Explosive Containing Tube	40.00	30.65	450.13	500	250/ 45-100	65,813	ASTM-A-27 GR60/30 Centrif. Cast.	35,000	3 Full Penetration Circumfer-ential Welds
Pressure tube	17.50	16.00	455.31	125/80	125/ 50-70	8675	ASTM-A-27 GR60/30 Centrif. Cast.	35,000	3 Full Penetration Circumfer-ential Welds
Reservoir	56.00	16.00	168.00	> 500	~ 250	70,000	Naval Steel Approx. 4630	104,000	5 Lamina-tions Internal Joints
Barrel	16.00	7.30	336.00	500/400	125/ 25-40	15,125	ASTM-A-27 GR60/30 Centrif. Cast.	35,000	2 Lamina-tions 1 Full Penetration Weld
Nozzle	16.00	7.30	20.40	500/260	125/40	783	ASTM-A-27 GR60/30 Static Cast.	35,000	
Detonator Plate	40.00	---	4.00	---	---	1430	ASTM-A-27 GR60/30 Plate	35,000	
Projectile	7.30	---	12.00	63/63	---	25.4	LA141A Static Cast.	15,000	

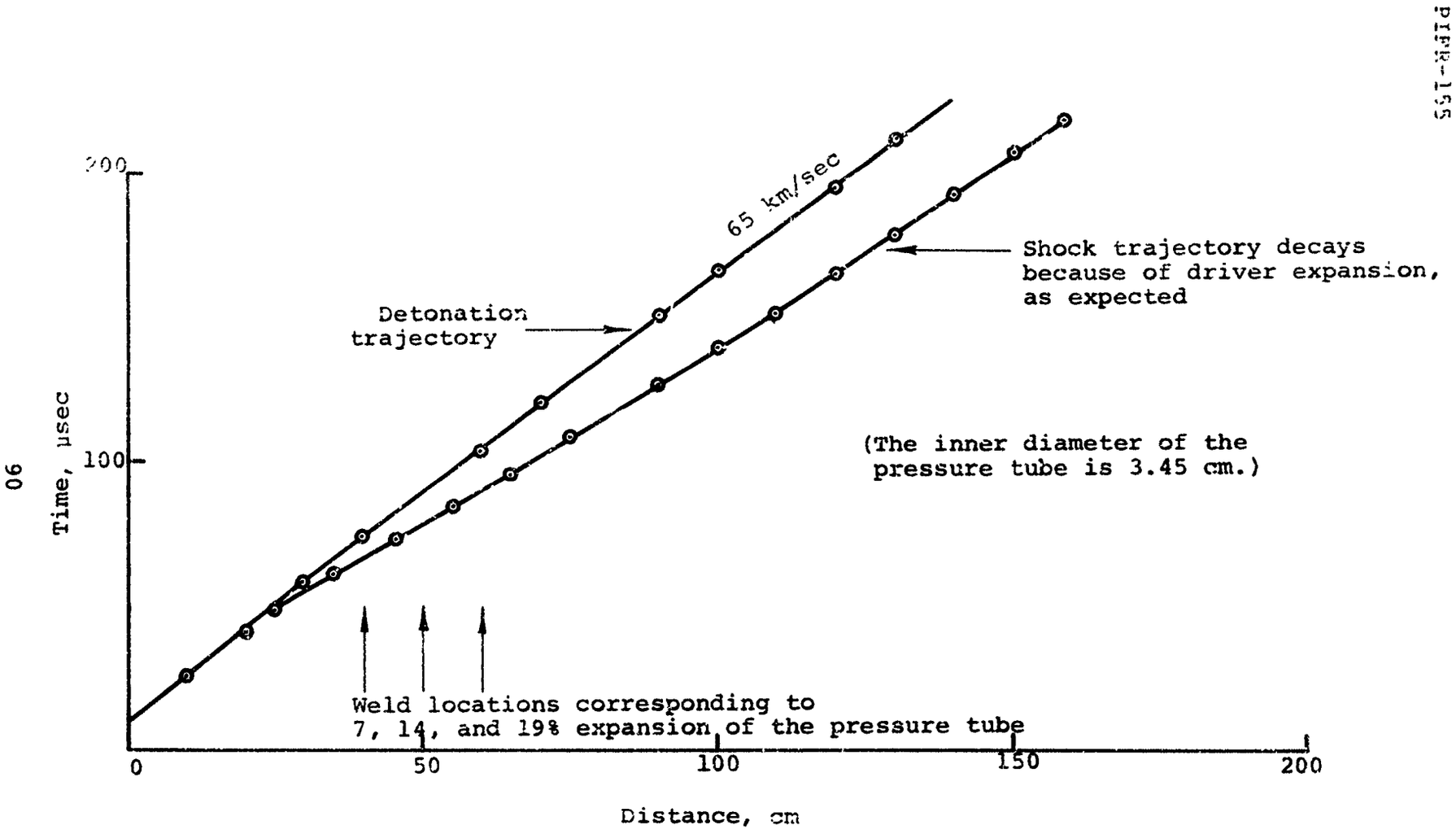

Figure 5.14 Performance of an explosive driver to test full-penetration circumferential welds in the pressure tube.

The manufactured parts were all individually shipped to the Physics International Tracy Test Site. The parts were cleaned and assembled at the site in the following manner. The reservoir section was placed on a reinforced concrete pad (Figure 5.15). The pressure tube was inserted into the explosive-containing tube to form the driver (Figure 5.16) and the driver was coupled to the reservoir. The detonator plate with the five Mach disc generators was then installed (Figure 5.17). The projectile was placed in the barrel (Figure 5.18), the nozzle was threaded onto the barrel, and the barrel assembly was inserted into the reservoir to complete the assembly of the gun (Figure 5.19). The heavy pieces were handled by means of a 70-ton crane (Figure 5.19) and adjustable stands with roller bearings.

Note: This piece was machined from a 16-inch surplus Naval gun breech.

Figure 5.15 The ALPHA-I reservoir section.

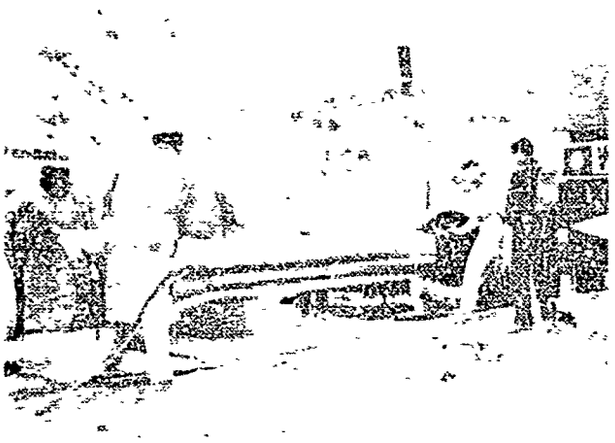

Figure 5.16 Assembly of the ALPHA-I explosive driver.

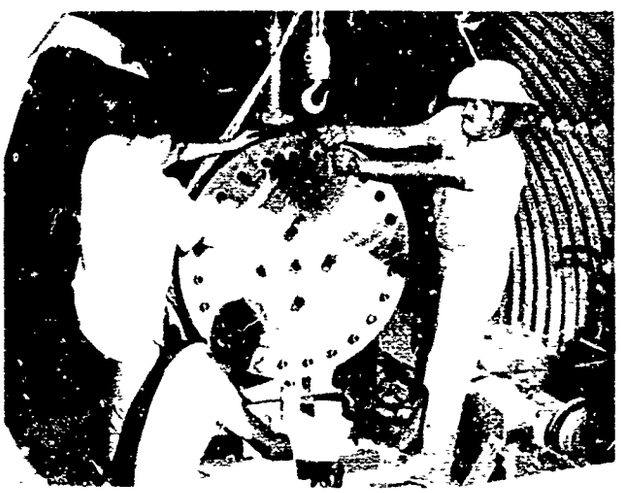

Figure 5.17 Installation of the ALPHA-I detonator plate.

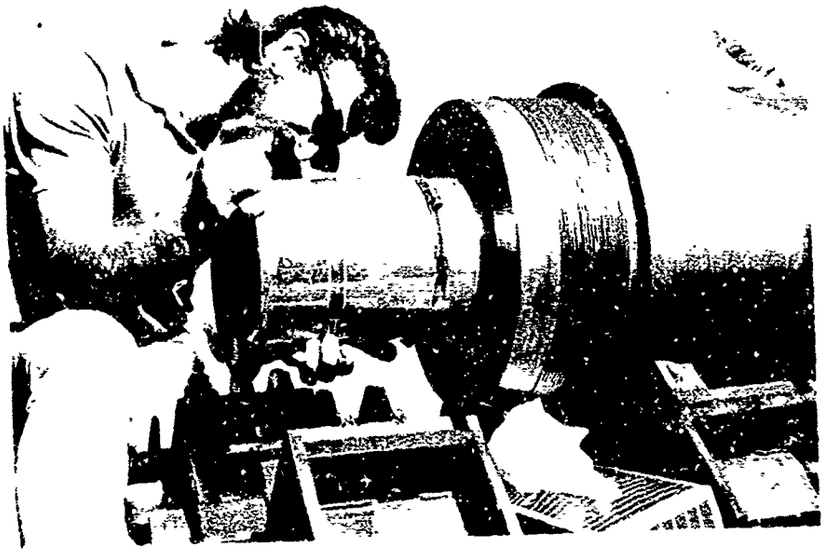

Figure 5.18 Installation of the ALPHA-I projectile.

Figure 5.19 The ALPHA-I gun showing construction of the arch over the gun.

Although no special precautions were taken to ensure cleanliness of the explosive chamber, the amount of dust accumulated in the chamber was considerably less than in the large driver used to test the solution of the preinitiation problem.

5.5 LOGISTICS OF THE ALPHA-I EXPERIMENT

A major part of the effort in the ALPHA-I experiment was devoted to covering the gun with a steel arch and burying the structure with sand. This was done to decouple the blast of the 9200 pounds of explosive from the atmosphere and to stop the shrapnel from the 86-ton steel gun as it blew up. Based on a study of blast wave focusing under various atmospheric conditions (Reference 7), a sand cover of 21 feet would permit the gun containing 9200 pounds of nitromethane to be fired on a day which would permit a maximum 500 pounds explosion; that is, the covering would provide an attenuation factor of about 20. This estimate is conservative since the above study is based on a detonation of a spherical charge; in the gun, the explosive geometry is a long cylinder and the explosive does not detonate simultaneously.

Considering the ratio of areal densities (thickness x density) of the explosive-containing tube (which forms the major portion of shrapnel) and the sand covering, the velocity of the shrapnel would be cut down by an enormous fraction. With a minimum of 21 feet of sand to penetrate, the shrapnel, which starts off at nearly 2 km/sec, would have a residual velocity of only a few feet per second.

After the ALPHA-I gun was assembled, the arch was constructed over the gun (Figure 5.20) and was then buried under a minimum of 21 feet of river bottom sand. Concurrent with construction of the arch, the gun was pressure tested to ensure no pressurized helium or nitromethane would leak.

The driver instrumentation that was installed consisted of piezoelectric pins to record the early detonation trajectory, barium titanate crystals to record the shock and detonation trajectory, and two sets of capped shorting pins to measure the expansion rate of the outer tube. Since it was too costly to provide optical coverage of the driver, these capped shorting pins were used to monitor the expansion of the outer tube and detect any anomalies arising if the explosive began to decompose prematurely.

Five X-ray stations were set up as the primary means of determining projectile velocity and condition. Each of the five X-rays was triggered by a 0.010-inch-thick foil range switch (Figure 5.21). Backup coverage of the range was provided by two hycam framing cameras located on the hillside overlooking the range and a streaking camera located in the control bunker. An inexpensive "failsafe" velocity measuring system using explosives was installed. This system would give the projectile velocity in the event of a complete electronic failure. A camera located on a hill upstream of the gun was used to give an overall picture of the explosion. The layout of the range instrumentation is shown in Figure 5.22.

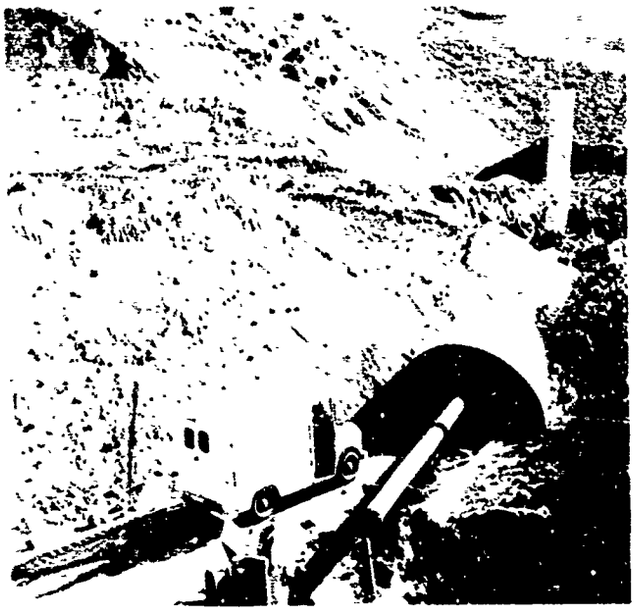

Note: The arch will be covered with sand to the level of the access tube.

Figure 5.20 The arch over the gun is shown completed.

Figure 5.21 Final Preparation of the range diagnostics after the gun has been buried.

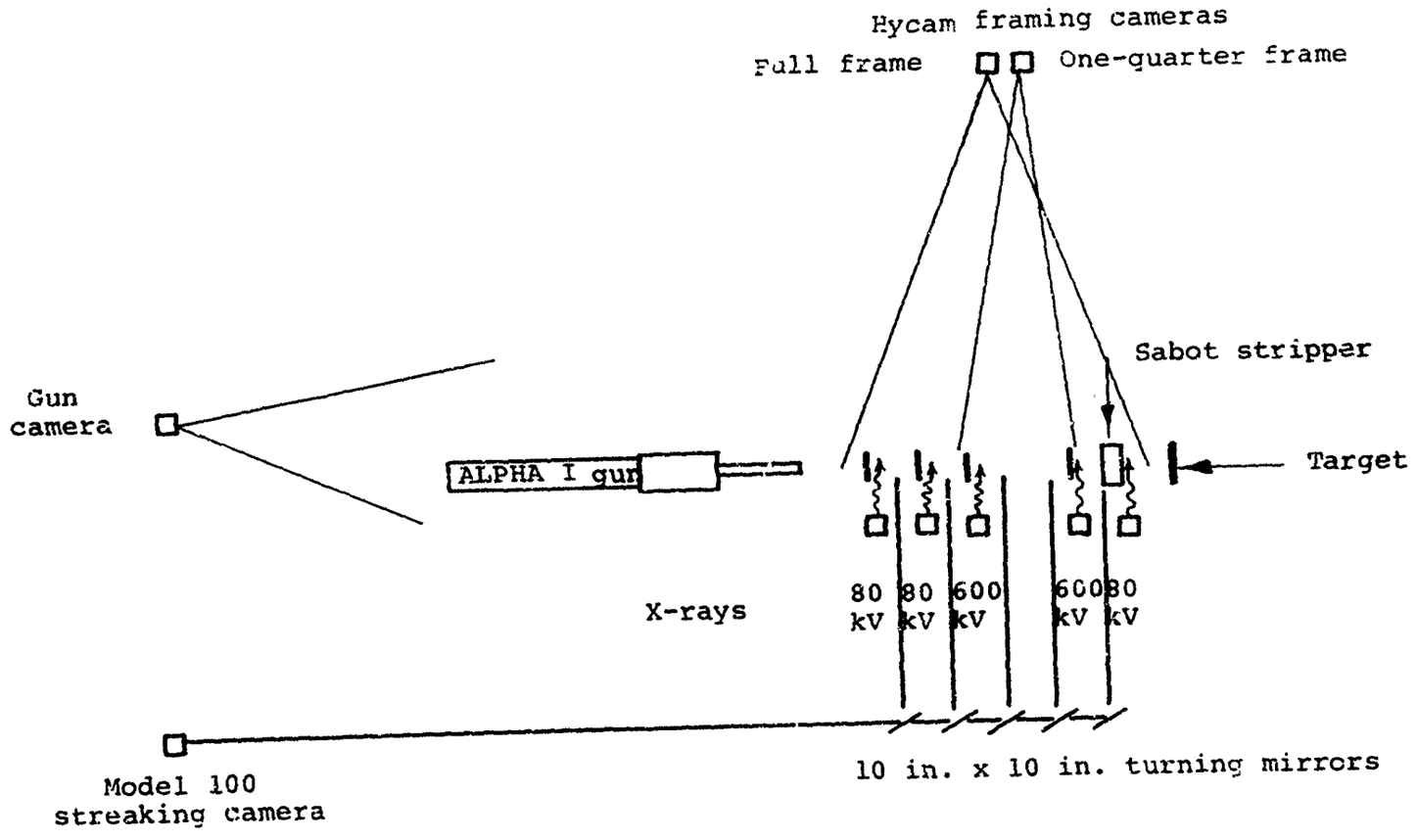

Figure 5.22 Range instrumentation layout for the ALPHA-I experiment.

The firing of the shot was conducted from an underground bunker 350 feet from the gun. Prior to the shot, the nitromethane was stored in the gun and the site was maintained on a ready status until proper weather conditions were obtained. Standard safety procedures were in force during all gas pressurization and explosive-loading operations.

SECTION 6

RESULTS OF THE ALPHA-I EXPERIMENT

Notification by weather report was received from the Lawrence Radiation Laboratory at 11:30 PST, November 20, 1969, that the atmospheric conditions were appropriate for firing the partially buried 9200 pounds of nitro-methane explosive. Prefiring operations, which included filling the gun with helium and pre-pressurizing the driver explosive, proceeded smoothly and the gun was fired four hours later at 15:50 PST. The postfiring condition of the area is shown in Figure 6.1.

Figure 6.1 Crater formed by the ALPHA-I experiment.

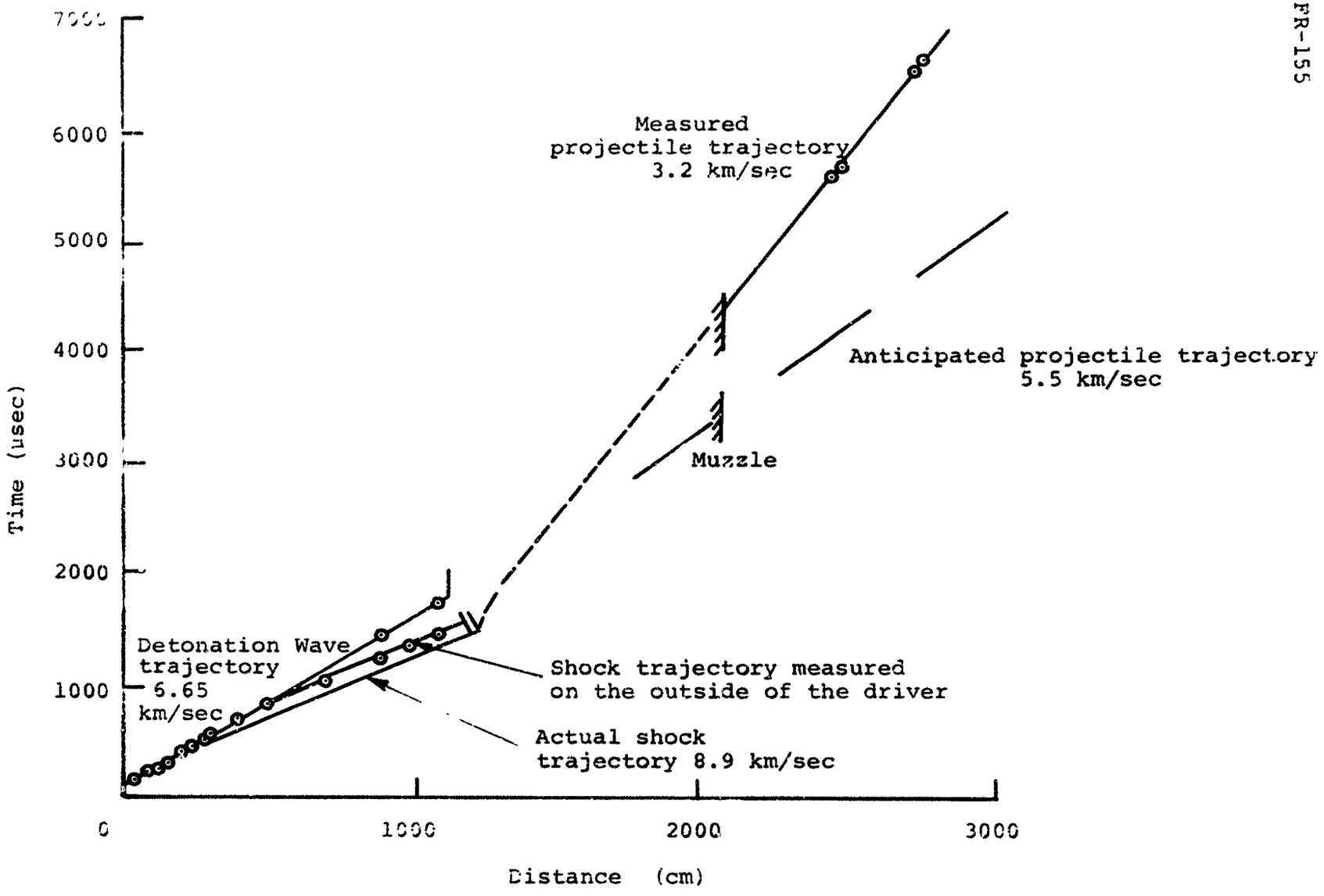

Figure 6.2 Observed performance of the ALPHA-I gun.

Analysis of the driver data indicated that the operation of the driver was normal. As illustrated in the x-t plane (Figure 6.2), the detonation wave and shock wave velocities were 6.7 km/sec and 8.9 km/sec, respectively, and showed no abnormality. A recovered portion of the pressure tube (Figure 6.3) exhibited excellent collapse characteristics. This piece, which formed the first 20 feet of the driver, verified that the operation of the

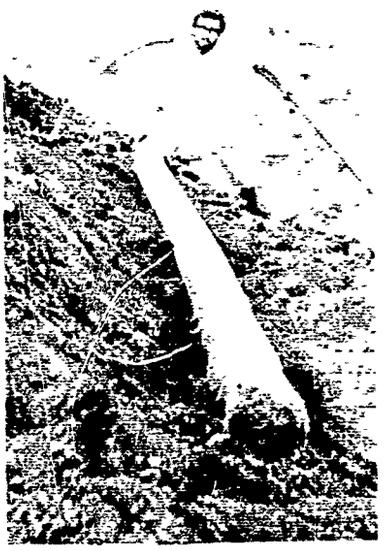

Figure 6.3 Recovered portion of the collapsed ALPHA-I pressure tube.

driver was as planned. As observed in the small-scale experiments, the remaining length of the pressure tube is always fragmented and not recoverable for inspection. A comparison of the large-scale and corresponding small-scale drivers in the dimensionless $\bar{x}$-$\bar{t}$ plane reveals that the driver design is scalable and that the shock trajectory is nearly that expected based on ideal driver theory (Figure 6.4). Measurements of the rate of expansion of

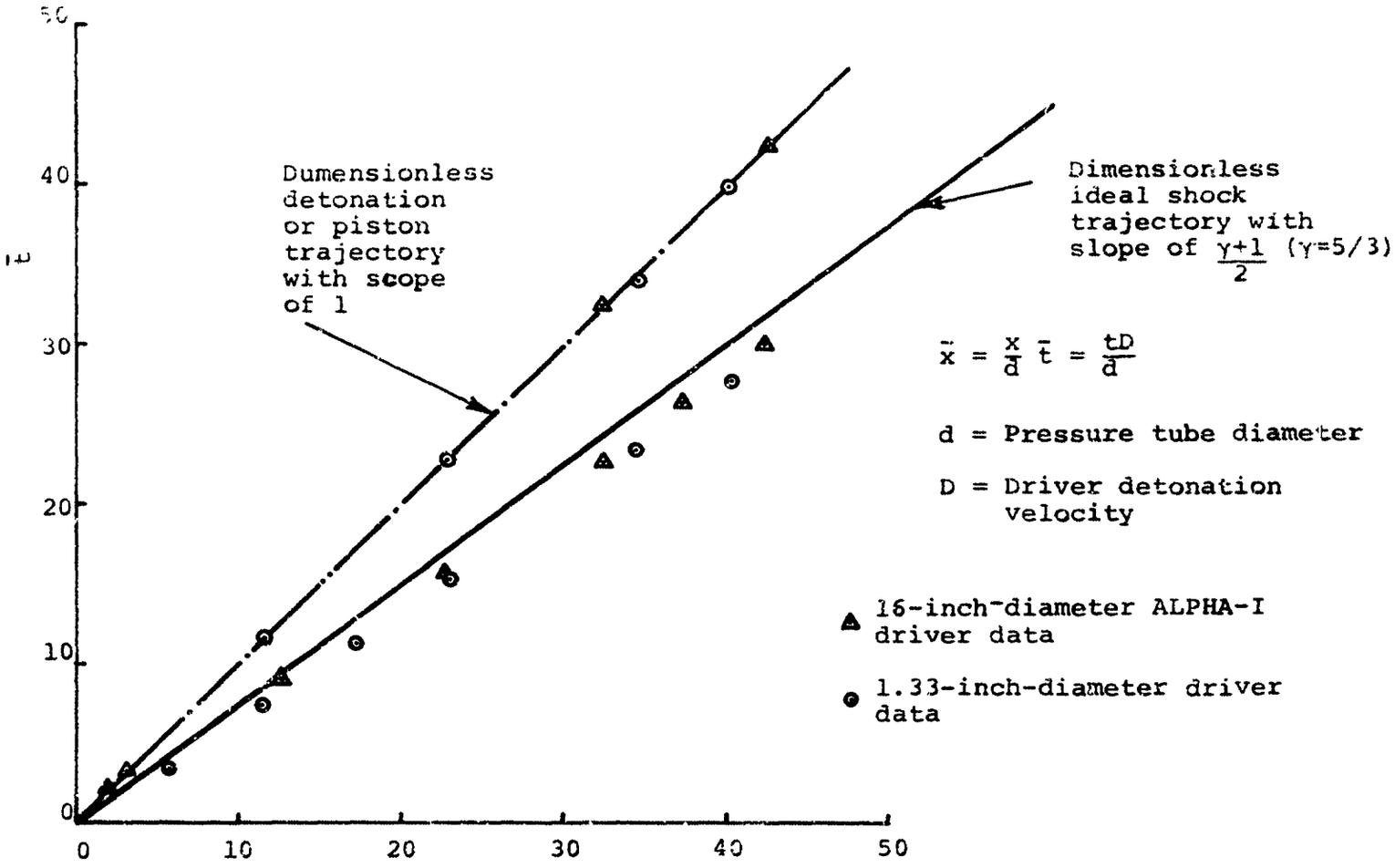

Figure 6.4 Performance of the 1.33-inch-diameter and 16-inch-diameter ALPHA-I drivers in the dimensionless $\bar{x}$-$\bar{t}$ plane.

the explosive-containing tube near the end of the driver showed approximately the expected expansion rate, and it is concluded that there was no ususual energy release during the period of pressure tube expansion such as would be expected if there were premature decomposition of the explosive. Based on the observed data, it was concluded that the performance of the explosive driver was normal and there was no evidence of premature decomposition of the explosive.

Three range radiographs (Figures 6.5 and 6.6) and two high-

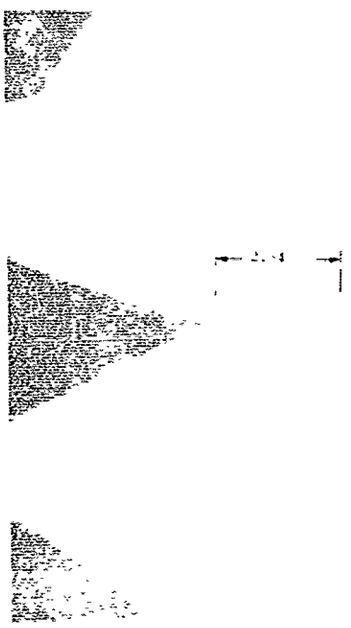

Note: The cone is flying at 3.1 km/sec into air at 1 atmosphere and is 23 barrel diameters downstream of the muzzle.

Figure 6.5 Range radiograph of the tip of the 6-inch-base-diameter ALPHA-I cone.

a. The cone is 39 barrel diameters downstream of the muzzle.

b. The cone is 55 barrel diameters downstream of the muzzle.

Note: The cone is flying at 3.1 km/sec into air at 1 atmosphere.

Figure 6.6 Range radiographs of the ALPHA-I cone.

speed camera records show that the projectile was launched in good condition to 3.2 km/sec. It should be noted that the projectile was subjected to the anticipated peak base pressure of nearly 40 kbar and the tip of the cone appeared to be in good condition (Figure 6.5). The sabot pieces separated as expected (Figure 6.5) on the basis of small-scale data. The X-ray downstream of the sabot stripper did not show the projectile, indicating that the cone was off course and collided with the stripper assembly. Since the cone was on course for the first X-ray, it is assumed that aerodynamic forces (the range atmosphere was air at 1 atmosphere) caused the deviation.

The anticipated projectile velocity of 7.5 km/sec was not achieved and the observed low projectile velocity (3.2 km/sec) was attributed to a brittle fracturing of the reservoir section in the early phase of the launch cycle. As described in Reference 3, the inside diameter of the reservoir expands over 50 percent during the acceleration of the projectile and it is vital to the successful operation of the gun that the inside surface of the reservoir not crack during the early part of the launch cycle. High-speed framing camera records show that the outside of small-scale gun reservoirs expand over 100 percent before rupture occurs. From this and other studies it was concluded that the inside surface of the small-scale reservoir sections remains intact until well over 30 percent expansion.

The reservoir section of the ALPHA-I gun was made from a 14-foot length of surplus 16-inch Naval gun with a 46-inch OD and a 16-inch ID. The section was laminated with five laminations (Figure 5.8) made of a medium-alloy steel (approximately a 4630 alloy according to analysis). The outer lamination was analyzed and found to have a yield point of 104,000 psi, a tensile strength

of 113,000 psi, and an elongation of 19-1/2 percent. It is possible that the inner (and most critical) lamination was particularly brittle because the piece had undergone numerous firings as a Naval gun. The inside surface yield point was estimated at 130,000 psi. The other ALPHA-I components were made from a low-alloy steel ASTM-A27 with a yield point of 40,000 psi, a tensile strength of 75,000 psi, and an elongation of 26.4 percent. The small-scale guns were constructed from 1015 steel, a similar low-alloy steel.

It is postulated that the inner laminations ruptured during the early phase of the launch cycle, thereby increasing the volume occupied by the hot reservoir gas and causing the reservoir pressure and sound speed to decrease more rapidly than programmed. Rupture occurring at 20- or 30-percent inner surface expansion is quite conceivable and would seriously degrade the performance of the gun. Examination of the remaining portion of the reservoir section (Figure 6.7) supports the hypothesis that the reservoir steel fractured early and did not expand properly. The upstream end, rather than having a substantial flare as exhibited in all the small-scale tests, is only slightly flared. Other causes of the low performance besides brittle fracture of the reservoir were considered but seem unlikely. The termination process of the explosive is a critical factor in the operation of the gun. The taper section (Figure 5.8) is supposed to collapse and seal off the reservoir section. The taper sections of the small-scale guns collapse perfectly (Figure 6.8) and remain closed. Since the ALPHA-I gun was scaled precisely, it is assumed that the taper section also collapsed properly. This was verified by a recovered portion of the ALPHA-I taper section (Figure 6.9) that indicates closure. It should be noted that in some of the small-scale tests the taper sections also fragment, but fragmentation probably occurs on a much longer time scale than the acceleration of the projectile.

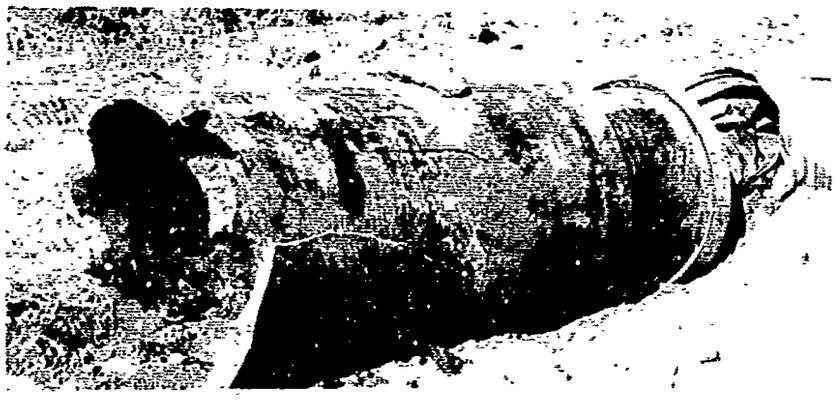

Figure 6.7 Recovered reservoir section of the ALPHA-I gun.

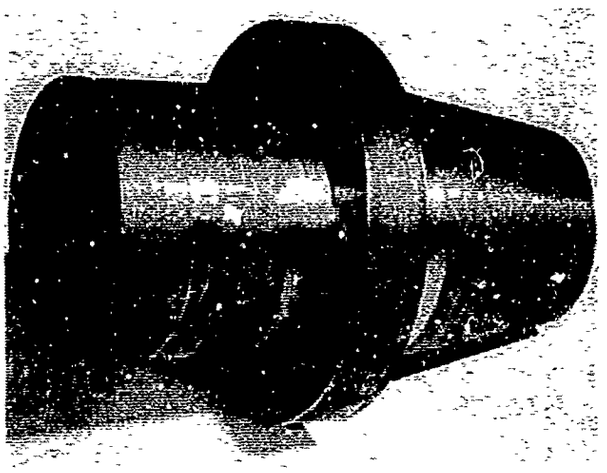

a. Before experiment

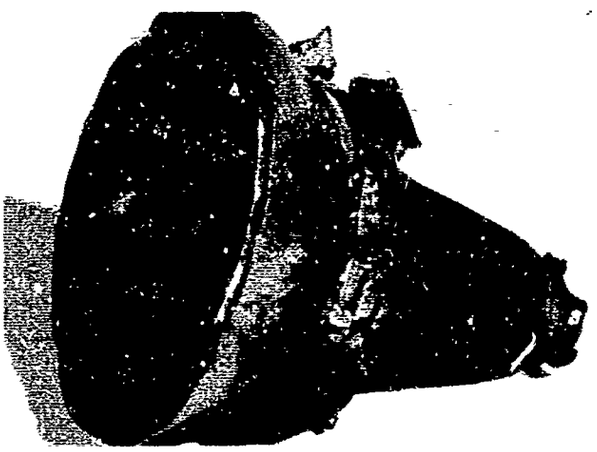

b. After experiment

Figure 6.8 Taper section from the small-scale replica of the ALPHA-I gun (Shot 538-11)

Figure 6.9 A recovered portion of the ALPHA-I taper section showing proper collapse.

Of special importance was the effect from the airblast and shrapnel which was smaller than expected. The gun was covered by a steel arch buried under a minimum of 21 feet of sand, thus the 9200 pounds of nitromethane and 86 tons of steel were decoupled from the ground and isolated from the atomosphere. The airblast generated by the shot was not felt by Control Point observers located 6000 feet from ground zero. Personnel in the bunker, only 350 feet from the shot, heard and felt only a dull rumble. Recovered shrapnel was confined to a radius of less than 300 feet from the shot. Observers at the neighboring Lawrence Radiation Laboratory test site concluded that subsequent 10,000 pound explosive experiments could be conducted under much less favorable atmospheric conditions than originally anticipated by using this same method of containment.

6.1 SUMMARY

The ALPHA-I experiment culminated the effort to accelerate large reentry shapes to reentry velocities. A 6-inch base-diameter slender cone was launched in good condition to 3.2 km/sec. The failure of the gun to accelerate the model to 5.5 km/sec as programmed has been attributed to premature fracturing of the expanding reservoir section. The reservoir section, which was constructed from a surplus 16-inch Naval gun for cost-scheduling reasons, was made from a fairly high strength steel when the most desirable property of the steel was high ductility. In future gun experiments, the reservoir section should be made from ductile low-alloy steel or lead. Both materials have been successful in small-scale experiments.

All other aspects of the ALPHA-I experiment were quite successful. The problems of projectile integrity and premature explosive decomposition appear to be solved. The base of the projectile was subjected to the anticipated peak pressure of nearly 40 kbar and the cone was launched in good condition. There was no observed effect of explosive decomposition for the maximum driver test time of over 390 μsec, confirming the results of an earlier large-scale driver experiment. The scalability of the ALPHA-I driver design was established over the range of pressure tube diameters from 1.37 to 16 inches.

The method of decoupling and burying the shot was very encouraging. The airblast and shrapnel problems associated with the detonation of 9200 pounds of nitromethane were much less than anticipated. The countdown and firing operations proceeded very smoothly, and the elapsed time between permission to fire and firing was only four hours.

The method of constructing the ALPHA-I gun including the use of full-penetration circumferential welds was developed in small-scale tests and appeared to be successful in the ALPHA-I experiment. Assembly of the full-scale gun was straightforward.

SECTION 7
CONCLUSIONS AND RECOMMENDATIONS

The primary purpose of these studies was to develop the explosive gun to launch large saboted models to reentry velocities. A secondary objective was to accelerate small projectiles to the highest possible velocity. To date, 2-gram projectiles have been accelerated to over 12 km/sec, and saboted models up to 4.5 inch diameter have been launched successfully to reentry velocities. Attempts to accelerate 6-inch-diameter and 7.3-inch-diameter models have not been completely successful.

A major portion of the research and development described in this report has been devoted to the explosive driver. The scalable operation of the explosive driver has been demonstrated over a range of pressure-tube diameters from 1/4 inch to 16 inches and with a variety of pressure-tube materials, driver gases and explosives. The precise operation of the explosive driver has been used to provide a controlled gasdynamic cycle for hypervelocity guns. The reproducibility, range accuracy, and the scalability of these guns have been well demonstrated.

During this program, the understanding of projectile-breakup mechanisms has been advanced by the use of sophisticated computer techniques. In the early development of the explosive gun, Lexan and polyethylene cylinders were fragmented or badly distorted during launch. Now, with a better understanding of projectile-failure mechanisms, saboted cones and spheres made from a lightweight lithium-magnesium alloy are launched intact with minimal distortion.

In addition to solving the projectile-integrity problem, several complex physical and physico-chemical phenomena associated with explosive drivers and guns have been quantitatively evaluated. The start-up process, or formation of the explosively formed piston of the driver, has been investigated. The formation of a jet by the collapsing pressure tube, the growth and interaction of the gaseous boundary layer with the collapse process, expansion of the driver pressure tube, and pre-initiation of the driver explosive have all been studied analytically and experimentally. As a result of these studies, the design of the explosive driver has been considerably advanced. The phenomena associated with a high-performance explosive gun, such as reservoir expansion and the detailed gasdynamics of the breech area, have also been thoroughly investigated. The only definite nonscalable phenomenon in this program was the premature initiation of the driver explosive in large-scale drivers. The severity of this phenomenon, however, has been significantly reduced by prepressurizing the driver explosive and is no longer considered a problem.

The launch cycle of the explosive gun has been specifically developed to launch a 6-inch-base-diameter, narrow-angle cone made of lithium-magnesium. Models having the same geometry, but with a density greater than lithium-magnesium ($\rho = 1.38$), would be launched to a lower velocity. Because the growth of a boundary layer limits the length of shocked gas that can be attained, higher-density projectiles of the same geometry would require larger-diameter drivers or higher pressures to overcome the length limitation. Driver and reservoir expansion, pre-initiation of the driver explosive, and projectile integrity are all problems that are made more difficult by higher pressures.

The experiment to field the ALPHA-I gun did demonstrate that assembling and firing large explosive guns is not difficult. The use of a steel arch and a reasonable amount of sand cover all but eliminates the overpressure and shrapnel hazards.

At this point, further development of the reentry gun should begin with a small-scale failure test to verify the mechanism of low performance of the ALPHA-I gun. This failure test should incorporate a high-strength, low-ductility, laminated reservoir such as used for the ALPHA-I gun. If this test verifies the suspected mechanism of low performance, future large guns similar to ALPHA-I should use lead or low-strength, high-ductility steel in the construction of the reservoir section. This would increase the costs of the large gun by 15 to 20 percent, but would ensure successful operation.

In addition, a program of small-scale tests should be conducted to evaluate the launching of slender cones with ablative coatings. These composite models could be X-rayed in flight with existing high-resolution techniques to determine if the ablative coatings survived the launch cycle of the explosive gun.

If these small-scale tests prove successful, a second large-gun experiment similar to ALPHA-I should be conducted. The explosive reentry gun concept would then have reached a sufficient state of development to be used on a range facility for testing realistic 6-inch-diameter slender cones in various reentry environments.

REFERENCES

1. J. D. Watson, E. T. Moore, Jr., D. Mumma, and J. S. Marshall, "Explosively-Driven Light Gas Guns," PIFR-024/065, Physics International Company, San Leandro, California (September 1967).

2. E. T. Moore, Jr., "Explosive Hypervelocity Launchers," NASA CR-982, National Aeronautics and Space Administration (February 1968). Prepared for NASA by Physics International Company.

3. J. D. Watson, "An Explosively Driven-Gun to Launch Large Models to Reentry Velocities," PIFR-098, Physics International Company, San Leandro, California (April 1969).

4. S. P. Gill, "Initiation and Decomposition of Nitromethane at 10-kbar Pressure," PITR-70-2, Physics International Company, San Leandro, California (March 1970).

5. H. F. Waldron, E. T. Moore, Jr., G. B. Steel, and C. S. Godfrey, "A Mechanism for the Conversion of the Chemical Energy of Explosives to the Kinetic and Internal Energy of a Gas," AIAA Paper No. 67-178, presented at the AIAA Fifth Aerospace Sciences Meeting, New York, New York (January 1967).

6. D. Mumma, "Explosive Gas Gun for Reentry Simulation," PIFR-024, Physics International Company, San Leandro, California (November 1965).

7. B. Perkins, Jr., and W. F. Jackson, "Handbook for Prediction of Air Blast Focusing," Report No. 1240, Ballistic Research Laboratories, Aberdeen Proving Grounds, Maryland (1964).

8. J. D. Watson and C. S. Godfrey, "An Investigation of Projectile Integrity Using Computer Techniques," Proceedings of the Fifth Hypervelocity Techniques Symposium, Vol. II, Denver, Colorado (March 1967).

REFERENCES (cont.)

9. R. F. Flagg, J. S. Marshall, Jr., J. D. Watson, and E. T. Moore, Jr., "Explosively-Driven Launchers," PIPR-098-SA-1, Physics International Company, San Leandro, California (April 1968).

10. J. E. Hay, J. Ribovich, F. H. Scott, and F. C. Gibson, "The Effect of Physical and Chemical Properties on the Sensitivity of Liquid Explosives," Fourth Detonation Symposium, U. S. Naval Ordnance Laboratory, White Oak, Silver Spring, Maryland (October 12, 1965).

11. H. S. Brahinsky and D. Northcutt, "Mollier Diagram for Equilibrium Air," Von Karman Gas Dynamics Facility, Arnold Air Force Station, Tennessee (February 1967).

12. A. E. Seigel, "Theory of High Speed Guns," Agardograph 91, NATO-AGARD Fluid Dynamics Panel, North Atlantic Treaty Organization (1965).

13. J. D. Watson, "High Velocity Explosively Driven Guns," PIFR-113, Physics International Company, San Leandro, California (July 1969).

14. "Physics International Hypervelocity Range Facility," A Preproposal Brief prepared for the Advanced Research Projects Agency by Physics International Company, San Leandro, California (February 1969).

APPENDIX A

A TWO-STAGE EXPLOSIVELY-DRIVEN GUN TO LAUNCH SMALL PROJECTILES TO VERY HIGH VELOCITIES

A small portion of the contract effort was used to support investigations of a two-stage-gun concept for accelerating small (0.17- to 2-gram) projectiles to very high velocities. The operation of the two-stage gun is illustrated schematically in Figure A.1. As shown in the illustration, the first stage consists of a standard linear gun of the type used in the ALPHA-I experiment. The second stage is formed by an explosive lens which collapses the barrel behind the accelerating projectile. The explosive lens, which is designed to phase the velocity of a detonating explosive, can be programmed to provide a piston that accelerates in such a manner as to keep a constant base pressure on the projectile.

Since the operation of the two-stage gun depends critically upon the gas conditions generated by the first stage, the initial studies were directed toward accurately calculating the performance of the first-stage gun (Figure A.2). Concurrently, an experimental program to develop the explosive lens resulted in a successful demonstration of its operation (Figure A.3).

The initial two-stage-gun experiments were only moderately successful. The 0.17-gram projectiles were launched to over 12 km/sec but were broken during the second-stage gasdynamic cycle (Figure A.4). The breakup of the projectile was attributed to improper matching of the first and second stages, and a new first-stage design was required to overcome this difficulty. A detailed discussion of this part of the program is found in References 1 and 2.

When the two-stage-gun experiments were resumed, the first stage was redesigned and the mass of the projectile was

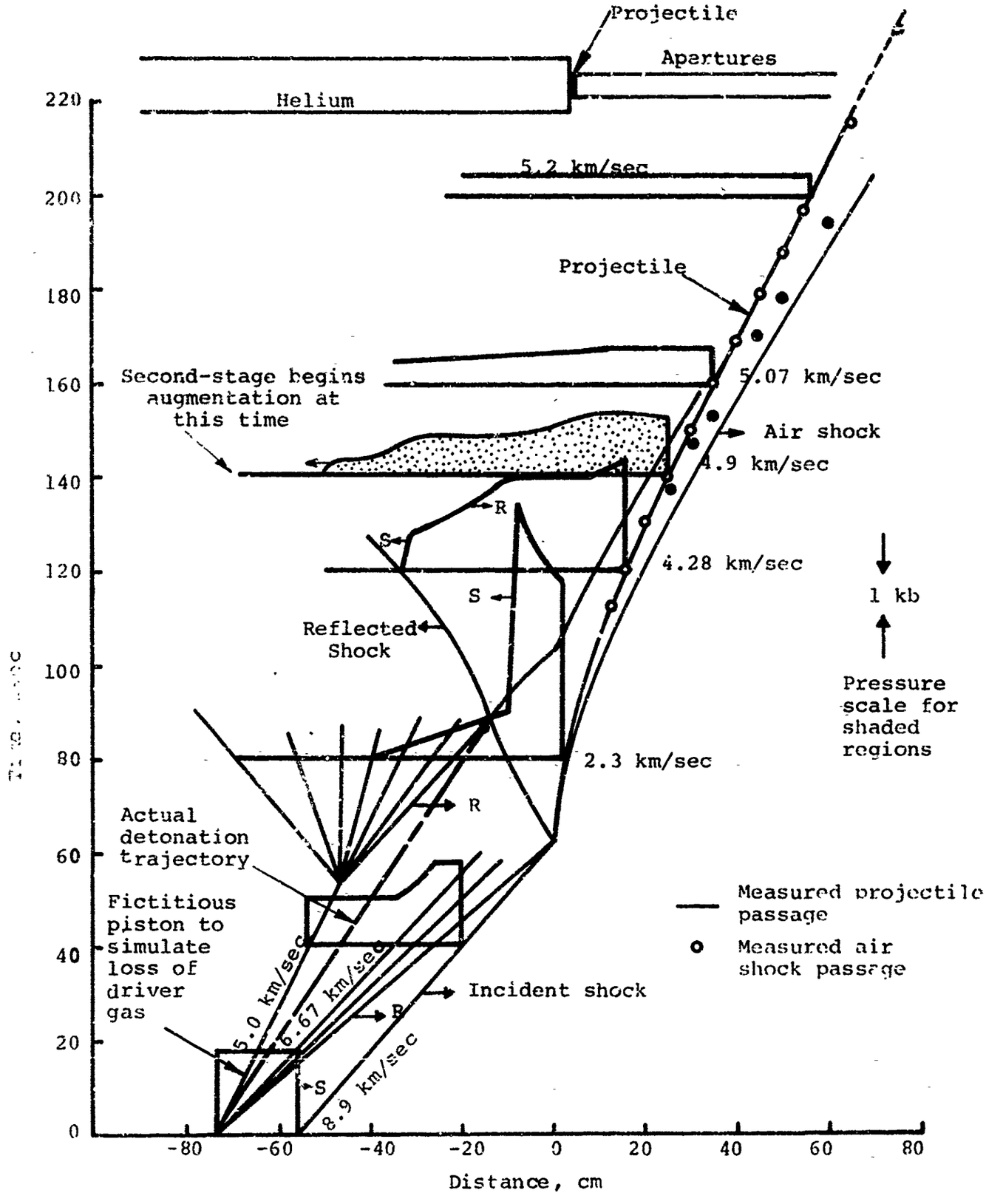

Figure A.1 Computed and experimental performance of first stage of a two-stage launching system.

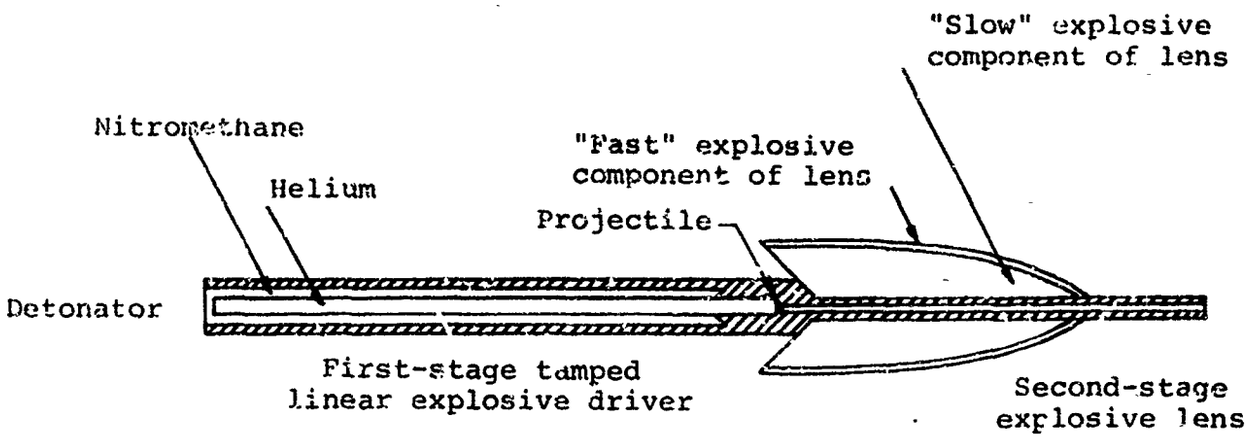

a. Initial configuration

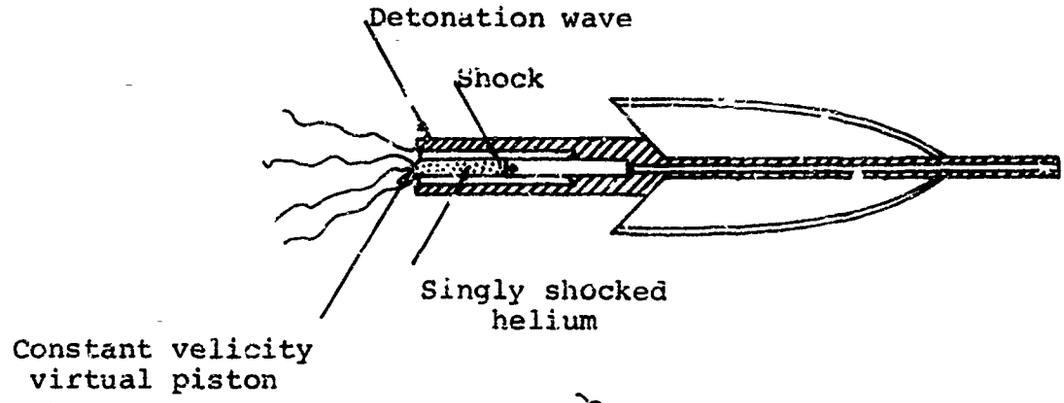

b. First-stage linear-driver operation

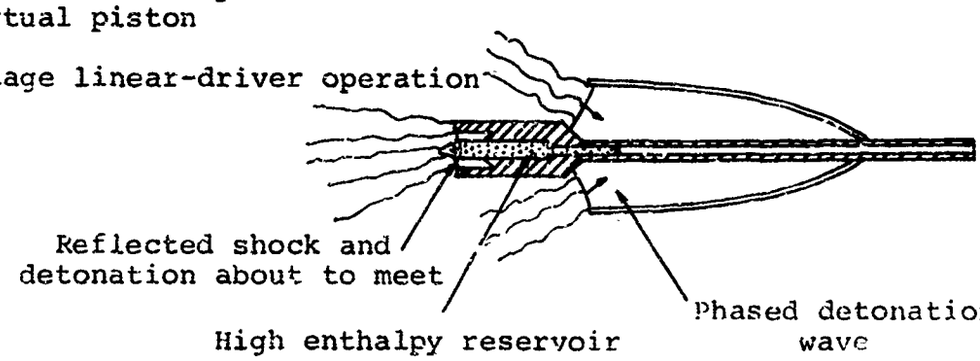

c. Second-stage initiated: projectile and driver gas being injected into explosive lens

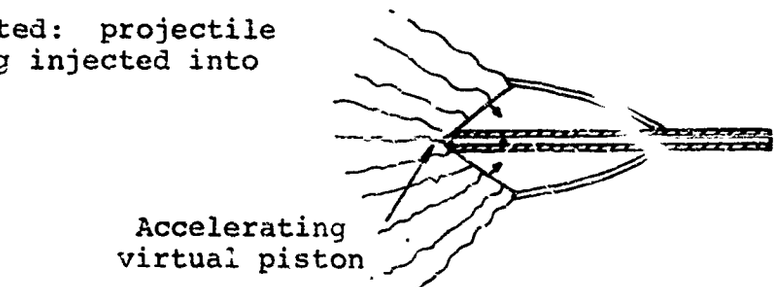

d. Explosive lens accelerates projectile to final velocity

Figure A.2 Operation of a two-stage explosively driven launcher.

3253

Pressure tube

t = - 1 μsec

t = 20 μsec

Bridgewire for determining timing

t = 40 μsec

t = 60 μsec

Note: Zero time taken as the arrival time of the phased detonation wave at the lens axis, or the location of the pressure tube.

t = 80 μsec

Figure A.3 High-speed framing camera record showing the operation of an explosive lens.

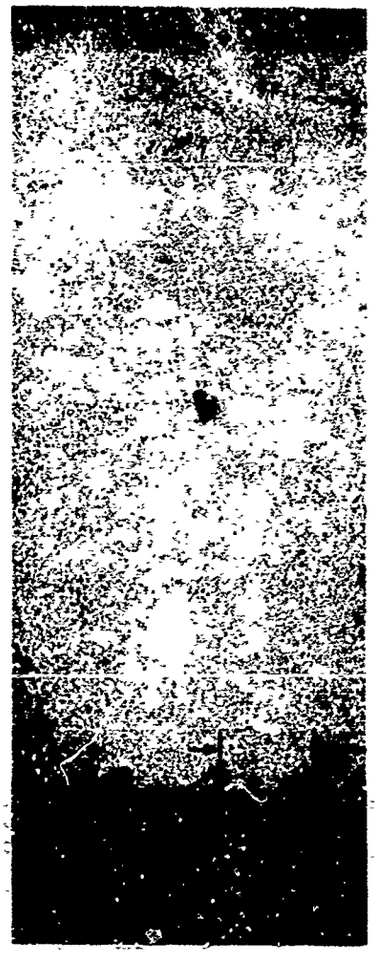

Projectile

Weight: 0.17 gram
Diameter: 0.66 cm
Length: 0.36 cm

Projectile is 60 cm downstream of the muzzle and is flying in air at 1 atmosphere.

1.27 cm

Figure A.4 Range radiograph of a 0.17-gram lithium-magnesium projectile in free flight at 1212 km/sec.

increased to 2 grams. The performance of the first-stage gun was limited by expansion of the reservoir and a new method was developed to overcome this limitation. Explosives were placed around the reservoir and, in addition to preventing reservoir expansion, they were used to collapse the reservoir and pump additional gas into the barrel behind the accelerating projectile. The action of this auxiliary pump cycle is illustrated in Figure A.5. When added to the new first stage, this auxiliary pump cycle resulted in an increase in projectile velocity from 8 km/sec to 10.2 km/sec.

A method for calculating the performance of the gun, even with an expanding or collapsing reservoir wall, was developed. This method is described fully in Reference 13. Several two-stage experiments were carried out using the results of these calculations and the successful first-stage gun with auxiliary pump cycle. The 2-gram projectiles were accelerated to over 12 km/sec (Figure A.6) and were launched in good condition (Figure A.7).

Several second-stage gasdynamic cycles were tested, but further increase in projectile velocity was negligible. It was postulated that the formation of the second-stage piston was being hindered by the unsteady, turbulent boundary layer developed behind the projectile. An experimental program will be necessary to optimize the second-stage parameters, to minimize the detrimental effect of this boundary layer on the second-stage piston. If this limitation can be overcome, then higher velocities, possibly up to 20 km/sec, will be achieved. A detailed discussion of this program is given in Reference 13.

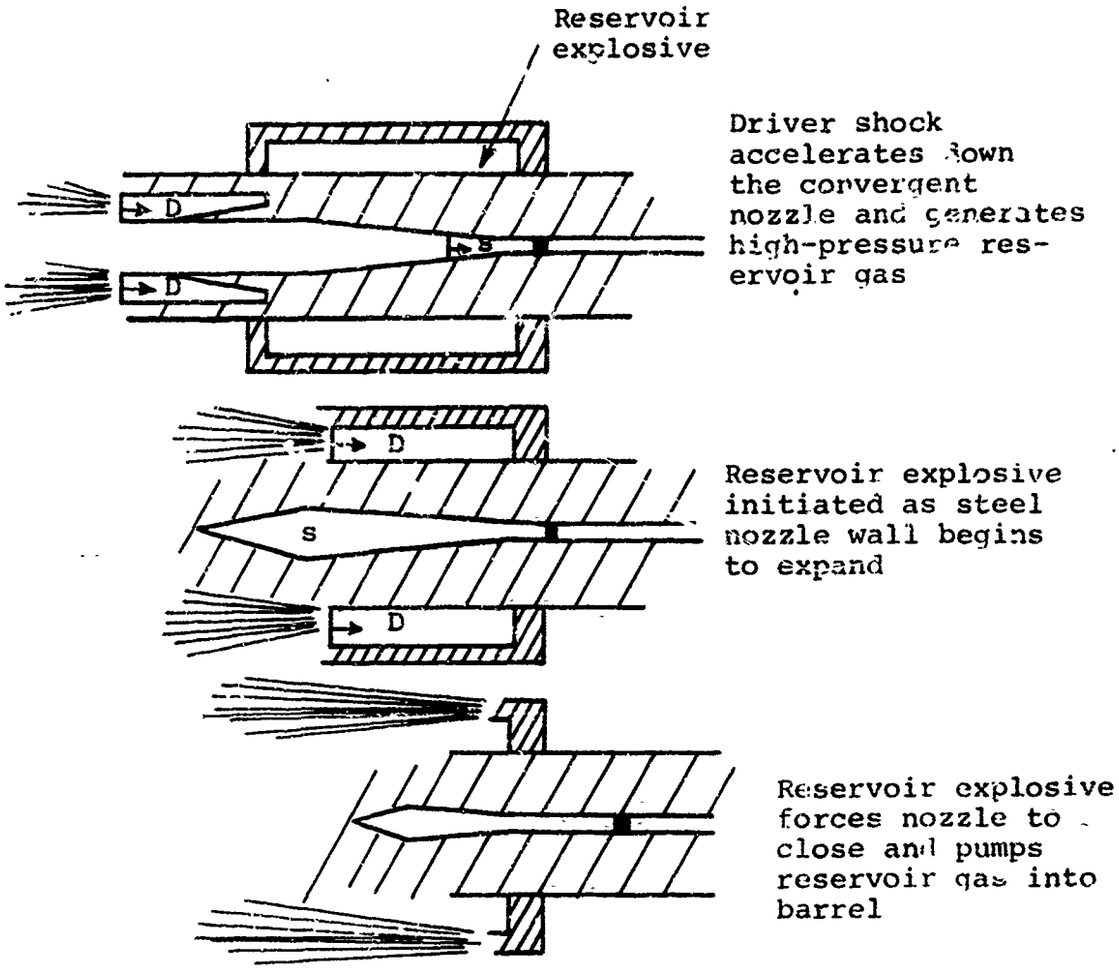

Figure A.5 Schematic operation of auxiliary pump cycle for two-stage gun.

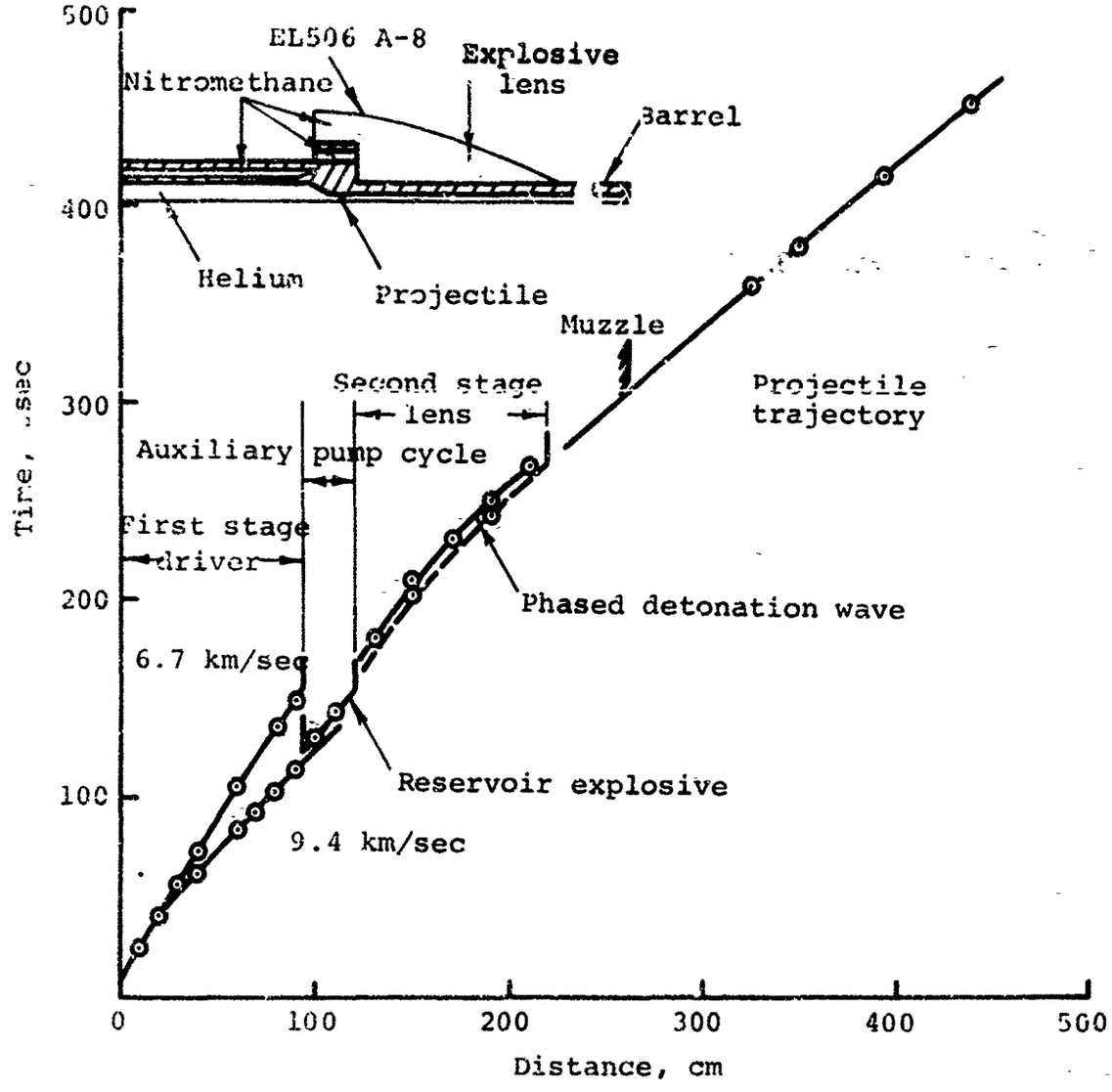

Figure A.6 Observed performance of a two-stage gun (Shot 397-12).

7269

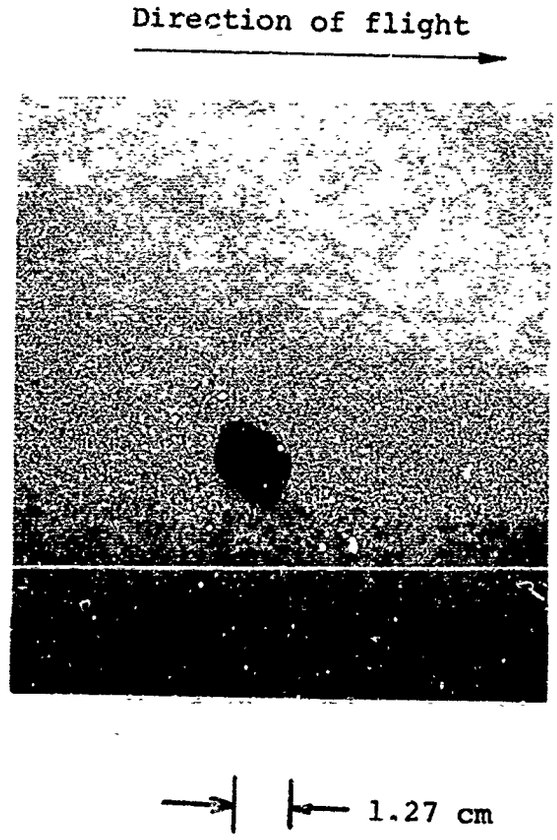

Model is 87.5 body diameters downstream of the muzzle. (Range atmosphere is helium at 1 atmosphere.)

Figure A.7 Range radiograph of a 2-gram, ½-caliber-long projectile launched to 12.0 km/sec by a two-stage gun (Shot 397-11).

APPENDIX B

PROPOSED HYPERVELOCITY RANGE FACILITY

A conceptual design has been proposed for a hypervelocity range facility for large, explosively-driven launchers similar to the ALPHA-I gun. Such a range facility will allow testing of 6-inch base-diameter cones with ablative heat shields over a free-flight distance of 1500 feet. Problems with material properties associated with the aerodynamics of ablating cones and the response of ablating models to dust and rain threats could be carried out. Microwave interaction problems, such as decoy simulation of reentry vehicles and jamming techniques, could be studied with the addition of sophisticated instrumentation. Detection and discrimination experiments could be conducted to investigate radiation signatures of reentry vehicles. It is envisioned that agencies interested in particular experiments would instrument and check out sections of the range tank at their plant and then move them into place in the range facility in accordance with a predetermined firing schedule for testing.

A prerequisite of range operation is that the gun and its 9200 pounds of explosive be entirely decoupled from the range housing. That is, the range housing must be protected from the airblast, ground shocks, and shrapnel hazards. A massive, reinforced-concrete berm was designed to isolate the range from the explosive blast and directed shrapnel. The berm design (Figure B.1) could protect the range from the explosion even if the gun were uncovered. The shrapnel hazard from pieces lobbed over the berm is eliminated by burying the entire range housing (Figure B.2). The gun barrel is held rigidly in place, although it is free to move a small distance axially at a sliding joint to minimize shock transmission into the range. Furthermore, all the range sections are effectively decoupled from each other by flexible rubber couplings commonly used in other range facilities.

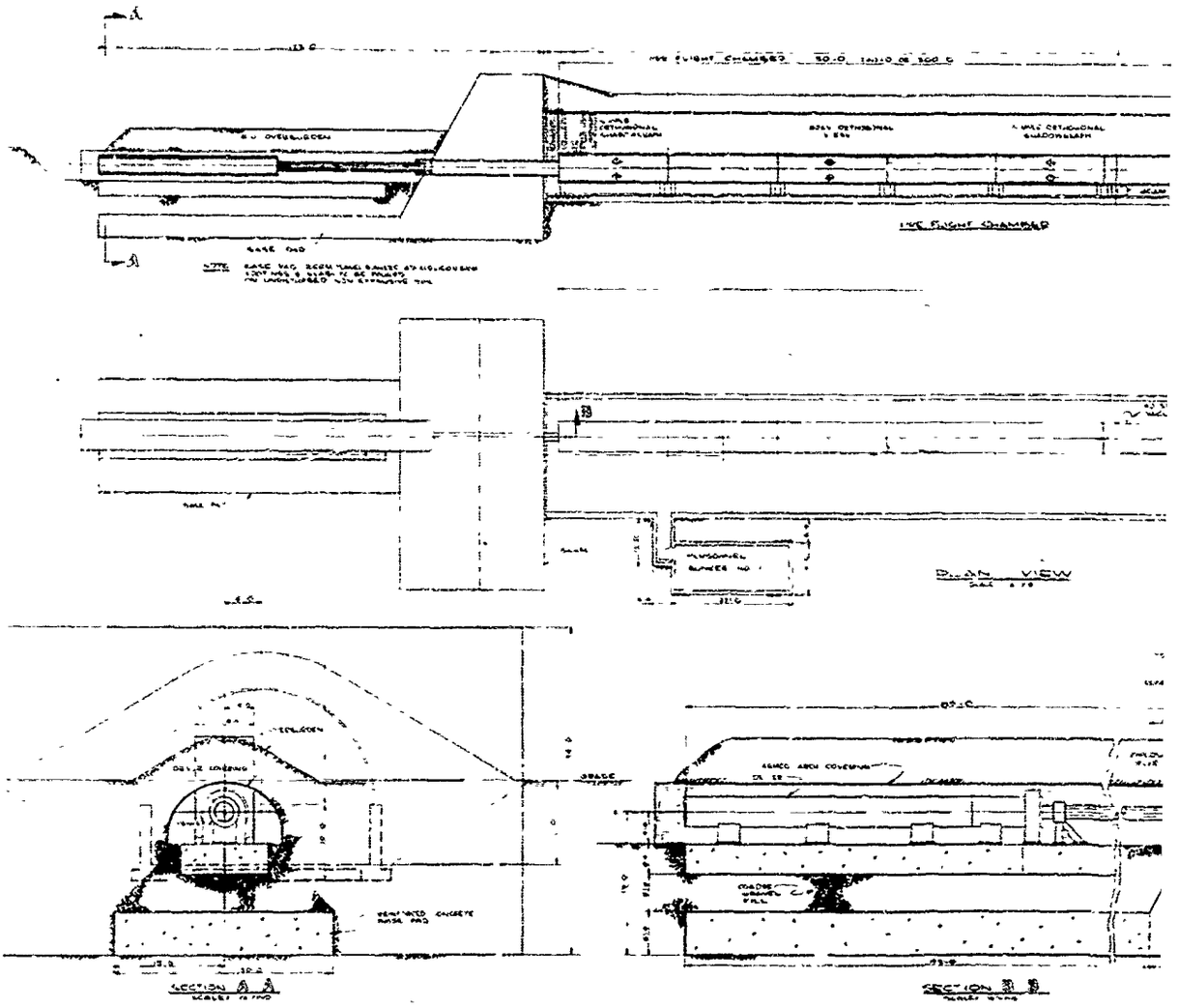

Figure B.1 Proposed hypervelocity range facility, range plot plan and elevation.

A

PIFR-155

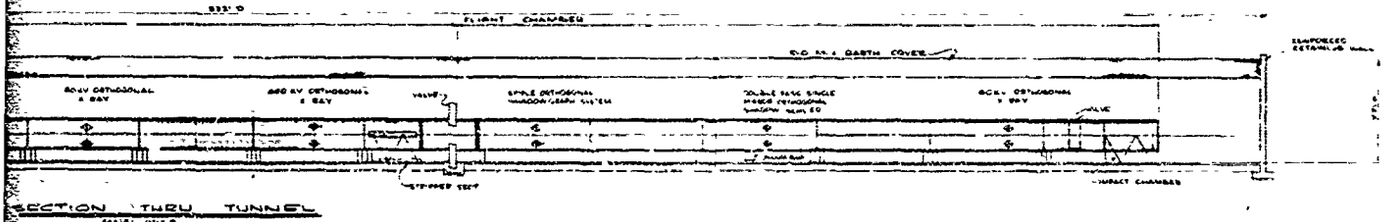

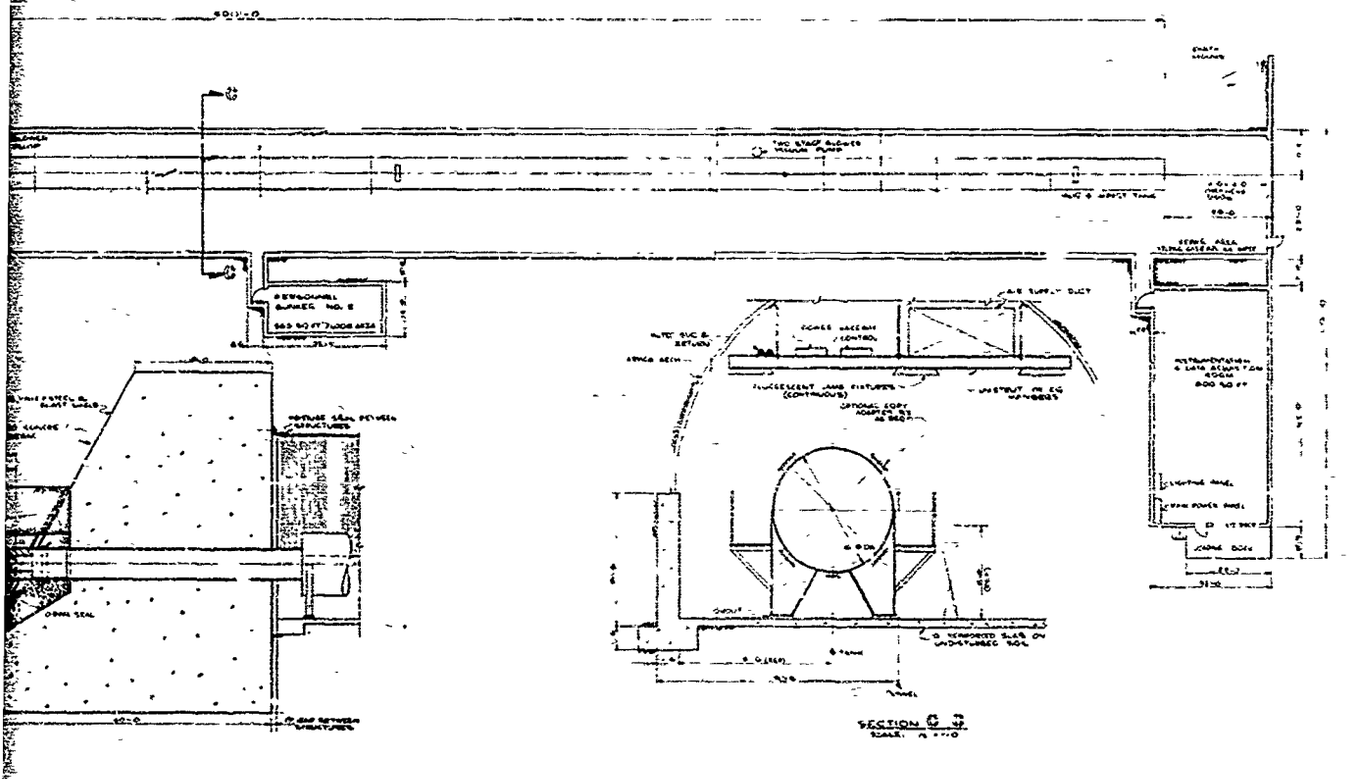

6503

B

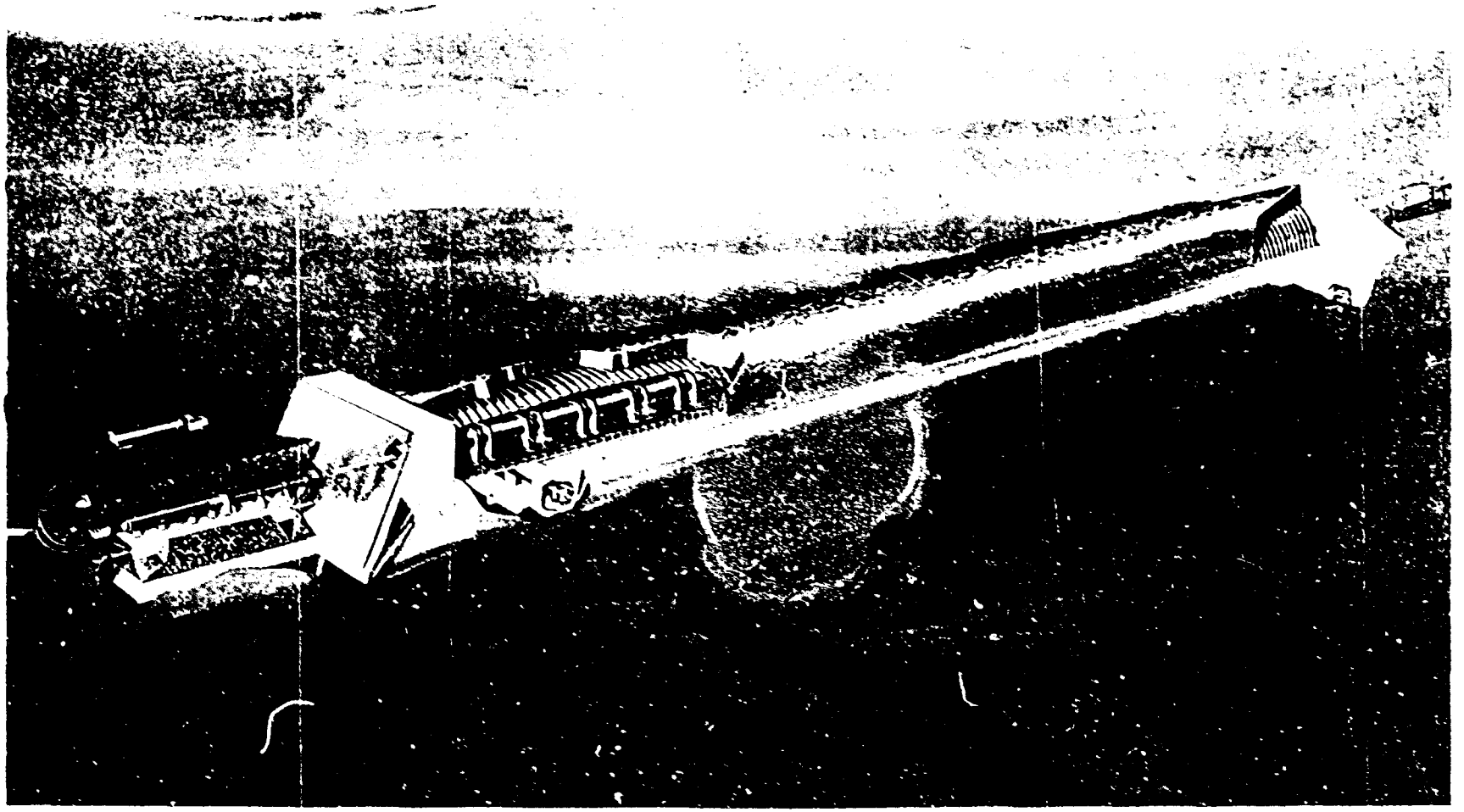

Figure B.2 Proposed Physics International Hypervelocity range facility for large explosive guns.

The proposed preflight chamber, consisting of that part of the range from the berm to the end of the sabot stripping tank, is shown in Figure B.1. The purpose of this section is to determine launch conditions, strip the sabot, and absorb muzzle gases and debris. The preflight chamber will consist of 30-foot-long by 8-foot-diameter tanks that are decoupled from one another and are easily interchangeable. The position of the sabot stripping tank, which determines the length of the preflight chamber, is variable (150, 240, or 300 feet from the muzzle).

The trajectory, attitude, and velocity of the projectile, the condition of the projectile and its ablative coating, and the sabot behavior are all monitored in this section. The preflight chamber may be operated at a different pressure than the flight chamber to give an aerodynamic assist to sabot stripping. The sabot pieces will be terminated in a bumper-impact section that will be able to absorb an impact of 30 pounds at 20,000 feet/second.

Following the preflight chamber, the flight chamber extends another 1200 to 1350 feet long, depending on the position of the sabot tank. It will be used primarily for evaluating the condition of the projectile and its ablative coating after sabot stripping and removal of the muzzle gases and debris from the wake. The flight chamber will consist of 30-foot-long by 12-foot-diameter tanks that will be decoupled from each other and will be interchangeable. The instrumentation in this section will allow detailed evaluation of the ablator condition and some wake measurements. In addition, dust and rain threat experiments may be carried out. The projectile will be terminated in an impact tank designed to absorb the load and prevent ejecta from contaminating the flight chamber.

Initially, state-of-the-art instrumentation will be used in the preflight and flight chambers. The diagnostic stations have been chosen to provide the maximum amount of information for the least cost and to permit a wide range of optical and X-ray techniques to be evaluated.

In the preflight chamber there will be two orthogonal 80-kV X-ray stations and two simple orthogonal shadowgraph stations. At each shadowgraph station there will be provision for direct reflection photography. These stations will be used primarily for determining projectile trajectory, attitude, and velocity. With coherent nanosecond light sources, high-resolution evaluation of the ablator condition is possible. An orthogonal 600-kV X-ray station will be included in the preflight chamber for analysis of the interior of the projectile for possible cracks formed during launch. In the flight chamber there will be four orthogonal 80-kV X-ray stations and fourteen simple orthogonal shadowgraph stations (including direct reflecting photography). There will also be two high-quality, double-pass shadowgraph or schlieren stations with a 24-inch field of view for flow-field visualization.

A large control room (Figure B.2) will be located 500 feet from the muzzle and will be centrally located along the length of the range. This room will contain firing, range control, and data recording functions. A completely interlocked system will integrate the firing, range control, and data acquisition procedures. Six small rooms are provided along the range to protect personnel who wish to make last-minute adjustments on their instruments.

A more detailed discussion of the design of the range facility can be found in References 3 and 14.

UNCLASSIFIED
Security Classification

DOCUMENT CONTROL DATA - R&D
(Security classification of title, body of abstract and indexing annotation must be entered when the overall report is classified)

1 ORIGINATING ACTIVITY *(Corporate author)*
Physics International Company
2700 Merced Street
San Leandro, California 94577

2a. REPORT SECURITY CLASSIFICATION

2b GROUP

3 REPORT TITLE
A Summary of the Development of Large Explosive Guns for Reentry Simulation

4 DESCRIPTIVE NOTES *(Type of report and inclusive dates)*

5 AUTHOR(S) *(Last name, first name, initial)*
Watson, J. D.

6 REPORT DATE	7a. TOTAL NO. OF PAGES	7b. NO OF REFS
August 1970	149	14

8a CONTRACT OR GRANT NO.	9a. ORIGINATOR'S REPORT NUMBER(S)
DA-04-200-AMC-796 (X)	ARPA Order No. 546
b. PROJECT NO.	Program Code No. 4730
c.	9b OTHER REPORT NO(S) *(Any other numbers that may be assigned this report)*
d.	

10 AVAILABILITY/LIMITATION NOTICES

11 SUPPLEMENTARY NOTES	12. SPONSORING MILITARY ACTIVITY
	Ballistic Research Laboratories Aberdeen Proving Ground Maryland 21005

13 ABSTRACT

This report describes the results of a program to develop an explosive gun capable of launching large saboted models to reentry velocities. A secondary objective was to accelerate small projectiles to the highest possible velocity. Saboted lithium-magnesium models up to 4.5-inch diameter have been launched successfully to 4.8 km/sec. Attempts to accelerate 6-inch-diameter and 7.3-inch-diameter models have not been completely successful. A new velocity-mass record was achieved by accelerating a 2-gram cylindrical projectile to 12.2 km/sec.

DD FORM 1 JAN 64 1473

UNCLASSIFIED
Security Classification

14 KEY WORDS	LINK A		LINK B		LINK C	
	ROLE	WT	ROLE	WT	ROLE	WT
Explosive gun						
Hypervelocity						
Explosives						
Simulator						

INSTRUCTIONS

1. ORIGINATING ACTIVITY: Enter the name and address of the contractor, subcontractor, grantee, Department of Defense activity or other organization *(corporate author)* issuing the report.

2a. REPORT SECURITY CLASSIFICATION: Enter the overall security classification of the report. Indicate whether "Restricted Data" is included. Marking is to be in accordance with appropriate security regulations.

2b. GROUP: Automatic downgrading is specified in DoD Directive 5200.10 and Armed Forces Industrial Manual. Enter the group number. Also, when applicable, show that optional markings have been used for Group 3 and Group 4 as authorized.

3. REPORT TITLE: Enter the complete report title in all capital letters. Titles in all cases should be unclassified. If a meaningful title cannot be selected without classification, show title classification in all capitals in parenthesis immediately following the title.

4. DESCRIPTIVE NOTES: If appropriate, enter the type of report, e.g., interim, progress, summary, annual, or final. Give the inclusive dates when a specific reporting period is covered.

5. AUTHOR(S): Enter the name(s) of author(s) as shown on or in the report. Enter last name, first name, middle initial. If military, show rank and branch of service. The name of the principal author is an absolute minimum requirement.

6. REPORT DATE: Enter the date of the report as day, month, year, or month, year. If more than one date appears on the report, use date of publication.

7a. TOTAL NUMBER OF PAGES: The total page count should follow normal pagination procedures, i.e., enter the number of pages containing information.

7b. NUMBER OF REFERENCES: Enter the total number of references cited in the report.

8a. CONTRACT OR GRANT NUMBER: If appropriate, enter the applicable number of the contract or grant under which the report was written.

8b, 8c, & 8d. PROJECT NUMBER: Enter the appropriate military department identification, such as project number, subproject number, system numbers, task number, etc.

9a. ORIGINATOR'S REPORT NUMBER(S): Enter the official report number by which the document will be identified and controlled by the originating activity. This number must be unique to this report.

9b. OTHER REPORT NUMBER(S): If the report has been assigned any other report numbers *(either by the originator or by the sponsor)*, also enter this number(s).

10. AVAILABILITY/LIMITATION NOTICES: Enter any limitations on further dissemination of the report, other than those imposed by security classification, using standard statements such as:

(1) "Qualified requesters may obtain copies of this report from DDC."

(2) "Foreign announcement and dissemination of this report by DDC is not authorized."

(3) "U. S. Government agencies may obtain copies of this report directly from DDC. Other qualified DDC users shall request through _____."

(4) "U. S. military agencies may obtain copies of this report directly from DDC. Other qualified users shall request through _____."

(5) "All distribution of this report is controlled. Qualified DDC users shall request through _____."

If the report has been furnished to the Office of Technical Services, Department of Commerce, for sale to the public, indicate this fact and enter the price, if known.

11. SUPPLEMENTARY NOTES: Use for additional explanatory notes.

12. SPONSORING MILITARY ACTIVITY: Enter the name of the departmental project office or laboratory sponsoring *(paying for)* the research and development. Include address.

13 ABSTRACT: Enter an abstract giving a brief and factual summary of the document indicative of the report, even though it may also appear elsewhere in the body of the technical report. If additional space is required, a continuation sheet shall be attached.

It is highly desirable that the abstract of classified reports be unclassified. Each paragraph of the abstract shall end with an indication of the military security classification of the information in the paragraph, represented as *(TS)*, *(S)*, *(C)* or *(U)*.

There is no limitation on the length of the abstract. However, the suggested length is from 150 to 225 words.

14 KEY WORDS: Key words are technically meaningful terms or short phrases that characterize a report and may be used as index entries for cataloging the report. Key words must be selected so that no security classification is required. Identifiers, such as equipment model designation, trade name, military project code name, geographic location, may be used as key words but will be followed by an indication of technical context. The assignment of links, roles, and weights is optional.